DEVELOPMENT OF POLYMERIC NANOSUSPENSION FOR THE ENCAPSULATION AND DELIVERY OF ANTIRETROVIRAL AGENTS

by

Anna Yusuf Aliyu

Submitted in partial fulfilment of the requirements for the degree of Master of Science

at

Dalhousie University
Halifax, Nova Scotia
April 2025

Dalhousie University is located in Mi'kma'ki, the
ancestral and unceded territory of the Mi'kmaq.
We are all Treaty people.

DEDICATION

This thesis is dedicated to all individuals living with HIV and to the numerous researchers, healthcare professionals, and advocates who have devoted their time, strength and resources to encourage the advancements of the science and treatment of HIV. May this work honor your contributions and serve as a step forward in the collective journey toward a world free of HIV.

TABLE OF CONTENTS

LIST OF TABLES

LIST OF FIGURES

ABSTRACT

The Human Immunodeficiency Virus (HIV) infection is a global, life-threatening epidemic that continues to affect millions, including the paediatric population. Effective antiretroviral therapy is crucial for managing HIV. However, poor adherence remains a significant problem, hindering successful clinical outcomes due to the complexity of HIV medications, which require at least a combination of three drugs. This is challenging especially for children, because efforts on designing innovative drug delivery systems such as fixed dose combinations and long acting injectables have been more directed at adults' patients meaning that young children tend to miss out on such advancements and their benefits which is mainly to simplify treatment to enhance convenience, adherence and efficacy. Consequently, there is a significant shortage of novel age-appropriate drug formulations for the paediatric population, particularly the very young children, typically ≤ 10 kg, such as neonates/newborns and infants. This research, therefore, specifically designed, for the first time, a flexible, orally delivered fixed dose nanosuspension formulation containing two key antiretroviral drugs, namely abacavir and lamivudine. This new nanosuspension formulation is intended for use in very young children (newborns to about 1 year) but is also suitable for older children, adolescents, adults, the elderly, or individuals who have difficulty swallowing. Formulation fabrication was achieved through the initial nanoencapsulation of abacavir and lamivudine within a biocompatible and biodegradable co-polymeric matrix to produce nanopowders that were subsequently dispersed into a synthesized methylcellulose/gelatin/xylitol-based pharmaceutical gel (fluid gel) carrier to generate the antiretroviral nanosuspension referred to herein. The reconstitutable nanosuspension formulation was found to (i) be physicochemically, physicomechanically, and environmentally stable; (ii) be compatible with the model antiretroviral agents employed; (iii) exhibit modulated drug release characteristics and zero order kinetics; and (iv) have no toxic effects on representative living cells.

LIST OF ABBREVIATIONS USED

3TC	Lamivudine
ABC	Abacavir
ADME	Absorption, distribution, metabolism and excretion
AIDS	Acquired immunodeficiency syndrome
API	Active pharmaceutical ingredient
ART	Antiretroviral therapy
ARV	Antiretroviral
C=O	Carbonyl group
CA	Citric acid
CCR5	C-C chemokine receptor type 5
CD4	Cluster of differentiation 4
CDC	Centers for disease control and prevention
C-H	Carbon-hydrogen bond
C-N	Carbon-nitrogen bond
C-O	Carbon-oxygen bond
CXCR4	C-X-C chemokine receptor type 4
CYP3A4	Cytochrome P 3A4
DDS	Drug delivery systems
DLS	Dynamic light scattering
DNA	Deoxyribonucleic acid
ELS	Electrophoretic light scattering
FDC	Fixed dose combination

FTIR	Fourier transform infrared
GEL	Gelatin
HBV	Hepatitis B virus
HEC	Hydroxyethyl cellulose
HEPG2	Human hepatocellular carcinoma
HIV	Human immunodeficiency virus
HPMC	Hydroxypropyl methylcellulose
ICH	International council for harmonisation of technical requirements for pharmaceuticals for human use
INSTI	Integrase strand transfer inhibitor
ƛ	Lamda
LAC	Lactose
LPV/r	Lopinavir/ritonavir
MC	Methyl cellulose
NaCl	Sodium chloride
N-H	Nitrogen-hydrogen
NNRTI	Non-nucleoside reverse transcriptase inhibitor
NRTI	Nucleoside reverse transcriptase inhibitor
OVAT	One variable at a time
PBS	Phosphate buffered saline
PDI	Polydispersity index
PEG/PVA	Polyethylene glycol/polyvinyl alcohol
PEP	Post-exposure prophylaxis

pH	Potential hydrogen
PI	Protease inhibitor
PrEP	Pre-exposure prophylaxis
PVA	Polyvinyl alcohol
PVP	Polyvinyl pyrrolidone
RNA	Ribonucleic acid
S=O	Sulphonyl group
SB	Sodium benzoate
SEM	Scanning electron microscopy
SSG	Sodium starch glycolate
STR	Single tablet regimen
TDF	Tenofovir disoproxil fumarate
TEM	Transmission electron microscopy
TPA	Textural profile analysis
tRNA	Transfer ribonucleic acid
UGT	Uridine glucuronosyltransferase
UNICEF	United nations international children’s emergency fund
UV	Ultraviolet
WHO	World Health Organization
XYL	Xylitol
α	Alpha
β	Beta

ACKNOWLEDGEMENTS

First and foremost, I would like to express my warmest gratitude to my supervisor, Dr. Oluwatoyin Adeleke, for her unwavering support and expert guidance, which have been instrumental in the success of this project. Her mentorship over the past two years has been invaluable, and I truly appreciate her constant encouragement, even in my moments of self-doubt, and professional insights whenever I needed them.

I am also very grateful to my examiners and committee members, Dr. Aik Jang Lau and Dr. Vahid Adibnia, for their constructive feedback and thoughtful advice. Dr. Lau's assistance in teaching me cell culture techniques and working with cells has been a key element in my professional growth and research. I also thank Dr. Adibnia for his expert guidance during my Dynamic Light Scattering (DLS) experiments. His contributions played an important role in the success of this project. I sincerely thank Dr. David Jakeman for his support as my graduate coordinator and all other faculty members for their encouragement and assistance.

I would also like to express my sincere gratitude to the College of Pharmacy for its support and graduate funding, which made this work possible. I extend my appreciation to Dr. Susan Mansour, past director, for her leadership, and Dr. Kyle Wilby, the current director, for his continued guidance. I am also grateful to the entire college administration, both past and present, including Wanda Dundas, Padampreet Kaur, Vignesh Hariharan, and Kaylon Fraser, for their assistance and support throughout this process.

I am deeply grateful to my colleagues and lab members, current and past, including Saba, Erica, Ajitha, Esther, and everyone else who has contributed to and supported me in various ways, academically or otherwise. You have all enriched this experience, and I sincerely appreciate all your efforts.

I would also like to extend my heartfelt thanks to my family, my parents, siblings, and friends for all their sacrifices, prayers, unwavering support, and encouragement throughout this journey. Their belief in me has been a constant source of strength, and I could not have completed this project without them.

Lastly, I give all the glory to God, whose guidance has carried me through every challenge. I truly believe that I could not have accomplished this without His help.

CHAPTER 1: INTRODUCTION

1.0. BACKGROUND AND STUDY RATIONALE

The Human Immunodeficiency Virus (HIV) is a virus that targets the immune system, specifically a type of white blood cell known as CD4 cells, which leads to the weakening of the immune system. This makes it easier for affected individuals to contract certain infections and diseases that a healthy immune system can normally fight off. It can be transmitted through contact with infected body fluids (e.g., blood, semen, vaginal secretions etc.) or vertically from an infected mother to her child. No cure exists for HIV yet, but treatment with antiretroviral medicines can manage the disease and allow individuals to live long and healthy lives (World Health Organization, 2023). HIV remains a major public health concern globally, both among adult and paediatric populations. The United Nations International Children's Emergency Fund (UNICEF) reported that an estimated 40 million people are infected with HIV, with more than 2 million infected children and more than 600 children contracting HIV every day in the past year. This highlights the critical need for more accessible and acceptable antiretroviral therapies tailored to the paediatric population (UNICEF., 2024).

The advancement of HIV management through antiretroviral therapy (ART) has come a long way and has enabled individuals to live long, healthy lives by suppressing the progression of the virus; however, there is still a significant gap in the treatment options for paediatric patients. The emergence of fixed dose combinations, which involves taking a single tablet (containing two or more antiretroviral agents) each day as opposed to several tablets every day or multiple times a day, has revolutionized the treatment of HIV. However, this impressive innovation is almost

entirely enjoyed by adult patients only (Caplan et al., 2018). HIV infected paediatric patients continue to experience regimen complexities that involve taking several pills and liquids daily or even multiple times a day due to the limited availability of child-friendly antiretroviral drug formulations and dosage forms. This problem has resulted in inconvenience for caregivers and ultimately lack of medication adherence in HIV positive children, which is an important requirement for the complete suppression of the virus (Mengesha et al., 2022). Several strategies are being implemented to eradicate the incidence of paediatric HIV cases. These recommended strategies include administering antiretroviral therapy (ART) to both HIV-positive mothers and their infants, scheduling caesarean deliveries for mothers with a high (i.e., over 1,000 copies per mL) or unknown viral load near delivery, and using formula instead of breastfeeding (Vijayan et al., 2021). While the eradication of paediatric HIV is highly anticipated, it is of paramount importance for child-friendly antiretroviral-containing dosage forms to be developed to ease the treatment regimen of all infected children.

Whilst monotherapy is traditionally the preferred treatment starting point for chronic conditions such as hypertension and diabetes, other diseases require the use of multiple drugs (polytherapy) from the onset of treatment (e.g., human immunodeficiency virus acquired immunodeficiency syndrome, tuberculosis, and malaria). Successful treatment of these chronic conditions is sometimes hampered by patient non-adherence to polytherapy. The options available for polytherapy are the sequential addition of individual drug products to deliver an effective multi-drug regimen or the use of a single fixed dose combination (FDC) therapy product. This research intends to critically review the use of FDC drug therapy and provide an insight into FDC products that are already commercially available. Shortcomings of FDC formulations are discussed from

multiple perspectives, and research gaps are identified. Moreover, an overview of fundamental formulation considerations is provided to aid formulation scientists in designing and developing new FDC products (Wilkins et al., 2024). This project aims to design, for the first time, a dual drug delivery system, which can also be referred to as a fixed dose combination formulation, composed of a dispersion of nanoparticulate carriers (nanopowders) containing abacavir and lamivudine in a fluid pharmaceutical gel matrix to produce a nanosuspension formulation. The flexible nature of the formulation designed is specifically intended to cater to paediatric patients weighing 10 kg and under as they are an underserved population, however, its applications extend beyond this demographic, because it can also benefit older children and adults experiencing dysphagia (difficulty swallowing) or who prefer oral liquids over solid dosage forms. The antiretroviral drugs of choice for this study, abacavir and lamivudine, which belong to the class of nucleoside reverse transcriptase inhibitors (NRTIs), were chosen because they are among the recommended first-line regimens for infants (Jesson et al., 2022). These drugs inhibit the virus' reverse transcriptase, causing DNA chain termination and preventing HIV replication. Abacavir is preferred over older agents like stavudine due to its favorable safety profile and lower risk of toxic effects such as lipodystrophy and metabolic abnormalities (Adkison et al., 2018). Both drugs have a well-established history of safety and efficacy in the paediatric population, making them ideal candidates for this study. Additionally, the successful nano-encapsulation of these two antiretrovirals will pave the way for the multi-drug encapsulation of several antiretrovirals, thus revolutionizing drug delivery and opening avenues for the administration of various pharmaceutical agents as well, which will improve convenience for both caregivers and patients. Thus, the proposed nano-based oral formulation will contain two backbone antiretroviral drugs for oral administration. Polymeric nanoparticles are known to improve the absorption, bioavailability,

and stability of drugs encapsulated within a formulation, thus making the proposed approach an attractive one for the concurrent incorporation of the two antiretroviral agents focused on herein (Begines et al., 2020). Formulations utilizing nanotechnology can also enhance the quality of life for young patients through better diagnosis, treatment, and prevention of various diseases. For instance, researchers developed a nanoparticle formulation of the liposoluble antiviral drug saquinavir to improve stability and taste masking for children (Abedin & Adeleke, 2024). Additionally, fluid gels can be used to safely administer medications to children as well as individuals who have trouble swallowing including elderly patients and patients in this category need to use suitable dosage forms to ensure effective swallowing (Mohd Shahrizan et al., 2022) Moreover, employing safe and biocompatible polymers for the fluid gel preparation will make the nanosuspension formulation less likely to cause adverse effects (Thang et al., 2023). The use of this double encapsulation drug delivery strategy will ensure that the formulation benefits from the advantages of both systems, which would produce a highly stable, biocompatible, and palatable drug product (Penazzato et al., 2022; Pereira et al., 2022). Since HIV is endemic in resource-limited countries, the provision of a fluid pharmaceutical gel as diluent instead of the usual water will not only make it convenient for caregivers to reconstitute. However, it will also decrease the risk of contamination in areas that lack clean water. Typically, water is used as a diluent for reconstituting suspension powders in clinical practice, but this is often faced with different demerits such as adding excess water to the powder for suspension which can dilute the concentration of the active ingredient(s), potentially affecting the effectiveness of the treatment (Daanish et al., 2023), limited availability of clean water. Consequently, this work focused on the use of a polymer-based fluid pharmaceutical gel carriers as an alternative diluent because of their known cost-effectiveness, low water content that can aid in maintaining stability thus ensuring that

the drugs remain safe for use and efficacious, plus their ability to enhance swallowing thus minimizing aspiration and choking risks and promote taste masking (Aziz et al., 2022).

1.1. STATE OF THE ART

Successful treatment of paediatric HIV is highly dependent on safe and effective antiretroviral drug formulations. Unfortunately, paediatric HIV formulations are lagging behind that of adults by 7-12 years, suggesting that more child friendly dosage forms need to be developed in order to fill this gap. Moreover, introducing more child-friendly formulations will be a welcome relief for many parents and healthcare providers who have faced challenges with helping infants and children tolerate current formulations (Penazzato et al., 2022). An effective paediatric ART aims to allow all children living with HIV to lead normal lives, reaching their full potential with sustained viral suppression throughout childhood and into adulthood (Sorour et al., 2023). Abacavir and lamivudine are considered the backbone of paediatric antiretroviral therapy, and currently, a fixed dose combination containing these two drugs is commercially available in the form of dispersible and scored oral tablets (UNICEF., 2020; WHO., 2023). Thus, no fixed dose liquid formulations can cater to the crucial needs of very young children, such as neonates and infants, typically those weighing 10 kg and below (National Institutes of Health, 2024). This requires caregivers to either break the tablet and/or dissolve it in water before administration. This practice can result in uneven splitting, dosing inaccuracies, chemical instability, or formulation contamination all of which can lead to significantly suboptimal therapeutic concentration, unwanted adverse effects and poor clinical outcomes (Saran et al., 2022) hence the glaring need for innovative drug delivery interventions that can improve the delivery of antiretroviral drugs to special patient populations.

1.2. RATIONALE FOR USING ABACAVIR AND LAMIVUDINE AS MODEL DRUGS FOR THIS STUDY

Although the general guideline of antiretroviral therapy is the same across all patients, the selection of drugs can differ from one patient to another due to different factors such as age Before 2010, stavudine and lamivudine were the nucleoside reverse transcriptase inhibitors (NRTIs), commonly known as the "backbones," used in combination with nevirapine for the treatment of HIV in children. However, WHO revised its guidelines and replaced stavudine with abacavir due to concerns about its toxicity (mitochondrial toxicity) (Margolis et al., 2014). The current guidelines now recommend lamivudine in combination with either zidovudine or abacavir as the preferred NRTIs for children. Tenofovir disoproxil fumarate (TDF), popular among adult patients, is not indicated for use in children under ten years of age due to potential long-term effects on bone and kidney health (Mega et al., 2020).

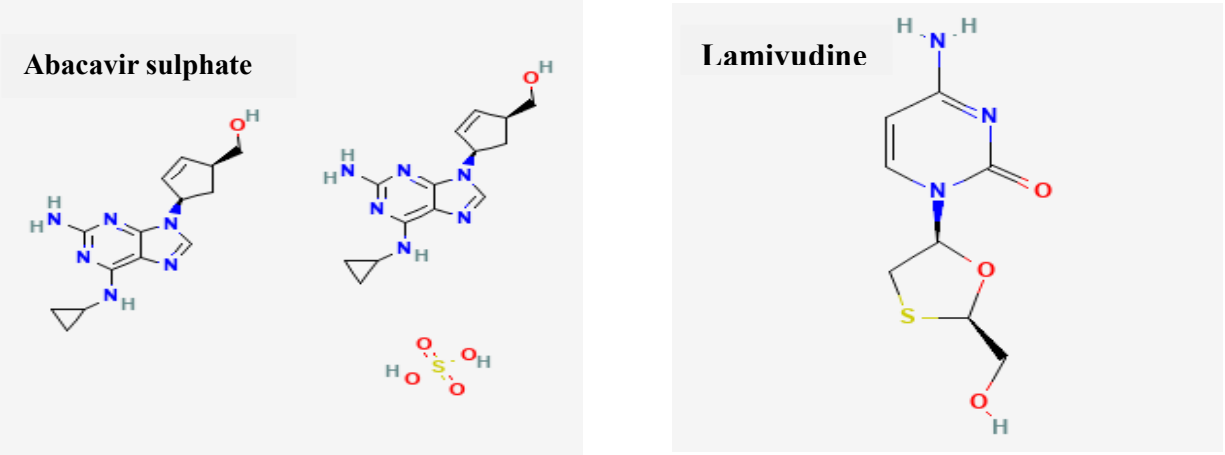

Figure 1.1. Chemical structure of abacavir sulphate and lamivudine (retrieved from PubChem NCBI, 2025)

Abacavir is a guanosine analog that belongs to the NRTI group. It demonstrates antiviral ability against HIV similar to NRTIs by preventing the transcription of viral RNA to DNA via its intracellular anabolite known as carbovir triphosphate (Fernandez & Munir, 2025). Lamivudine is another NRTI that is used in the treatment of both HIV and hepatitis B (HBV) infections. It is a dideoxynucleoside cytosine analog that inhibits viral replication through a process similar to that of other NRTIs. Lamivudine is an important antiviral agent because human polymerases do not primarily recognize its active form as a substrate because it is an L-(-)-nucleoside enantiomer, not a D-enantiomer, but instead competes with natural cytidine triphosphate to block reverse transcriptase DNA synthesis in both HIV and HBV. In addition, the selective nature of the active 3TC minimizes its risk of harmful side effects due to its ability to only weakly inhibit mammalian DNA polymerases (α and β) and mitochondrial DNA polymerase (Taylor et al., 2025).

The combination of abacavir and lamivudine is frequently used due to their complementary mechanisms of action, which not only enhance antiviral efficacy but also reduce the potential for the development of drug resistance (Antiretroviral Therapy - PAHO/WHO | Pan American Health Organization, 2020). Both drugs are well tolerated in paediatric populations, with long half-lives (abacavir 20 hours and lamivudine about 19 hours) (Sivasubramanian et al., 2010)), enabling one-daily dosing, thus improving adherence. These drugs also show excellent oral bioavailability and have favorable pharmacokinetic properties for children, allowing for effective viral load suppression and improved immune function (Achenbach et al., 2010; Quercia et al., 2018). Importantly, lamivudine is effective in patients co-infected with HIV and HBV, making this combination therapy beneficial in areas with high rates of this co-infection (Quercia et al., 2018). Additionally, abacavir and lamivudine are known for their good safety profiles and cost-

effectiveness. Compared to tenofovir-based regimens, they have the benefit of reducing the risk of renal and bone toxicity, making them a suitable option for individuals with renal insufficiency and osteoporosis (Lim et al., 2021). The drugs were also compatible with the excipients and experimental methods selected for this study. Thus, the choice of a combination of abacavir and lamivudine as model bioactives for the nanosuspension formulation reported herein is not only based on their established efficacy but also their suitability for paediatric treatment and compatibility with selected excipients and experimental processing techniques.

1.3. DRUG DELIVERY TECHNOLOGY APPLIED IN THIS STUDY

The pharmaceutical formulation of choice for this study is one-of-a-kind that is specifically designed for young children, thus, an oral delivery system in the form of a liquid nanosuspension was chosen. The process included three key phases: first, the nanoencapsulation (primary encapsulation) of the active drugs (abacavir and lamivudine); second, the synthesis of a pharmaceutical gel which functioned as the diluent and final a secondary encapsulation stage that involved the incorporation of the drug loaded nanoparticulates into the fluid pharmaceutical gel matrix by gentle physical agitation to produce the nanosuspension formulation. With the nanosuspension being a dual drug delivery system of two antiretroviral agents, the first phase entailed the separate polymeric nanoencapsulation of abacavir and lamivudine to minimize systemic toxicity that are associated with drugs (A. Kumari et al., 2014) as well as reduce potential physical and chemical incompatibilities (between these bioactive compounds) which could lead to formulation instability and decreased bioavailability of the active ingredients (Wilkins et al., 2024). In other words, this initial drug nanoencapsulation process is targeted at improving the compatibility of the combined active drug substances and the overall nanosuspension formulation

stability (Kumari et al., 2022). The second phase encompassed the creation of a polymer-based pharmaceutical gel, which was fluid in nature and thus served as the diluent, carrier for the palatability enhancers and preservative as well as the secondary encapsulant for the abacavir and lamivudine nanopowders to further shield/preserve the drug nanopowders to enhance formulation instability while also improving biocompatibility. In the final phase, the abacavir and lamivudine nanopowder and the fluid gel were physically combined under mild agitation to produce the dual drug delivery system herein referred to as the fixed dose nanosuspension formulation.

All the excipients used in this study were biocompatible and biodegradable and were carefully selected from the widely utilized United States Food and Drug Administration (US FDAS) list of Generally Recognised as Safe (GRAS) pharmaceutical excipients. Briefly, for the nanoencapsulation process, polyvinyl alcohol and polyvinyl pyrrolidone were employed as stabilizers to prevent particle aggregation. Kollidon CL-SF was used as a disintegrant, lactose as a bulking agent and sodium chloride as a salting out agent. The synthesis of the fluid pharmaceutical gel required the use hypromellose (hydroxypropyl methylcellulose), methylcellulose and gelatin as the gelling agents and viscosity modifiers, sodium starch glycolate served as a dissolution enhancer/suspending agent, polyethylene glycol as co-solvent for water and plasticizer, polyvinyl alcohol acted as an additional surfactant and solubilizer, xylitol as sweetener/palatability enhancer and sodium benzoate as preservative. More details about these pharmaceutical additives are provided in subsequent chapters.

1.4. STUDY DESIGN

This research project began with a systematic review of the existing literature regarding HIV treatments, focusing specifically on commercially available fixed dose combination drug product for the paediatric population. Following the identification of the gap between adult and paediatric fixed dose formulations where there are significantly fewer marketed products presented in appropriate dosage forms for the paediatric population, the treatment guidelines for paediatric HIV were thoroughly reviewed to inform the selection of appropriate antiretroviral drugs for suitable pharmaceutical formulation development. Subsequently, an oral liquid formulation was developed using nanotechnology to encapsulate the drugs and a pharmaceutical gel to physically disperse the nanoencapsulated drugs to produce a nanosuspension. This strategy allows for easy reconstitution by providing a ready-made fluid gel to function as the diluent for the nanosuspension formulation thereby eliminating the need to use the conventional diluent, water thereby preventing contamination, improving environmental stability and maintaining formulation quality/wholeness.

Furthermore, several methods of synthesizing nanoparticles were reviewed, and the salting-out technique which involves the use of water and toxic organic solvent, as described by Konan et al. (2002), was adapted with modifications to suit the specific needs of this project. Specifically, this investigation made use of the highly beneficial 'green synthesis' approach (Singh et al., 2018; Huston et al., 2021) by excluding the use of harmful chemical organic solvents by retaining water, a more environmentally friendly option (Singh et al., 2018), as the sole solvent for the modified salting out technique used to produce the drug loaded nanopowders. Abacavir was nanoencapsulated in a polyvinyl alcohol (PVA)/polyvinylpyrrolidone (PVP)/lactose/Kollidon CL-SF multipolymeric blend, while Lamivudine was encapsulated in a PVA/lactose co-polymeric

blend using a modified salting out technique. Both nanoparticles were fabricated separately, and their physicochemical characteristics were determined. Using Transmission Electron Microscopy (TEM) coupled with the ImageJ software, the nanoparticle size and shape measurements were achieved, and then Dynamic Light Scattering (DLS) was employed to confirm the hydrodynamic dimensions of the particles, while Scanning Electron Microscopy (SEM) was utilized to assess the particles' surface morphologies. Drug content analysis employing Ultraviolet (UV) Spectroscopy was used to determine the encapsulation efficiency and drug loading efficiency of the nanopowders and their flow properties in the anhydrous state was quantified using the bulk and tapped density method. To assess the long-term stability of the drug loaded nanopowders, fluid pharmaceutical gel and the nanosuspension formulation, environmental stability studies were conducted following the International Conference on Harmonization (ICH) standard methods for stability testing.

Subsequently, the pharmaceutical gel, intended for the secondary encapsulation, dispersion and palatability enhancement of the drug loaded nanopowders was developed using a combination of swellable, gel-forming polymeric excipients. A selection of excipients was made based on their ability to form stable and biocompatible fluid gels appropriate for both abacavir and lamivudine. The gel preparation process involved the use of water in combination with suitable polymeric biomaterials such as carboxymethyl cellulose, gelatin and methylcellulose. The production and optimization of the fluid pharmaceutical gel variants were systematically facilitated using the Plackett-Burman design of experiments computational approach employing the Minitab® Statistical Software (Version 21.1.0, Minitab LLC, State College, PA, USA). This methodical optimization strategy used to identify the most influential physicochemical factors from a set of variables that influences the formulation/product performance (Ekpenyong et al., 2017). The

optimization process focused on the overall physical appearance of the pharmaceutical gel, including homogeneity**,** flow properties**,** gel strength**,** and pH. Once the gel was optimized, it was characterized for its rheological properties such as viscosity, and SEM analysis performed to elucidate the gel's microstructure. The final optimized gel was further characterized for its physicochemical and physicomechanical properties such as gel strength, pH, physical appearance, viscosity and stability, ensuring that it remained suitable for the nanosuspension formulation development.

To produce the fixed dose antiretroviral nanosuspension formulation, the nanoparticulate drug carriers (nanopowders) were then dispersed/suspended into the optimized fluid pharmaceutical gel, to produce a stable liquid nanosuspension. The final nanosuspension formulation contained 40 mg of abacavir and 20 mg of lamivudine per 5mL and it characterized by determining its drug content**,** physicochemical properties (e.g., color, pH and smell)**,** and environmental stability over time. Stability testing was carried out under controlled temperature, humidity and light conditions as described under the guidelines provided by the ICH. Physicochemical quantities namely drug content, physical properties like colour, smell, pH changes and textural properties of the nanosuspension formulation were all evaluated as indicators of stability to determine the quality of the formulation after storage over a specified duration. Although, there are no commercialized abacavir/lamivudine nanosuspensions, some of its properties were compared with three commercially available suspension-like oral liquid formulations to determine any significant similarities or differences. Additionally, in vitro cytotoxicity studies were conducted to evaluate the biocompatibility of the formulation using a representative human cell line, and the in vitro drug release behaviour was studied to assess the formulation’s ability to completely release both drugs

relative to the unformulated drug. Drug-excipient compatibility was also investigated using the Fourier transform infrared spectroscopic method by analysing the chemical composition of the nanosuspension, placebo and unformulated drug to identify any anomalies and irreversible interactions. The schematic presented in figure 1.3. summarises the different phases of this study design.

1.5. WORKING PRINCIPLES OF THE PROCEDURES AND TYPES OF EQUIPMENT USED

1.5.1. Fourier Transform Infrared Spectroscopy

Fourier Transform Infrared Spectroscopy (FTIR) examines how matter interacts with electromagnetic radiation, producing a characteristic spectrum for each molecule. This unique "spectral fingerprint" allows FTIR to distinguish between different molecular structures (Fadlelmoula et al., 2022). It relies on the vibrations of atoms. Infrared spectroscopy examines the vibrations of molecules. Different parts of a molecule, called functional groups, absorb infrared light in specific ways. These patterns aid in the identification of which groups are present in a molecule (Berthomieu & Hienerwadel, 2009). The technique is widely used to identify unknown substances and assess the quality and quantity of components within a sample. (Tkachenko & Niedzielski, 2022). FTIR is also valued for its simplicity and effectiveness in detecting physical or chemical variations in drug–excipient mixtures (Segall, 2019).

1.5.2. Dynamic Light Scattering and Electrophoretic Light Scattering

Dynamic Light Scattering (DLS), also known as photon correlation spectroscopy or quasi-elastic light scattering, is a technique used to measure the size of particles or macromolecules in a solution.

It works by analyzing how particles move randomly (Brownian motion) due to collisions with molecules in the surrounding liquid. The speed of this movement depends on the size of the particles, the temperature, and the viscosity of the solvent. In general, smaller particles move faster, while larger particles move more slowly. DLS can estimate their size by observing how particles shift positions over time. In a solution where all particles are roughly the same size (monodisperse), the signal produced changes in a simple, predictable way. However, in mixtures with particles of different sizes (polydisperse), the signal is more complex. It represents a combination of different movement rates, each contributing to the overall pattern (Stetefeld et al., 2016).

Zeta potential, an important indicator of the stability of colloidal dispersions, is commonly measured using electrophoretic light scattering (ELS). In this method, a voltage is applied across two electrodes placed at opposite ends of a cell containing the particle suspension. The charged particles move toward the electrode with the opposite charge, and their speed is measured as electrophoretic mobility, which reflects how fast they move per unit electric field. The measured mobility is converted to zeta potential using Henry's equation, which relates particle movement in a fluid to their surface charge (Kaszuba et al., 2010).

1.5.3. Scanning Electron Microscopy (SEM) and Transmission Electron Microscopy (TEM)

Transmission Electron Microscopy (TEM) uses a high-energy electron beam to view the internal structure of very thin samples. Electrons are generated by heating a tungsten filament and focused onto the specimen using magnetic lenses. As the beam passes through the sample, some electrons are scattered while others transmit through, depending on the density and composition of the material. Heavier atoms scatter electrons more, creating contrast in the image. The transmitted

electrons form a highly magnified, black-and-white image on a fluorescent screen or digital camera. TEM allows visualization of fine internal details such as organelles, protein structures, and even individual atoms under special conditions (Kannan, 2018).

Scanning Electron Microscopy (SEM) uses a focused beam of high-energy electrons to scan the surface of a sample. Electrons are generated by an electron gun (often using a tungsten filament) and accelerated to energies typically between 0.1–30 keV. The beam is focused on a small spot using electromagnetic lenses. When the electron beam hits the sample, it interacts with the surface layers, generating signals such as secondary or backscattered electrons. These signals are detected and converted into an image. The image contrast depends on the type and amount of signal collected, which relates to the sample's surface structure and composition (Chen et al., 2015).

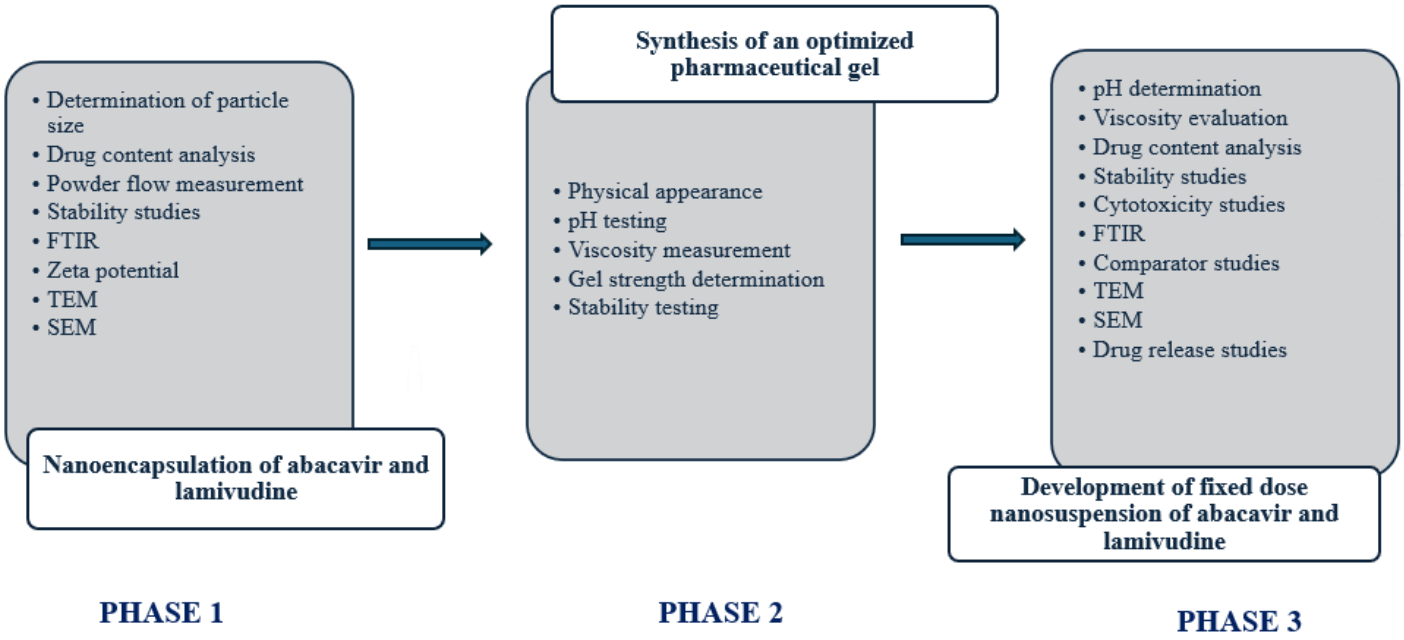

Figure 1.2. An illustration of the study design.

1.5. RESEARCH AIM AND OBJECTIVES

This project aims to design an orally delivered, reconstitutable nanosuspension formulation containing a fixed dose combination of two core antiretroviral drugs, Lamivudine and Abacavir. This oral drug delivery system is intended to reduce regimen complexity, allow water-free and manageable reconstitution, and facilitate easier administration for both children and their caregivers, as well as applicability in adolescents, adults, and the elderly who prefer liquid formulations to solids or individuals having trouble swallowing. The work seeks to enhance formulation stability, improve palatability and patient acceptance, enable easy reconstitution by decreasing the added complexity and risk of contamination from the need to reconstitute with water, which is typically non-potable due to water insecurity in low-income areas where the incidence of HIV is generally highest (Nagata et al., 2022). In other words, the fluid pharmaceutical gel serves as a stable, ready-to-use diluent which aids patient convenience, compliance and environmental stability and eliminate the typical need for refrigeration of liquid formulations of anti-infective agents (Al-Ramahi et al., 2015; Mack et al., 2021) thus improving delivery and storage in third world countries where infectious disease such as HIV/AIDS are prevalent. Additionally, this innovative approach aims to address the issue of shortages for the paediatric population and medication burden by adding to the range of available antiretroviral formulations for special populations (e.g., neonates, infants, children). The following objectives are therefore planned to accomplish the specific project aim described here:

Objective 1: To select appropriate biocompatible and biodegradable polymeric and non-polymeric excipients for the nanoencapsulation of the selected antiretroviral drugs and synthesis of the fluid

pharmaceutical gel carrier system to ensure formulation stability and suitability for the special populations targeted

Objective 2: To separately prepare drug-loaded nanopowder employing a modified salting out technique and the fluid gel systems using wet milling and mechanical agitation

Objective 3: To optimize the pharmaceutical gel carrier system using the computer aided Plackett Burman design of experiments approach

Objective 4: To determine the physicochemical properties of the abacavir/lamivudine nanoparticles such as particle size, zeta potential, morphology, drug loading efficiency and encapsulation efficiency, powder flow, structural integrity, and particle morphology employing suitable scientific characterization procedures

Objective 5: To measure the characteristics of the optimized fluid gel by assessing its physicomechanical and physicochemical properties such as viscosity, visual homogeneity, microscopic structure, gel strength (textural) and pH

Objective 6: To develop and characterize the fixed dose nanosuspension by assessing its drug content, drug release behaviour, pH, and surface morphology, and structural elucidation of the drugs

Objective 7: To evaluate the short-term stability of the drug loaded nanopowders, optimized fluid gel and final nanosuspension formulation under varying environmental conditions to determine its potential shelf life and appropriate storage condition(s)

Objective 8: To assess the *in vitro* cytobiocompatibility of the synthesized nanosuspension formulation under biorelevant conditions utilizing the human hepatocellular carcinoma G2 (HepG2) cells

1.6. CLOSING REMARKS

This chapter covered the general background of HIV/AIDS and detailed the research rationale by describing the current advancements in the treatment of HIV infection, particularly in the paediatric population. The general overview of the study design including the research aim and objectives and experimental methods employed, were also discussed. The next chapter will provide more detailed information on HIV/AIDS, its epidemiology and treatment as well as a comprehensive overview of nanomedicine and fluid pharmaceutical gels as innovative drug carriers useful for disease pharmacotherapy.

CHAPTER 2: LITERATURE REVIEW

2.0. OVERVIEW OF THE DISEASE

The human immunodeficiency virus (HIV) is a viral infection that specifically targets and weakens the immune system of the human body specifically the cytotoxic (CD4) T cells which are responsible for fighting off several illnesses and diseases, resulting in the weakening of the immune system and making the infected individuals more susceptible to various kinds of diseases such as tuberculosis, and certain types of cancer (e.g., cervical, lung) that healthy people are generally immune to. If left untreated for a long time, HIV can progress to the most advanced stage, known as acquired immunodeficiency syndrome (AIDS) (WHO, 2023).

The human immunodeficiency virus belongs to the retroviridae family and the lentivirus genus. The retroviridae family is distinct from other viruses due to their process of reverse transcription, where the ribonucleic acid (RNA) genome is converted into deoxyribonucleic acid (DNA) and integrated into the host's genome, which leads to lifelong infection (Swinkels et al., 2024). The life cycle of HIV begins when the virus uses glycoprotein on the surface of its structure to bind to the host's CD4 T cells receptor facilitated by the chemokine coreceptors 5 and 4 (CCR5) (CXCR4), which are present on the host cellular membrane. Once the virus attaches itself to the host cell, the reverse transcriptase enzyme begins reverse transcription, using the host transfer RNA (tRNA) as primers. Afterwards, the virus's newly synthesized DNA is integrated into the host's DNA with the integrase protein and continues to replicate (Swinkels et al., 2024). After infection, HIV can produce about 10 million to 10 billion new viral cells every day and significantly reduces the lifespan of CD4 cell and their number begins to decline continuously

while the virus increases making the host more vulnerable to infections due to immunological failure (Wilkins., 2020).The acquired immunodeficiency syndrome (AIDS) is the most advanced phase of this disease resulting from a prolonged lack of treatment. It is characterized by a very high viral load and severely damaged immune system. Individuals with AIDS may easily transmit the disease and have high risk of acquiring opportunistic infections (WHO, 2023).

The human immunodeficiency virus is known to be transmitted through infected bodily fluids such as blood, semen, rectal and vaginal fluids and breast milk (Brandt et al., 2017). HIV must enter the bloodstream through contact with a mucous membrane (e.g. rectum, mouth, vagina, and penis) or open cuts, sores etc. for transmission to happen. There are three ways in which HIV is primarily transmitted from one person to another: (i) through sexual intercourse without appropriate protection with an infected individual; (ii) sharing needles, syringes or other sharp objects with an infected individual and (iii) through vertical transmission from an infected mother to her child either during pregnancy, delivery or breastfeeding. However, HIV cannot be transmitted through certain bodily fluids such as saliva, tears, sweat or casual human contact like hugging, shaking hands, or sharing public spaces like swimming pool toilet seats or food utensils (National Institute of Child Health and Human Development., 2021).

The progression of HIV is long and complex, starting from the point of transmission and infection to the eventual end-stage disease. HIV infection can be categorized into three stages, the first being acute infection, which typically occurs within the first few weeks to months of HIV infection. This stage is characterized by a high viral load and acute damage to the immune system and can clinically present with symptoms such as sore throat, nausea and vomiting, night sweats, rash, and

others. These symptoms are usually mild and typically resolve in most patients within one to three weeks. Following the acute infection phase, there is an asymptomatic phase typically lasts for several years. During this phase, viral replication continues persistently, and CD4 cell counts gradually decrease. Symptoms that may appear include lymphadenopathy (swollen lymph nodes). Finally, the last stage of HIV infection is AIDS where the immune system is highly compromised making the infected individual susceptible to opportunistic infections such as tuberculosis and tumors (Chinese Medical Association., 2022).

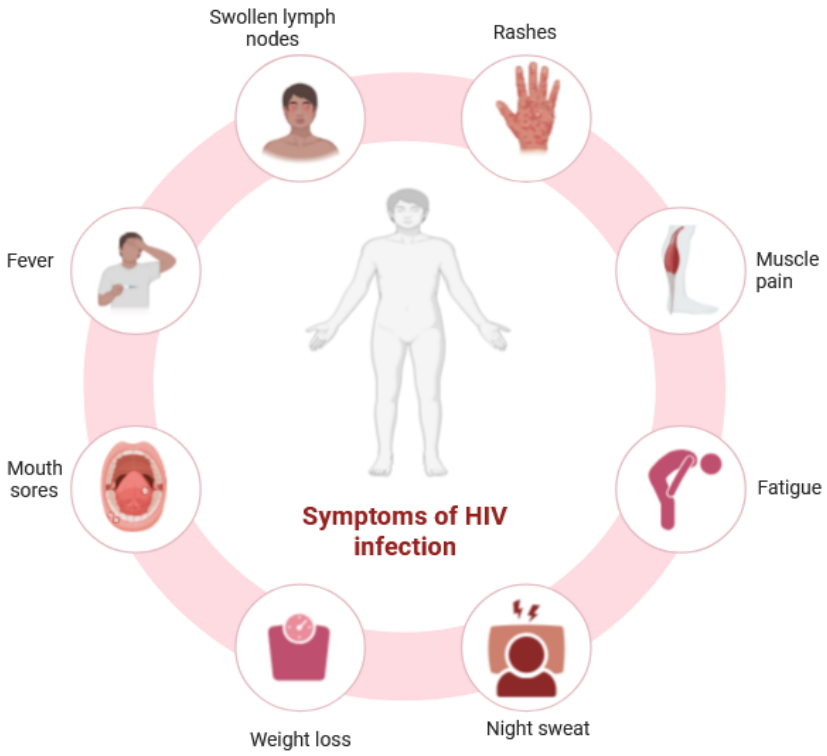

Figure 2.1. Symptoms of HIV infection (created with BioRender.com)

According to the World Health Organization (WHO), the human immunodeficiency virus continues to be a major public health concern worldwide with an estimated number of 39.9 million people living with HIV at the end of 2023 and about 40 million lives claimed by this infectious disease since the beginning of the epidemic (WHO, 2023). In 2023, out of the approximate 40 million global HIV cases, about 2.3 million were children aged 0 to19 years old. Every day, around 685 children contracted HIV, and approximately 250 children died of AIDS-related causes, primarily due to insufficient access to HIV prevention, care, and treatment services (UNICEF, 2024). Although HIV/AIDS remains a global concern, it is most prevalent in resource-limited settings such as sub-Saharan Africa and parts of Asia. Sub-Saharan Africa, which makes up only 2% of the global population, accounts for one-third of the world's HIV infections. However, in recent years, there has been an increasing prevalence of HIV in some European countries, such as Portugal and Spain, as well as in the United States. Significant progress has been made in addressing the HIV pandemic, with a decline in the incidence of HIV and AIDS-related mortality in many countries, largely due to the widespread use of antiretroviral therapy and efforts to prevent both vertical (mother-to-child) and non-vertical transmission of HIV. Despite these improvements, there is still substantial evidence of perinatal transmission, with approximately 4 million children having been infected worldwide (Govender et al., 2021).

Children living with HIV need to start ART immediately to ensure proper growth and development into adolescence and adulthood. However, children under 5 years are less likely to be diagnosed and initiated into treatment compared to older individuals, while those not receiving ART have a high mortality rate. Additionally, studies have shown that the lack of child-friendly formulations poses a barrier to ART adherence in neonates and infants, leading to a lack of virological

suppression in this population. Therefore, developing child-friendly ARV formulations will simplify medication administration for caregivers and make it easier for children to take their medications. This will improve adherence, which is essential for their healthy growth and development (Schlatter et al., 2016; Agathis, 2023; WHO, 2024).

2.1. CLASSIFICATIONS OF ANTIRETROVIRAL DRUGS

There is no known cure for the Human Immunodeficiency Virus (HIV) infection yet. However, the management of HIV has come a long way from the approval of the first antiretroviral (ARV) drug, zidovudine, in 1987 to the introduction of multi-drug therapy known as antiretroviral therapy (ART). The introduction of ART revolutionized the management of HIV; it decreased the incidence of acquired immunodeficiency syndrome (AIDS), mortality rates, improved quality of life, and reduced the risk of transmission. ART typically consists of a combination of at least three or more ARVs in two or more different classes, and the drug combinations vary depending on factors like comorbidities and coinfections, potential for drug-drug interaction, drug resistance, viral load, and CD4 cell count (Foka & Mufhandu, 2023).

Along with several non-pharmacological strategies, ARVs are being used in healthy individuals as a preventive measure in either pre-exposure prophylaxis or post-exposure prophylaxis, otherwise known as PrEP and PEP, respectively. PrEP involves the use of at least two ARVs in individuals at high risk of contracting HIV, such as adults or adolescents who are sexually active with more than one partner or whose partner is HIV positive, people who inject illegal substances, etc., to prevent transmission of the disease. Several studies have shown that the risk of HIV infection decreases by 92% with PrEP compared to placebo. However, its effectiveness is highly dependent on

consistent use. PEP, on the other hand, refers to the use of ARVs for a short period (usually 28 days) after a confirmed or suspected exposure to HIV, preferably within the first 72 hours (Huynh et al., 2024). Furthermore, ARVs can also be used to prevent the vertical spread of HIV due to their ability to suppress viral replication, thus lowering the risk of maternal transmission. ARVs can also be given to newborn babies whose mothers are HIV positive to prevent them from contracting the disease (Cardenas et al., 2023).

There are six main classes of antiretroviral drugs, and they are classified according to their method of inhibiting viral replication and are discussed below:

2.1.1. Nucleoside Reverse Transcriptase Inhibitors (NRTIs)

Zidovudine was the first antiretroviral drug to be discovered, which demonstrated the inhibition of HIV replication. This activity was carried out by the triphosphate metabolite of zidovudine through the selective inhibition of the virus' reverse transcriptase enzyme, which is crucial for HIV replication (Cihlar & Ray, 2010). The reverse transcriptase enzyme is responsible for the transcription of viral RNA into the host's DNA, allowing the virus to reproduce. Thus, the introduction of NRTIs prevents the increase in viral multiplication by blocking this important step of the HIV life cycle. This class of antiretrovirals is considered very important in the treatment regimen of HIV infection, and a combination of two drugs from this class is recommended for every current treatment of HIV-infected individuals. Antiretroviral drugs that belong to this class are zidovudine, tenofovir, abacavir, lamivudine, emtricitabine and didanosine (Tressler & Godfrey, 2012).

2.1.2. Non-Nucleoside Reverse Transcriptase Inhibitors (NNRTI)

The mechanism of NNRTIs to inhibit the replication of HIV is not fully understood; it is, however, generally believed that they act by binding to the drug-binding pocket of the HIV reverse transcriptase enzyme, which causes a shift in the position of the template primer. This alteration prevents the binding of deoxyribonucleotide triphosphates (dNTPs), thus inhibiting the formation of a functional RT-DNA-dNTP complex. NNRTIs share drug binding pockets, which makes them prone to cross resistance due to the development of mutations in the HIV strains; this is especially noteworthy among first-generation NNRTIs such as nevirapine and delavirdine because they have a low genetic barrier to resistance, meaning they can develop resistance quickly. However, newer NNRTIs such as rilpivirine and doravirine have a higher genetic barrier (i.e. they do not develop resistance quickly), making them effective against HIV strains that are resistant to earlier NNRTIs (Y. Wang et al., 2019). The distinct antiretroviral action, high specificity, and low toxicity of NNRTIs make them a valuable component in ART in combination with NRTIs (Vanangamudi et al., 2020).

2.1.3. Protease Inhibitors (PI)

Protease is an essential protein for HIV maturation, and protease inhibitors act by blocking the active site of the HIV protease, which disrupts the maturation of the virus and prevents it from becoming fully infectious. Protease inhibitors are crucial elements of antiretroviral therapy as they have been associated with lower resistance levels compared to NNRTI-based regimens. However, they are commonly linked to several adverse effects, including dyslipidemia, insulin resistance, lipodystrophy, lipoatrophy, and increased risk of cardiovascular and cerebrovascular diseases. Additionally, studies have shown that there is no significant difference in the adverse events

between PI monotherapy and combination with integrase inhibitors or NRTIs, which suggests that PIs may be primarily responsible for the most severe side effects. Drugs that belong in this class include saquinavir, indinavir, ritonavir, atazanavir, duranavir, lopinavir etc (Lv et al., 2015).

2.1.4. Integrase Strand Transfer Inhibitors (INSTI)

INSTIs have significantly improved the treatment of HIV. They act by targeting the integration step in the HIV life cycle, which is very important for ensuring permanent infection. This process is carried out by the integrase enzyme, which is produced by the HIV genome. The integrase enzyme facilitates the reactions needed to insert the reverse-transcribed HIV DNA into the host cell's DNA. The first INSTI was approved in 2007, which makes them a relatively new group compared to NRTI, NNRTI, and PI. At present, four INSTIs are approved for use in the treatment of naïve individuals with HIV, which include the first-generation raltegravir and elvitegravir, and second-generation dolutegravir and bictegravir, with the newest addition being cabotegravir. Second-generation INSTIs are globally preferred as first-line treatment for HIV naïve patients as several clinical studies report that they are superior to NNRTI and PI treatment regimens. INSTIs demonstrate a high genetic barrier to resistance and minimal drug-drug interaction due to its primary metabolism by uridine diphosphate glucuronosyltransferase (UGT) 1A1; they exhibit excellent viral suppression rates and have good tolerability (Zhao et al., 2022).

2.1.5. Fusion Inhibitors

HIV fusion inhibitors prevent the virus from merging with the host cell, thereby reducing cellular damage (Wang et al., 2019). They act by binding to the virus's envelope protein, preventing the structural changes needed for the virus to fuse with the host's CD4 cell. Without the ability to enter

the host cell and start an infection, HIV cannot replicate inside the host cells **(Yusuf Aliyu & Adeleke, 2024).** Several fusion-inhibiting peptides have demonstrated potent antiviral activity, their short half-life and their susceptibility to drug resistance make them clinically inadequate (Wang et al., 2019).

2.1.6. Post-Attachment Inhibitors

Post-attachment inhibitors work by blocking the receptors on the surface of the cytotoxic T-cells and preventing HIV from binding to the CD4 receptor, which is important for the virus to enter the cell and continue its life cycle. Thus, they disrupt the virus's replication process, as it needs to enter the CD4 cells to replicate. Fostemsavir is an example of a drug in the treatment of HIV belonging to this class **(Yusuf Aliyu & Adeleke, 2024).**

2.2. TREATMENT GUIDELINES FOR ANTIRETROVIRAL THERAPY

It is recommended that antiretroviral therapy be started as soon as possible after diagnosis, preferably within seven days, and ideally on the same day as the diagnosis or at the first clinical visit if the patient is ready. Before the initiation of treatment, several essential laboratory tests are to be carried out, such as viral levels, CD4 cell count, ART resistance, and any potential co-infection or opportunistic infections. If an individual tests positive for an opportunistic infection, ART should be initiated within two weeks after starting treatment for most opportunistic infections (Gandhi et al., 2024). Current HIV treatment involves a daily oral regimen of three antiretroviral drugs. This typically includes two NRTIs and a third agent, which may be an INSTI, NNRTI, or PI. These treatment regimens are highly effective, convenient, and generally well tolerated, and

they help HIV infected individuals maintain a normal life expectancy and reduce the risk of HIV transmission (Phanuphak & Gulick, 2020).

Several factors influence the selection of suitable antiretroviral agents. Thus, the recommendation of initial ART regimens for all individuals with HIV should prioritize optimal regimens that offer a high rate of viral suppression, minimal toxicity, low pill burden, and low risk of drug interaction. On that note, factors such as cost and access to healthcare play a significant role. In cases involving active opportunistic infections, the choice of ARVs follows the general principles of starting treatment while also considering potential drug-drug interactions with the medications used to treat or prevent opportunistic infections (Saag et al., 2020). For instance, many individuals who are coinfected with HIV and tuberculosis, a very common opportunistic infection in HIV patients, require simultaneous treatment with ARV and anti-TB medications, which improves survival but also presents certain challenges, such as drug interactions. For instance, rifampicin, an antitubercular drug, is a cytochrome P450 enzyme inducer, and certain NNRTIs, including rilpivirine, doravirine, etc., are primarily metabolized by CYP3A4. When combined with rifampicin, the concentrations of these ARVs are significantly reduced to the point where they should not be used together (Pooranagangadevi & Padmapriyadarsini, 2022). Drug resistance and the patient's age are important factors in determining the appropriate antiretroviral agents (Saag et al., 2020).

In paediatric patients, the same regimen recommendations, such as starting therapy immediately after diagnosis regardless of age or weight, are applied. The choice of ART, however, should be personalized based on current guidelines and patient-specific factors such as age, body weight,

cognitive development, and other factors that can affect adherence such as the ability to swallow pills or tolerate unpleasant taste. Recommendations should also consider the convenience of administration for the patient and their family (i.e., caregivers) along with the most up-to-date information on efficacy and safety (Lim et al., 2021). For instance, tenofovir disoproxil fumarate has been linked to a higher risk of bone loss compared to other NRTIs like abacavir and low bone mass has been observed in the paediatric population particularly those with perinatally acquired HIV and therefore, should be avoided in these groups (Shiau et al., 2020). Overall, the complexity of this population highlights the need to tailor every patient's ARV selection to ensure that both the patient and their family can effectively adhere to the treatment to achieve optimal viral suppression (Lim et al., 2021).

Although two-drug regimens in the early days of HIV treatment did not meet expected efficacy and safety standards, research interest in these therapies has persisted. This is primarily due to their potential to reduce long-term therapy exposure, minimize specific drug toxicities, and lower overall treatment costs. As a result, several randomized trials have been conducted to assess the viability of various dual-drug therapies. While some two-drug regimens have failed to meet the desired efficacy or safety outcomes in early studies, others have shown virological non-inferiority compared to standard three-drug treatments. This success has led to the inclusion of the first long-acting antiretroviral regimen, consisting of two drugs, in treatment guidelines (Gibas et al., 2022).

2.3. CURRENT TRENDS IN ANTIRETROVIRAL FORMULATIONS

Adherence to antiretroviral therapy is a crucial factor in determining the effectiveness of HIV treatment, and as such, several research studies have been dedicated to improving patient

adherence to antiretrovirals. From a pharmacotherapeutic point of view, simplifying regimens and improving their tolerability are key strategies to enhance optimal adherence. In that regard, the simplification of ART regimens with fewer pills and less frequent dosing has been shown to improve ART adherence, thus, effective viral suppression and improved patient outcomes.

Figure 2.2. Description of fixed dose combination (created with BioRender.com)

This was achieved with the development of single-tablet regimens (STRs) containing fixed dose drug combinations, which have been linked to better adherence compared to multi-tablet regimens (MTRs) (Caplan et al., 2018). Fixed dose combinations (FDCs) combine multiple drugs into a single dosage form with specific doses, and an STR is a type of FDC that includes drugs from two or more classes, which effectively serves as a complete regimen for HIV treatment. Over the past years, advances in FDCs in the treatment of HIV have significantly transformed antiretroviral therapy. Modern ART regimens no longer require patients to take numerous pills at various intervals throughout the day. Instead, many regimens can now be taken as a once-daily STR (Caplan et al., 2018; Kim & Weon, 2021).

The latest innovative approach to the treatment and prevention of HIV/AIDS is a long-acting injectable formulation, which the FDA approved in January of 2021. It consists of two

antiretroviral drugs (cabotegravir and rilpivirine) to be administered either monthly or bi-monthly. Although a typical antiretroviral therapy consists of at least three drugs, clinical trial reports show that the two-drug regimen of the long-acting injectable is as effective in suppressing viral replication as the orally delivered three-drug regimen. Research has shown that HIV patients considered the new therapy more convenient compared to the traditional daily pill(s) regimen. Moreover, due to the private nature of injectables, they will be less likely to face stigma or discrimination as it tackles the challenge of having to pack several bottles of medication(s) for long periods (Pinto et al., 2023). The injectable cabotegravir and rilpivirine is recommended in individuals with no history of treatment failure or known or suspected resistance to either drug, but only after viral suppression has been successfully achieved with oral ART (Gandhi et al., 2024). Unfortunately, the long-acting injectable is not approved for use in children under 12 years (Sherman et al., 2024).

Despite efforts to simplify treatment regimens and improve antiretroviral adherence, newborns and infants face limited antiretroviral therapy options due to their inability to swallow tablets, as most available single-tablet regimens are formulated for adolescents and adults. Paediatric STRs are typically available as dispersible or scored tablets and are recommended as first-line treatment for children aged 3 years or older and weighing at least 25 kg. The only liquid FDC available for young children, particularly neonates and infants, is lopinavir/ritonavir (LPV/r), which comes as an oral suspension for neonates and infants. However, a complete regimen requires two NRTIs in addition to the LPV/r. Other ARV agents are available in different dosage forms such as oral suspensions, powders or chewable tablets, but until children reach the appropriate age (3 years) and weight (25 kg and above) each medication must be administered separately making treatment

cumbersome for the caregivers of such minors. This creates a significant challenge to adherence because complex regimens often lead to missed regimens and subtherapeutic effects (C. Lee et al., 2021). Since FDC therapy offers have been proven to simplify medication administration and improve safety by reducing confusion, the lack of FDC options for young children means they do not benefit from the convenience and improved patient adherence that FDC therapy provides (Wilkins et al., 2024). Given these limitations, addressing the gap in age-appropriate formulations is imperative. There is a critical need for the development of more age-appropriate FDC formulations tailored specifically for neonates', infants and young children to ensure they can receive the same benefits of simplified drug regimens and improve access to effective treatment, leading to better adherence, improved health outcomes, and reduced risks of drug resistance which ensures that this underserved population receives the best possible care as adults.

2.4. DRUG DELIVERY SYSTEMS

Drug delivery systems (DDS) are technological systems designed to contain or house drug molecules in appropriate physical forms, such as tablets or solutions, for effective administration. They can be referred to as pharmaceutical formulations, drug carriers, dosage forms, etc. These systems enhance the speed at which drugs reach their intended target sites in the body and improve therapeutic efficacy while reducing unwanted drug accumulation in non-target sites. There are different types of drug delivery systems depending on the intended route of drug administration (e.g., oral, ophthalmic, transdermal, subcutaneous) (Ezike et al., 2023).

Drug delivery systems are crucial in the field of pharmaceutics because the direct use of active pharmaceutical ingredients (APIs) (i.e. drugs, bioactives) in their raw form is not recommended

due to several practical challenges such as difficulty in handling and accurate dosing of highly potent drugs which can be difficult or even impossible without a proper delivery system, in some cases, administering drugs directly into body cavities such as rectal or vaginal routes is impractical due to the possibility of drug degradation, local irritation or injury at the administration site because of the high drug concentration. Additionally, APIs can be sensitive to environmental factors such as light, humidity, temperature, and pH changes, which can compromise their stability and/or efficacy. Furthermore, many APIs have an undesirable taste or smell, which may negatively impact patient compliance. Therefore, to overcome these challenges, APIs are typically prepared with excipients to help in shaping the formulation and aid handling, increase stability during storage and use, mask unpleasant taste, facilitate accurate and convenient dosing, and improve overall patient acceptability and clinical outcomes (Adepu & Ramakrishna, 2021).

Although several delivery systems exist, the selection of the most appropriate route of administration is very important for achieving the desired therapeutic effect. Thus, different factors must be considered when choosing an appropriate route of administration, including the properties of the drug, the condition being treated, and the intended therapeutic timing (Coelho et al., 2010).

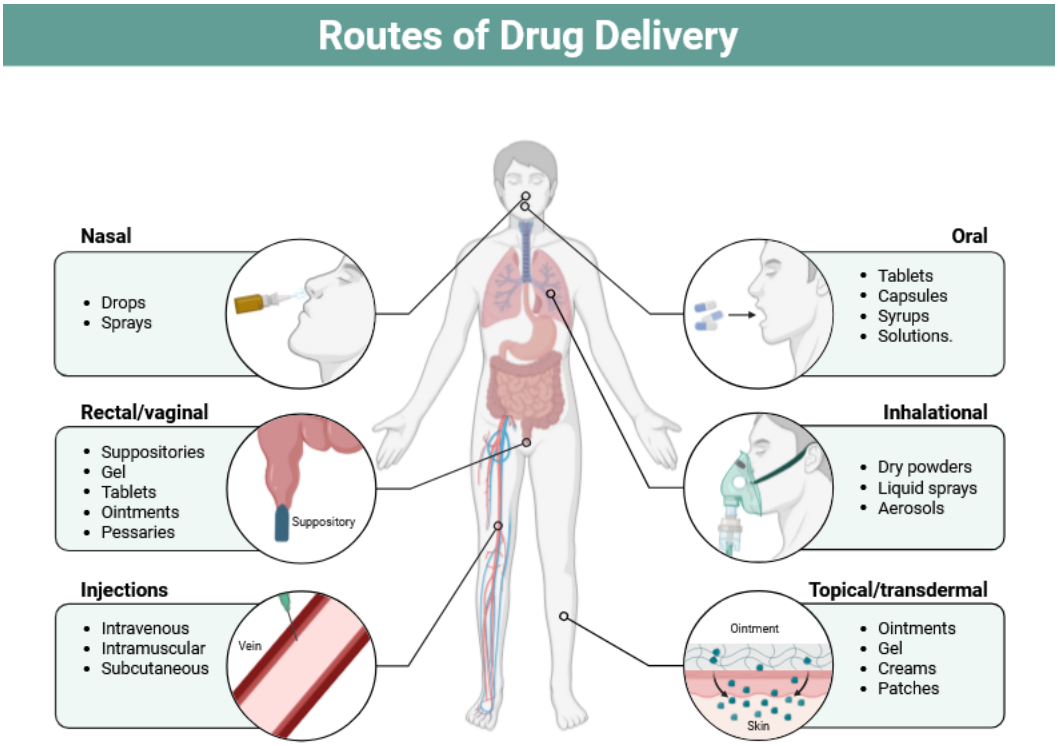

Figure 2.3. Illustration of some common routes of drug administration (image was adapted from Adepu & Ramakrishna, 2021).

Every drug delivery system offers distinct advantages and disadvantages, and in this light, oral delivery systems are the most used administration route due to their numerous advantages. These include convenience, cost-effectiveness, and ease of manufacturing on a large scale, and most importantly, patient compliance with oral formulations is generally higher compared to other parenteral routes like intravenous, subcutaneous, or intramuscular injections, making it the most preferred option for many therapeutic applications (Alqahtani et al., 2021). An oral drug delivery system is a method of administering medications through the mouth, where the drug is absorbed in the gastrointestinal tract. This system is designed to ensure that the drug reaches its intended site of action after passing through the digestive system. Oral drug delivery systems come in

various forms, including solids (e.g., tablets, capsules, powders, etc.) or liquids (e.g., syrups, suspensions, etc.) (Mohammadzadeh & Javadzadeh, 2018). Just like in adults, various routes of administration can be used in paediatric populations, but the oral route is preferred due to its simplicity, convenience, and non-invasive nature. Liquid formulations such as solutions, suspensions, elixirs, syrups, etc., are especially favored for their flexibility in dosing and ease of swallowing. These fluid forms are particularly useful for younger children who may have difficulty swallowing solid forms. The ability to adjust the dose in liquid formulations makes them suitable for the entire paediatric population, from neonates to adolescents (Khan et al., 2022).

2.4.1. Orally Delivered Pharmaceutical Suspensions

Generally, suspensions are a mixture of fine solid particles dispersed in a liquid, usually an aqueous or viscous medium, with the solid particles evenly distributed throughout the continuous phase, otherwise known as the dispersion medium (e.g., the diluent). Oral suspensions are often preferred for paediatric patients, as they address challenges associated with solid medications, such as difficulty swallowing and the risk of choking. Additionally, suspensions improve bioavailability by presenting the drug in a liquid/fluid state, which enhances absorption. They also help mask unpleasant tastes, making them more palatable for children. (Gaikwad et al., 2024). A pharmaceutical suspension is a type of coarse dispersion where the internal phase, made up of insoluble solid particles, is evenly distributed within the external phase with the particles maintained uniformly throughout the complete suspending medium. Oral suspensions can be categorized based on the size of the dispersed particles into colloidal, coarse, or nanosuspensions (Kumar et al., 2016).

2.4.1.1. Ready-Made Versus Reconstitutable Oral Suspensions

Suspensions can be classified as either ready-made or reconstitutable types. Ready-to-use suspensions, as the name suggests, can be administered without the need for reconstitution (Kathpalia et al., 2014), whereas reconstitutable suspensions are distinctive dosage forms designed for either poorly soluble or hydrophilic drugs combined with excipients to create a dry powder or granule. This dry formulation is meant to be mixed with potable water at the point of dispensing to form a suspension for oral administration. This approach helps to address stability issues commonly encountered with other liquid formulations, such as drug degradation caused by prolonged contact between the drug and excipients in an aqueous medium (Rampedi et al., 2023). The reconstitution of dry powder for suspensions typically requires the use of distilled or boiled and then cooled tap water. This process can be inconvenient, negatively impact product stability, and may increase the risk of contamination if potable water is unavailable (Al-Ramahi et al., 2015).

2.4.1.2. Nano-Structured Suspensions (Nanosuspensions)

While many commonly available oral suspensions are microparticulate in nature (i.e., made up of particles that are greater than 1 μm in size), nanosuspensions are colloidal dispersions in which the drug-excipient particles have diameters of less than 1 μm. The key principle behind this technology is to reduce the size of the formulation particles to a submicron level. Nanosuspensions are particularly useful for poorly soluble drugs, offering low toxicity and enhanced chemical stability. Nanoformulations can be given via various routes of administration, including oral, parenteral, pulmonary, etc., delivery (Manoharan et al., 2010). The main advantages of nanosuspensions include their increased dissolution rate and enhanced saturation solubility, which result in improved bioavailability as well as reduced risk of adverse effects. Formulating a drug as a

nanosuspension has also been suggested as a strategy to improve chemical stability compared to solution formulations, as it minimizes degradation that can occur in liquid dosage forms (Malamatari et al., 2016).

The emergence of nanotechnology has opened new possibilities for drug delivery in recent years. A variety of nanoscale devices, such as nanoparticles, nanopowders, etc., have become the most widely used delivery systems at the nanometer scale. These nanoparticles are typically spherical and range from 1 to <1,000 nm. The small size of these delivery systems offers several advantages, including enhanced tissue penetration, prolonged circulation time in the blood stream, improved cellular uptake, etc. Besides, the use of nanocarriers for delivering multiple drugs have gained popularity as they can help reduce toxic side effects, thus improving therapeutic outcomes to a good extent (Manoharan et al., 2010; Tu et al., 2021). Nanotherapeutics often demonstrate higher therapeutic effectiveness compared to traditional micro/macro-configured drug delivery systems because of their small size, large surface area, and the ability to modify their surface. These characteristics contribute to lower toxicity, better bioavailability, improved pharmacokinetics, and better therapeutic outcomes. As a result, nanotherapeutics can address challenges faced by conventional drugs and have the potential to meet future treatment needs in the medical market (Zhang et al., 2020).

Nanoparticles have a high surface area to volume ratio due to their nanoscale size, which enables them to carry large amounts of medication and travel quickly through the bloodstream. This increased surface area enhances their mechanical, magnetic, optical, and catalytic properties, which makes them suitable for a variety of pharmaceutical applications (Haleem et al., 2023).

Polymeric nanoparticles are nanoscale materials that are made from polymers and used in delivering therapeutic agents, in diagnostics, and in biomedical applications (Greenwood, 2023). They have gained significant attention in recent years due to their advantages, which include the protection of drug molecules, controlled release, and specific targeting, all of which contribute to improved therapeutic outcomes. Most of the polymers used for nanoformulation synthesis are biodegradable, which is highly desirable for safety and sustainability. However, the choice of polymer for nanoparticle formulation is generally based on the intended pharmacotherapeutic applications (Manoharan et al., 2010; Crucho & Barros, 2017).

2.4.2. Pharmaceutical Gels/Fluid Gels

Pharmaceutical gels are usually created by thickening a liquid with different excipients capable of producing a gel-like network. They are commonly formulated using gelling agents like hypromellose, carbopol, and others, along with additional ingredients such as stabilizers and antimicrobial agents (Sharma et al., 2022). Fluid gels, also known as sheared gels, are a type of pharmaceutical gel formulation consisting of suspended gel particles formed by applying shear force during the gelation process in biopolymer solutions. These types of gels maintain a pourable, viscoelastic fluid consistency while preserving the gel microstructure within their network, further enhancing their functionality in pharmaceutical formulation (Mahdi et al., 2014).

Fluid gels offer several key advantages in oral drug delivery, such as enhanced viscosity, which improves taste masking, making medications more palatable, especially for paediatric patients. The smooth, viscous texture of fluid gels also facilitates easier swallowing, thus reducing the chances of discomfort or choking. Additionally, the gel structure provides improved stability by

preventing sedimentation and ensuring uniform distribution of the active ingredients. This makes pharmaceutical gels not only safer options but also an effective means of improving patient acceptability and, subsequently, medication adherence and effective pharmacotherapy (Aziz et al., 2022).

In addition to their application in formulations designed for paediatric or geriatric populations by aiding taste masking and ease of swallowing, fluid gels have gained increasing popularity in oral delivery systems because they can be used to modify the release properties of oral liquids, offering controlled or sustained release of the drug (Mohd Shahrizan et al., 2022). For instance, research has shown that they can prevent the premature release of active ingredients in simulated gastric conditions, which shows their potential to achieve sustained release in oral liquids, demonstrating their ability to improve drug release profiles, offering better therapeutic outcomes, especially for young patients (Mahdi et al., 2014). Furthermore, they have been shown to enhance suspension stability and improve the palatability of drugs, which leads to better patient compliance, thus, fluid gels can be used as diluents for reconstitutable suspensions, offering several benefits such as improved stability of the suspension, better drug release profile, and overall improvement of patient experience. (Aziz et al.., 2022).

2.5. CLOSING REMARKS

This chapter has highlighted the global prevalence of HIV and the diverse treatment options available across all age groups, with a specific focus on the challenges faced by paediatric patients. It also provided insight into the challenges faced by paediatric patients that negatively impact their treatment outcome, with a major focus on the limited suitable formulations and the need for more

child-friendly dosage forms that can aid medication adherence in children and subsequently improve therapeutic outcomes. Additionally, the chapter discussed the potential of innovative drug delivery systems, particularly nanosuspensions using nanotechnology and pharmaceutical gels, to address these challenges. Enabling fixed dose combination formulations that could help bridge the current gap in paediatric HIV treatment options. The next chapter will explore the materials and methods used in this project to develop and evaluate an ARV nanosuspension formulation, aiming to further advance the therapeutic landscape for paediatric patients.

CHAPTER 3: MATERIALS AND METHODS

This chapter provides a detailed account of the methods employed to synthesize and characterize abacavir and lamivudine nano-based suspensions. The methodology is structured into three key phases. Phase 1 focuses on the preparation of placebo formulations and the nanoencapsulation of abacavir and lamivudine, alongside the experimental techniques used for their characterization. Phase 2 outlines the development of the pharmaceutical gel and includes the characterization of the optimized gel formulation. Finally, Phase 3 details the synthesis and characterization of the fixed dose combination suspension of abacavir and lamivudine.

3.0. MATERIALS USED

Sodium chloride (certified ACS crystalline) was purchased from Fisher Chemical (Ottawa, Canada). Kollidon® CL-SF and Kollicoat® IR (polyethylene glycol/polyvinyl alcohol) were obtained from BASF (Ludwigshafen, Germany). Lactose monohydrate (laboratory grade) was sourced from Ward's Science (Mississauga, Ontario, Canada). Fully hydrolyzed polyvinyl alcohol (molecular weight = 60,000) and hydroxyethyl cellulose were supplied by Sigma-Aldrich (Darmstadt, Germany). Polyvinylpyrrolidone (molecular weight 10,000) and methyl cellulose (4000 cPs viscosity) were purchased from Thermo Scientific (Mississauga, Ontario, Canada). Sodium starch glycolate and hydroxypropyl methylcellulose were acquired from Spectrum Chemical Manufacturing Corporation (Gardena, CA, USA). Abacavir and lamivudine were sourced from BOC Sciences (Shirley, NY, USA). Food-grade gelatin, citric acid, and sodium benzoate were obtained from Elo's Premium (Toronto, Canada). Food grade xylitol was sourced from NOW® (Ontario, Canada). Phosphate-buffered saline (PBS) and hydrochloric acid were

acquired from Sigma-Aldrich (Missouri, USA). Human hepatocellular carcinoma cells (HEPG2 cells, lot 70044360) were obtained from the American Type Culture Collection (ATCC, Manassas, VA, USA). MEM/EBSS culture medium (lot AK30767270), MEM non-essential amino acids (lot AJ30738460), L-glutamine, 200 mM (lot AH30021570), Penicillin 10,000 U/ml, streptomycin 10,000 µg/ml (lot J220009), trypsin EDTA 0.25% (lot J220037), and phosphate-buffered saline (PBS), no Mg and Ca, 0.0067M, were all supplied by Avantor, Hyclone™ (Utah, USA). Fetal bovine serum (FBS, lot 2385094RP) was obtained from Thermo Fisher Scientific, Gibco (Burlington, ON, Canada). Trypan blue, 0.4% (lot RNBK8799), Dextran (lot BCCF4787), and Triton X-100 (lot SLCJ6163) were sourced from Sigma-Aldrich (Oakville, ON, Canada). The CellTiter-Glo assay kit (lot 0000543560) was procured from Promega (Madison, WI, USA).

3.1. EXPERIMENTAL PHASE 1 — SYNTHESIS AND CHARACTERIZATION OF THE NANOENCAPSULATED ABACAVIR AND LAMIVUDINE

This experimental phase involved preparing the abacavir and lamivudine nanopowders, which served as the dispersed phase of the fixed dose nanosuspension formulation.

3.1.1. Preparation of Placebo Formulations

Four different placebo (drug-free) nanopowder formulations (F1, F2, F3, and F4) were prepared using the salting-out technique method described by Konan and colleagues (Konan et al., 2002) with modifications made to suit the purpose of this project. Each placebo nanopowder formulation was created by preparing two separate solutions (i.e., A and B). Solution A was prepared by weighing all the ingredients for each formulation, except for polyvinyl alcohol (PVA) and/or sodium chloride (NaCl), using a VWR-160AC analytical balance (Avantor, Canada), and transferring them to a labeled glass beaker. Then, 10 mL of deionized water was measured with a glass measuring cylinder and added to the labeled beakers for F1, F2, F3, and F4. Each mixture was stirred for 20 minutes at 40°C ± 0.5°C and 300 rpm using a Fisherbrand™ Isotemp™ hot plate stirrer (Chelmsford, USA). For Solution B, sodium NaCl and/or PVA were carefully weighed out using the VWR analytical balance and placed in a labelled beaker to which 20 mL of deionized water was added. The resulting mixture was homogenized at 20,000 rpm for 1 minute using a Fisherbrand™ homogenizer with a 5/7 mm generator probe. After this, Solution A was gradually added to Solution B, and the resulting mixture was homogenized at 20,000 rpm for 20 minutes. To prevent heat generation (overheating) during the homogenization process, the respective beakers were placed in an ice bath. After complete homogenization, the nanoprecipitates formed were transferred into a labelled pan and placed in the freezer (Eppendorf CryoCube F570N ULT, Fisher

Scientific, Toronto, ON) set to -80°C ±1°C until completely solidified. Subsequently, the frozen samples were lyophilized utilizing a Scientific Pro freeze dryer (Harvest Right LLC, Salt Lake City, UT, USA) under a vacuum of 924 Pa ± 115 Pa and at a temperature of -18°F ± 0.5°F for 72 hours. The final lyophilized placebo products were physically examined and then stored away in air-tight, opaque aluminum sachets for further testing as necessary.

Table 3.1: Composition of placebo formulations

Placebos	GEL (g)	PVP (g)	LAC (g)	KOL (g)	PVA	NaCl
F1	1.0	0.0	0.0	0.0	3.0	0.0
F2	0.0	0.5	0.5	0.5	3.0	0.0
F3	0.0	0.0	1.0	0.0	3.0	8.0
F4	0.0	0.5	0.5	0.5	3.0	8.0

GEL = gelatin; PVP = polyvinylpyrrolidone; LAC = lactose; KOL = Kollidon CL-SF; PVA = polyvinyl alcohol; NaCl = sodium chloride. Each formulation contained 30 ml of deionised water.

3.1.2. Nanoencapsulation of Abacavir and Lamivudine

Abacavir and lamivudine nanopowders were synthesized separately, employing the placebo carrier systems described in Table 3.1 above. Lamivudine was encapsulated in a polyvinyl alcohol (PVA) matrix (i.e., F3; Table 3.1), while abacavir was encapsulated in a PVA/polyvinyl pyrrolidone (PVP) co-polymeric matrix (i.e., F4; Table 3.1). Additionally, both abacavir and lamivudine were co-formulated using the PVA/PVP matrix (F4). The respective nanopowder drug formulations contained 40 mg of abacavir and/or 20 mg of lamivudine per 250 mg of excipients. All nanoformulations were prepared using the same procedure and experimental parameters outlined in section 3.1.1. Following lyophilization, the products were visually assessed for their overall physical presentations and any noticeable changes in color or odor. The drug-loaded nanoformulations were subsequently transferred into airtight amber sachets and stored at room

condition. These formulations were prepared in triplicate to confirm the reproducibility of the results.

Table 3.2: Composition of abacavir and lamivudine nanopowders

	PVP (g)	KOL (g)	LAC (g)	PVA (g)	NaCl (g)	DRUGS (g)
ABC NP	0.5	0.5	0.5	3	8	2.4
3TC NP	0	0	1	3	8	1

ABC = abacavir; 3TC = lamivudine; PVP = polyvinylpyrrolidone; LAC = lactose; KOL = Kollidon CL-SF; PVA = polyvinyl alcohol; NaCl = sodium chloride. Each formulation contained 30 ml of deionised water

3.1.3. Characterization of Abacavir and Lamivudine Nanoparticles

3.1.3.1. Preliminary Size Determination Using Transmission Electron Microscope (TEM)

About 1 mg of abacavir and lamivudine nanoparticles were individually placed into 1.5 mL capacity Eppendorf® Flex-Tubes® microcentrifuge tubes, followed by the addition of approximately 1 mL of deionized water. Each mixture was vortexed using a Fisherbrand™ vortex mixer (Thermo Fisher Scientific, Toronto, ON) at 700 rpm for 5 minutes to ensure thorough dispersion. The resulting nanoparticle dispersion was then deposited onto a coated TEM grid and transferred into the microscope (JEOL 1230 TEM, JOEL USA Inc., Peabody, MA) for imaging. TEM images were captured at a magnification of 80,000×, with a scale of 200 nm, and a high voltage (Hv) of 80 kV. Once the images were obtained, particle size analysis was performed using ImageJ software (Version 1.54p, National Institutes of Health, Bethesda, USA). The scale was manually set to 200 nm, and the image type was set to 8-bit. Particle sizes for each image were measured, and the average particle size was calculated, along with the standard deviation. Additionally, the TEM images were analyzed to assess the shape of the nanoparticles.

3.1.3.2. Fourier Transform Infrared Spectroscopy

A Fourier transform infrared (FTIR) spectrophotometer (Nicolet iS20 Mid-Infrared FTIR Spectrometer, Thermo Fisher Scientific, Mississauga, Ontario, Canada) equipped with the OMNIC™ specta material characterization software was used to obtain the FTIR spectra for each nanoencapsulated drug with each free (unformulated) drug employed as a reference. The sample holder was first cleaned with 70% ethanol and Kimtech™ lint-free wipes to eliminate any contaminants before and in-between each sample measurement. Thereafter, background readings were collected as needed to remove any interferences. Sample measurements (about 2 mg per sample) were performed in the transmission mode producing individual spectrum within vibrational frequencies of 400 – 4000 cm^{-1}. Each spectrum was obtained as an average of 32 sample scans to reach the desired signal-to-noise ratio and spectra resolution was fixed at 16 cm^{-1}. The obtained spectra were then analyzed and the drug loaded nanoparticles were compared to their respective free drugs by assessing their functional groups and possible inter- and intra-molecular interactions.

3.1.3.3. Encapsulation Efficiency (EE)

The encapsulation efficiency (EE) of the drug-loaded nanoparticles was determined using the method outlined by (Derman, 2015). 1g of each nanoencapsulated drug formulation was accurately weighed using a VWR-160AC analytical balance and separately transferred into labeled 15 mL capacity Falcon centrifuge tubes (Avantor, Toronto, ON). 10 mL of the buffer pH 1.2 was measured using a HENK-JECT syringe and added to each Falcon tube. Buffer pH 1.2 was prepared by dissolving 2 g of NaCl and adding 7 mL of concentrated hydrochloric acid (HCl), which was then diluted to 1 L with deionized water as described in the United States Pharmacopeia (USP,

2020). The pH of the buffer was measured using a calibrated Thermo Scientific™ Orion Star A211 pH meter (Thermo Fisher Scientific, Canada) and adjusted as needed.

The drug formulation and buffer mixtures were then subjected to centrifugation using a Sigma-Aldrich Hettich RotoFix 32 centrifuge (Rotor 1617, Darmstadt, Germany) at 5000 rpm for 20 minutes. The supernatant was carefully collected and diluted with the same buffer and the solution was filtered using a 0.45 μm sterile nylon syringe filter (Fisher Scientific, Toronto, ON) into a quartz cuvette. The concentration of the free drug was determined using a Thermo Scientific™ Genesys 150 UV-Visible spectrophotometer (Thermo Fisher, Madison, USA) at specific wavelength of maximum absorbance i.e., lambda maximum (λ_{max}). As a result, abacavir and lamivudine were measured at λ_{max} of 296 nm and 280 nm respectively. Each drug's filtered placebo solution in buffer pH 1.2 served as blank measurements to exclude possible interfering background absorbances associated with the presence of the different formulation additives. Abacavir and lamivudine concentrations were calculated by fitting the recorded absorbance values into previously established linear equations (abacavir: y = 48.565 mx and R^2 = 0.9988; lamivudine: y = 70.967 mx and R^2 = 0.9993) obtained from the calibration curve of each pure drug. Each sample was prepared and measured in triplicate to ensure reproducibility. The encapsulation efficiency (EE) was calculated using the formula (López-Cabeza et al., 2021) represented by equation 3.1.

EE (%) = Total drug - free drug ÷ total drug × 100 **(Equation 3.1)**

3.1.3.4. Drug Loading Efficiency (DLE)

The drug loading efficiency (DLE) was determined by weighing 0.5 g of each drug loaded nanoformulation sample using a VWR-160AC analytical balance. The weighed sample was then transferred to a 200 mL capacity glass beaker, and 100 mL of buffer pH 1.2 (prepared as described in Section 3.1.3.3) was added. The mixture was homogenized using a Fisherbrand™ homogenizer with a 5/7 mm generator probe at 5000 rpm for 5 minutes. Subsequently, the mixture was agitated on a Fisherbrand™ Isotemp™ hot plate magnetic stirrer at 500 rpm and 60°C for 40 minutes. After homogenization and agitation, the solution was diluted with the buffer (pH 1.2) and filtered using a 0.45 µm Fisher Scientific sterile nylon syringe filter into a quartz cuvette inserted into the UV spectrophotometer. The concentration of abacavir and lamivudine were determined by measuring the absorbance, with blanking performed using the placebo formulations prepared in the same manner as the drug-loaded nanoparticles. Analysis was conducted using the Thermo Scientific™ Genesys 150 UV-Visible spectrophotometer, with abacavir measured at its λ_{max} of 296 nm and lamivudine measured at λ_{max} of 280 nm. The drug concentrations were calculated based on a previously established calibration curve for both drugs (Please refer to section 3.1.3.3.). Measurements were carried out in triplicate to ensure reproducibility. The drug loading efficiency (DLE) was calculated using equation 3.2 (Srisuwan & Baimark, 2014).

$$\text{DLE}\ (\%) = \text{Actual drug load} \div \text{theoretical drug load} \times 100 \qquad \textbf{(Equation 3.2)}$$

3.1.3.5. Hydrodynamic Diameter, Polydispersity Index and Zeta Potential

The particle size and polydispersity index (PDI) were measured using dynamic light scattering (DLS), while the zeta potential was determined via electrophoretic light scattering (ELS) utilizing

the Anton Paar Litesizer™ 500 instrument (Anton Paar, Montreal, Canada). Sample preparation for DLS analysis followed the method described by (Guo et al., 2020). A 100 mg/mL concentration of each drug-loaded nanoparticle formulation was prepared by dispersing the nanoparticles in deionized water and vortexing at 700 rpm for 1 minute using a Fisherbrand™ Fisher Analog vortex mixer (Fisher Scientific, Pittsburgh PA, USA). The suspension was then filtered using a 0.45 µm Avantor™ VWR® non-sterile nylon syringe filter (VWR International LLC, Mississauga, ON, Canada) to remove any contaminants. Approximately 10 µL of the sample was transferred to a disposable Omega cuvette (Anton Paar, Ashland, VA, USA), and measurements were performed using the backscatter measurement angle at 21°C. For the ELS measurements, the nanoparticle suspension was dispersed in warm (37℃ ± 0.5℃) phosphate buffered saline (PBS) solution and vortexed to achieve a final concentration of 50 µg/mL. An Omega cuvette was used for these measurements, which were performed at 25°C with a voltage of 200 V applied. All measurements were carried out using the Kalliope particle analysis software (Version 2.30.4) and measured in triplicate and the results were reported as mean values with the standard deviation.

3.1.3.6. Powder Flow

The flowability of abacavir and lamivudine nanopowders was determined by calculating the Hausner ratio, following the United States Pharmacopeia (USP) guidelines (Shah et al., 2023). Approximately 10 g of each powder sample was accurately weighed using a VWR-160AC weighing balance. The powders were then transferred into a 50 mL graduated glass cylinder. The volume of the powder was recorded to determine the bulk density. Subsequently, the cylinder was subjected to continuous tapping until no further change in volume was observed. The tapped volume was recorded after the tapping process and the tap density was calculated. This procedure

was repeated three times for both the abacavir and lamivudine nanopowders to ensure reproducibility. The Hausner ratio was calculated using equation 3.3 and standard values for the different flow characteristics are presented in Table 3.3.

$$\text{Hausner ratio} = \text{tapped} \div \text{bulk density} \qquad \textbf{(Equation 3.3)}$$

Table 3.3: Hausner ratio flowability scale description

Flow character	**Hausner ratio**
Excellent	1.0 –1.11
Good	1.12 – 1.18
Fair	1.19 – 1.25
Passable	1.26 – 1.34
Poor	1.35 – 1.45

3.1.3.7. Scanning Electron Microscopy (SEM)

Particulate surface morphology of the nanopowders of abacavir and lamivudine versus the free drugs and placebo formulations were investigated using a Zeiss Sigma 300 Field Emission Scanning Electron Microscope (FESEM, United States). A small amount (about 2 mg) of each dry sample was affixed to 13 mm diameter aluminum SEM stubs using carbon double-sided adhesive tabs. To enhance conductivity and reduce charging effects during imaging, the samples were sputter-coated with a thin layer of gold/palladium using a Leica EM ACE 600 high vacuum coater set to 30 mA (Rod et al., 2019). Following the coating process, the samples were individually inserted into the FESEM machine and imaged at an accelerating voltage (EHT) of 5 kV. Images were captured at magnifications of 50,000x and 100,000x using the Secondary Electron Detector (SE2). These images were analyzed to assess the surface morphology and evaluate the presence or absence of particle agglomeration.

3.1.3.8. Stability Studies

The stability of the nanopowders was assessed over a 3-month period, with evaluations conducted biweekly for the first 4 weeks and subsequently every 4 weeks. The samples were stored at a controlled temperature of 22.5°C ± 2°C and relative humidity of 37% ± 11%, conditions that mimic those typically found in a pharmacy medication cabinet and/or day-to-day use (WHO, 2015). Temperature and humidity were monitored using two ThermoPro TP167-2-CA hydrometer thermometers (TP157, ThermoPro, China). At each time point, the samples were visually inspected for any changes in physical appearance, such as color alteration or odour development. Additionally, the drug content of the nanopowders was determined to determine the presence or absence of drug degradation using the method and formula outlined in Section 3.1.3.4 and Equation 3.2. respectively

3.2. EXPERIMENTAL PHASE 2 — DEVELOPMENT, OPTIMIZATION AND EVALUATION OF THE PHARMACEUTICAL/FLUID GEL

This experimental phase focused on the preparation of the optimized pharmaceutical gel, which served as the diluent (dispersion phase) for the fixed dose nanosuspension formulation.

3.2.1. Preliminary Screening Using One-Variable-at-a-Time (OVAT)

The initial stages of preparing the pharmaceutical/fluid gel (i.e., the dispersion medium) was conducted using the one variable at a time (OVAT) approach. In this process, five different gelling agents; hydroxypropyl methylcellulose (HPMC), hydroxyethyl cellulose (HEC), sodium starch glycolate (SSG), methylcellulose (MC), and gelatin (GEL) were employed. Each gelling agent was utilized in combination with other excipients to prepare five gel formulations. All other manufacturing parameters remained constant across the different formulas, including stirring rate, time, water content, preservative and wet milling duration. The preparation of the gels began by accurately weighing all ingredients using a VWR-160AC analytical balance. The weighed ingredients were then transferred into a KYG grinder (M200B, China) and were wet milled with 30 mL of pre-boiled deionized water for one minute to ensure uniform dispersion. After milling, the resulting mixture was transferred into a glass beaker, which was subsequently sealed with parafilm to prevent evaporation. The beaker was placed on a Fisherbrand™ Isotemp™ hot plate magnetic stirrer and agitated at 60°C and 600 rpm for 30 minutes.

Table 3.4: Tabular representation of preliminary pharmaceutical gel screening

	HPMC (g)	HEC (g)	SSG (g)	XYL (g)	PEG/PVA (g)	MC (g)	GEL (g)	CA (g)	SB (g)
HG 1	0.1	0	0.2	1	0.1	0	0	0	0.1
HG 2	0	0.2	0.1	1	0.1	0	0	0.05	0.1
HG 3	0	0	0.2	1	0.1	0.1	0	0	0.1
HG 4	0	0.3	0.1	1	0.1	0	0	0.05	0.03
HG 5	0	0	0.2	1	0.1	0.1	0.1	0	0.03

HPMC = hydroxypropyl methylcellulose; HEC = hydroxyethyl cellulose; SSG = sodium starch glycolate; XYL = xylitol; PEG/PVA = polyethylene glycol/polyvinyl alcohol; MC = methyl cellulose; GEL = gelatin; CA = citric acid; COL = colorant. For all formulations, the total volume of deionized water used was 30 mL

3.2.2. The Plackett-Burman Experimental Design for the Gel Development and Optimization

The next phase of the optimization process was conducted using the Minitab Statistical Software, version 21.1 (Minitab Inc., State College, PA, USA), employing the Plackett-Burman design template. This design incorporated eight factors: HPMC, HEC, SSG, XYL, PEG/PVA, MC, GEL, and CA which were varied at three levels (low, mid, or high). The fixed variables in all formulations were sodium benzoate (0.03 g) and deionized water (30 mL).

Table 3.5: Limits for variables

Levels	HPMC (g)	HEC (g)	SSG (g)	XYL (g)	PEG/PVA (g)	MC (g)	GEL (g)	CA (g)
Low	0	0	0.1	1	0.1	0	0	0
Mid	0.05	0.15	0.15	1	0.2	0.05	0.1	0.05
High	0.1	0.3	0.2	2	0.3	0.1	0.2	0.1

HPMC = hydroxypropyl methylcellulose; HEC = hydroxyethyl cellulose; SSG = sodium starch glycolate; XYL = xylitol; PEG/PVA = polyethylene glycol/polyvinyl alcohol; MC = methyl cellulose; GEL = gelatin; CA = citric acid. For all formulations, 0.03 g of sodium benzoate was added, and the total volume of deionized water used was 30 mL

The design had three center points and generated a total of 15 different formulations. Each formulation was prepared by weighing the ingredients, followed by wet milling and magnetic agitation, as described in Section 3.2.1. All 15 gels were prepared in triplicate and transferred to

50 mL falcon tubes after cooling down. They were then stored under ambient conditions, wrapped in foil paper, and stored under room conditions (temperature of 22.5 ± 2°C and relative humidity of 37 ± 11%). Two researchers evaluated the gels on days 7, 14, and 28 under fluorescent light for any visible changes in physical appearance, focusing on homogeneity and flow properties. Additionally, their pH and gel strength were quantified.

Table 3.6: Plackett-Burman experimental design template

Formulations	HPMC (g)	HEC (g)	SSG (g)	XYL (g)	PEG/PVA (g)	MC (g)	GEL (g)	CA (g)
HG 1	0.1	0	0.1	1	0.3	0.1	0.2	0
HG 2	0.05	0.15	0.15	1.5	0.2	0.05	0.1	0.05
HG 3	0	0.3	0.2	2	0.1	0.1	0.2	0
HG 4	0.1	0.3	0.1	2	0.1	0	0	0.1
HG 5	0.1	0.3	0.1	2	0.3	0	0.2	0
HG 6	0	0.3	0.1	1	0.1	0.1	0.2	0.1
HG 7	0.05	0.15	0.15	1.5	0.2	0.05	0.1	0.05
HG 8	0.1	0	0.2	2	0.1	0.1	0	0
HG 9	0	0	0.1	2	0.3	0.1	0	0.1
HG 10	0	0	0.2	2	0.3	0	0.2	0.1
HG 11	0	0.3	0.2	1	0.3	0	0	0
HG 12	0.1	0.3	0.2	1	0.3	0.1	0	0.1
HG 13	0.1	0	0.2	1	0.1	0	0.2	0.1
HG 14	0.05	0.15	0.15	1.5	0.2	0.05	0.1	0.05
HG 15	0	0	0.1	1	0.1	0	0	0

HPMC = hydroxypropyl methylcellulose; HEC = hydroxyethyl cellulose; SSG = sodium starch glycolate; XYL = xylitol; PEG/PVA = polyethylene glycol/polyvinyl alcohol; MC = methyl cellulose; GEL = gelatin; CA = citric acid; for all formulations, 0.03 g of sodium benzoate was added, and the total volume of deionized water used was 30 mL

3.2.2.1. Physical Appearance Screening

The physical appearance of the gels prepared was assessed using a grading scale based on the following criteria — *(1) Homogeneous, optimal flow:* the gel is uniform and pourable, with no separation or excessively thick consistency ;*(2) Phase-separated, intermediate flow:* the gel shows

some phase separation, but the consistency is moderately fluid ; *(3) homogeneous, suboptimal flow:* the gel is uniform (i.e., no phase separation) but too viscous to pour easily or too watery; and *(4) homogeneous, intermediate flow:* the gel is uniform (absence of phase separation) but exhibits intermediate flow properties i.e., neither too viscous but not easily pourable.

3.2.2.2. Gel Strength Determination

Following physical appearance evaluation, gel strength was measured as a textural quantity using a CTX™ Texture Analyzer (AMETEK® Brookfield, MA, USA) equipped with a 5 kg load cell and a TA10 cylinder probe (diameter: 12.7 mm, length: 33 mm). The texture analyzer was set with the following parameters: trigger force of 0.05 N, deformation of 0.1 mm, test speed of 0.5 mm/s, pre-test speed of 2 mm/s, and two test cycles. A 6 mL sample of each gel was measured using a syringe and transferred into a 10 mL glass beaker, which was then positioned on the equipment stage. Gel strength was measured under the texture profile analysis (TPA) parameter. Each gel's measurement was carried out three times and the averages and standard deviation were determined.

3.2.2.3. pH Measurement

Next, the pH of each gel was measured using a Thermo Scientific™ Orion Star A211 pH meter (Thermo Scientific, Mississauga, ON, Canada). Before use, the pH meter was calibrated with standard 4.0 and 7.0 pH buffers. The probe was then rinsed with deionized water and blotted dry with lint-free Kimtech™ wipes. Subsequently, the pH meter was immersed in each gel sample, and the pH was recorded. The pH measurement was repeated for each gel in triplicates, and the results were averaged.

Following the preparation and evaluation of the 15 fluid gel formulations, a response surface regression analysis was conducted using Minitab® Statistical Software (Version 21.1.0, Minitab Inc., State College, PA, USA) to identify the suitable combinations of polymers for the development of the optimized gel. The optimization was based on the three evaluated response parameters: physical appearance, pH, and gel strength. For each parameter, target values were defined as follows:

- *Physical appearance* was targeted toward homogeneity and optimal flow (ranking of 1 on the grading scale).
- *pH* was targeted toward values closest to neutral (close to 7) to reduce the risk of irritation.
- *Gel strength* was set to achieve moderate strength (about 0.05N) to allow the nanopowder dispersion while maintaining flowability.

The optimization process utilized a composite desirability function, which integrated individual desirability scores for each response into a single global desirability index (ranging from 0 to 1). Higher values indicate a better match between the experimental outcomes and the specified target, with a composite desirability of ≥ 0.90 considered acceptable. Regression statistics, including R^2 values and p-values, were generated for each response to assess the significance of each parameter. The final optimized formulation was generated based on the computed ideal levels of the eight variables, and a validation run was performed. The formulation was prepared using the predicted composition, and the resulting experimental values for PA, pH, and GS were compared to the predicted values using ANOVA to confirm the accuracy and robustness of the design model

Table 3.7: Optimized pharmaceutical gel

Formulation	HPMC (g)	SSG (g)	XYL (g)	PEG/PVA (g)	MC (g)	GEL (g)
OG	0.1	0.1	2	0.1	0.1	0.2

HPMC = hydroxypropyl methylcellulose; SSG = sodium starch glycolate; XYL = xylitol; PEG/PVA = polyethylene glycol/polyvinyl alcohol; MC = methyl cellulose; GEL = gelatin. For all formulations, 0.03 g of sodium benzoate was added, and the total volume of deionized water used was 30 mL

3.2.3. Evaluation of the Optimized Pharmaceutical Gel

3.2.3.1. Physical Appearance

The physical appearance of the optimized gel was evaluated in triplicate after preparation. A researcher inspected each sample and classified it based on the grading scale outlined in Section 3.2.2.1. The classification was then compared with the predicted outcome derived from the experimental design, which indicated the gel should be classified as (1) homogeneous, optimal flow.

3.2.3.2. Gel Strength

Gel strength (GS) was assessed using the CTX™ Texture Analyzer with the same settings described in Section 3.2.2.2. The measured value was compared to the predicted gel strength value of 0.0523 N from the experimental design. The gel strength of the optimized formulation was measured in triplicate, and the average value and standard deviation were calculated and reported.

3.2.3.3. pH Measurement

The pH of the optimized gel was determined using the Thermo Scientific™ Orion Star A211 pH meter, following the procedure outlined in Section 3.2.2.3. The measured pH was then compared to the predicted value of 5.7 from the design. The gel was tested three times, and the average pH and standard deviation were recorded for analysis.

3.2.3.4. Viscosity Determination

Viscosity was measured using the IKA® ROTAVISC ME-VI (HELISTAND S098, IKA Works, Inc., United States) viscometer, which was equipped with disc spindle 9 (SP-9). A 50 mL sample of the gel was poured into a glass beaker, and the viscometer was set to 200 rpm. The viscosity was recorded approximately 30 seconds after allowing the readings to stabilize. This process was repeated three times. The viscosity (mPa·s) and the M% values were calculated, and the average and standard deviation of the measurements were recorded.

3.2.3.5. Scanning Electron Microscopy (SEM)

The gel samples were initially fixed for 2 hours in 2.5% glutaraldehyde (Electron Microscopy grade), prepared in 0.1 M sodium cacodylate buffer. After fixation, the samples were rinsed three times for 10 minutes each with 0.1 M sodium cacodylate buffer. The samples were then secondarily fixed for 2 hours in 1% osmium tetroxide, followed by a quick rinse with distilled water. Next, the samples were dehydrated in a graded ethanol series: 50% ethanol for 10 minutes, 70% ethanol for 10 minutes (x2), 95% ethanol for 10 minutes (x2), 100% ethanol for 10 minutes, and finally, dried 100% ethanol for 10 minutes (x2). The samples were then subjected to critical point drying using a Leica EM CPD300 Automated Critical Point Dryer. The dried gel samples were installed to SEM stubs, sputter-coated with a thin layer of gold/palladium, and analyzed using a Zeiss Sigma 300 Field Emission Scanning Electron Microscope (FESEM), following the procedure and parameters described in Section 3.1.3.7. The SEM images obtained represented the surface morphology of the gel.

3.2.3.6. Stability Studies

The stability of the optimized pharmaceutical gel was evaluated over a period of 3 months, with assessments conducted on Day 0, and at weeks 2, 4, 8, and 12. The following parameters were used as stability indicators:

- Physical Appearance: The optimized gel was observed under fluorescent light by a researcher at each time point. The gel's overall appearance and flow properties were assessed and classified according to the previously established grading scale described in section 3.2.2.1.
- Gel Strength: The gel strength was measured using a CTX™ Texture Analyzer, following the protocol outlined in Section 3.2.2.2. Measurements were performed at each time point in triplicate, and the average and standard deviation of the results were calculated.
- Gel pH: The pH of the gel was determined using the Thermo Scientific™ Orion Star A211 pH meter, as described in Section 3.2.2.3. The test was repeated three times for the sample, and the average pH and standard deviation were calculated and recorded.

3.3. EXPERIMENTAL PHASE 3 — FORMULATION OF ABACAVIR AND LAMIVUDINE FIXED DOSE NANOSUSPENSION FORMULATION

This phase of the experiment focused on preparing the fixed dose combination of abacavir and lamivudine suspension.

3.3.1. Synthesis of Abacavir and Lamivudine Nanosuspension

The suspension was prepared by accurately weighing 500 mg of abacavir and lamivudine nanoencapsulated nanopowders, using a VWR-160AC weighing balance. Each drug was transferred to a glass vial containing 10 mL of pharmaceutical gel, which had been precisely measured with a 10 mL syringe. The vial was then sealed and manually agitated until the powders were thoroughly dispersed within the gel. The final suspension contained 40 mg of abacavir and 20 mg of lamivudine per 5 mL of suspension. The vial was covered with foil and stored for subsequent experiments.

3.3.1. Testing The Abacavir/Lamivudine Nanosuspension

3.3.1.1. Determination of Physical Properties of the Nanosuspension

The physical properties of the drug loaded nanosuspension formulation were determined by examining the overall physical presentation of the nanosuspension to visually observe the color and the smell which was done by a researcher (to minimize errors) who sniffed the preparation and recorded their observation.

3.3.1.2. Textural Strength of Nanosuspension

The textural strength of the suspension was measured using a CTX™ Texture Analyzer, following the previously described settings in Section 3.2.2.2. The textural strength of the test suspension was then matched with that of three marketed paediatric oral suspensions namely Motrin®, Tylenol®, and Advil®. These three comparator products were randomly selected because they are fluid formulations designed for paediatric population and are available over the counter while abacavir/lamivudine combination is not commercially available as a liquid preparation. Measurements were executed using the same parameters and method described in Section 3.2.2.2. Quantifications were all conducted in triplicate for all test samples and the average value and standard deviation were calculated.

3.3.1.3. Nanosuspension pH Measurements

The pH of the suspension and those of the reference paediatric oral liquid suspensions (Motrin, Tylenol, and Advil) were measured using a Thermo Scientific™ Orion Star A211 pH meter, following the same procedure described in Section 3.2.2.3. The pH measurement was repeated for each sample in triplicate, and the average value along with the standard deviation were recorded. The pH values of the suspension were compared to those of the reference paediatric oral liquid suspensions.

3.3.1.4. Viscosity Measurement

The viscosity of the suspension and the reference formulations were measured using the IKA® ROTAVISC ME-VI viscometer (HELISTAND S098, IKA Works, Inc., Wilmington, NC), using the same experimental method and parameters as described in Section 3.2.2.4. This comparison

allowed for an evaluation of the viscosity the suspension in comparison to commercially available formulations.

3.3.1.5. Fourier Transform Infrared Spectroscopy (FTIR)

The FTIR analysis was conducted using a Thermo Scientific™ FTIR Spectrometer. A small amount of the placebo formulation, prepared at the same concentration and following the same process as described in Section 3.3.0, was used as the blank. The placebo was placed in the sample holder, and the holder was cleaned with a Kimtech™ lint-free wipe and 70% ethanol before introducing the suspension sample. The sample holder was then carefully closed, and the spectra were collected and analyzed using the procedure outlined in Section 3.1.3.2.

3.3.1.6. Scanning Electron Microscopy

The suspension was prepared and dehydrated following the same procedure outlined in Section 3.2.3.5. Images of the sample were captured using the Zeiss Sigma 300 Field Emission Scanning Electron Microscope (FESEM), with the same imaging parameters as described in sections 3.1.3.7 and 3.2.3.5.

3.3.1.7. Drug Release Kinetics

The drug release studies were conducted following the protocols outlined by the United States Pharmacopeia (USP) using simulated intestinal fluid (pH 1.2), which was prepared as described in section 3.1.3.3. The buffer was added to 500 mL of glass bottles, and the bottles were placed in a preheated water bath set to 37°C, with the temperature monitored using a thermometer. Once the buffer reached 37°C, 5 mL of the suspension was measured using a syringe and added to the

preheated buffer, which was agitated at 100 rpm. Samples were withdrawn at the following time intervals: 5, 10, 15, 20, 30, 40, 50, 60, 90, 120, 160, 200, and 240 minutes. At each time point, 10 mL of the sample was collected into glass vials, and 10 mL of fresh, warm plain buffer was added to the dissolution medium to maintain sink conditions. The same procedure was carried out for the placebo formulation, which was used as a blank. The collected samples were filtered using a Fisher Scientific nylon 0.45 μm non-sterile filter, and the resulting solutions were diluted with the fresh buffer as needed. The drug concentrations were then determined using a Thermo Scientific™ Genesys 150 UV-Visible spectrophotometer. The UV analysis was conducted after blanking the spectrophotometer with the placebo solution sampled at each time point. Abacavir was quantified at a wavelength of 296 nm, while lamivudine was analyzed at 280 nm. The entire procedure was repeated in triplicate for three different preparations to ensure reproducibility. The amount of abacavir and lamivudine released over time were calculated and analyzed.

Additionally, dissolution studies for both unformulated drugs (i.e., 40 mg of abacavir and 20 mg of lamivudine) were conducted in triplicate using the same media, following the same procedure. These studies were analyzed using the UV spectrophotometer, with blanking performed using the simulated intestinal fluid. The results obtained served as reference data for the encapsulated/formulated drugs (i.e., abacavir and lamivudine). All resulting data were analyzed using the KinetDS version 3.0 open-source software, which aided the selection of the most suitable release model based on mathematical computations for zero-order, first-order, second-order, and Korsmeyer-Peppas models (Adeleke et al., 2020).

3.3.1.8. Stability Studies

Stability studies were conducted under conditions recommended by the International Council for Harmonisation (ICH) guidelines, specifically under intermediate conditions of 30°C ± 2°C and 65% ± 5% relative humidity. (González-González et al., 2022) These conditions were simulated using a VWR® Gravity Convection Oven 3.7, (Radnor, PA, USA), with beakers containing water to generate the required humidity. The environmental temperature and humidity were continuously monitored using two ThermoPro TP167-2-CA thermohygrometer to ensure consistency. The suspension was prepared and transferred into glass vials, which were then wrapped in foil paper to protect them from light and then stored in the oven incubator throughout the test period. Evaluations were conducted weekly for a duration of 28 days (4 weeks). At each time point, the following parameters were assessed:

- Physical Appearance: The overall appearance, color, and smell of the suspension were visually inspected for any signs of changes.
- pH: The pH of the suspension was measured following the procedure described in section 3.2.2.3
- Textural Suspension Strength: The textural strength was measured as described in section 3.2.2.2
- Drug Content: The drug content was quantified according to the method described in Section 3.1.3.4

3.3.1.7. In vitro Cytobiocompatibility Assay

HepG2 cells, derived from human hepatocellular carcinoma, were utilized for the cytotoxicity assay. They were chosen because they offer greater accessibility, cost-effectiveness, and

reproducibility, making them particularly suitable for in vitro screening and toxicity profiling. While they do not fully replicate the metabolic capacity of normal hepatocytes, their stable growth and liver-like characteristics make them a reliable model for preliminary toxicity evaluations (Gerets et al., 2012).

- Samples Tested: The samples used in the study included unformulated (pure) abacavir and lamivudine solution, the placebo suspension formulation consisting of placebo nanopowder (without drugs) and the final optimized gel, and the drug-loaded nanosuspension of abacavir and lamivudine. Triton X-100 was used as the positive control (Riss et al., 2004), while Dextran served as negative control (Lau et al., 2010), and phosphate-buffered saline (PBS) at pH 7.4 was used to normalize the data.

- Plating of cells: The cytotoxicity test was conducted over a period of three days. On day 1, culture media was prepared by warming and thawing the necessary ingredients in a 10 L Isotemp GPD10 water bath (Fisherbrand, Mississauga, Toronto, ON) set to 37°C. The media consisted of minimum essential medium (MEM), non-essential amino acids (1X), L-glutamine (2 mM), penicillin G-streptomycin (100 U/mL, 100 µg/mL), and fetal bovine serum (FBS) (10% v/v). This was prepared in a biological safety cabinet (Class II, Type A2, Thermo Scientific, Model 1385) while maintaining sterile techniques throughout the procedure. HepG2 cells were cultured in T75 flasks with the prepared culture media and incubated at 37°C in a 5% CO2 atmosphere using a Heracell Vios 160i CR CO2 incubator (Thermo Scientific, Dartmouth, NS, Canada) for approximately one week. After the cells had proliferated, they were detached using 2 mL of Trypsin-EDTA and incubated for 5 minutes. The reaction was stopped by adding 5 mL of complete culture media, which was then

transferred into a sterile 50 mL Falcon tube. The tube was centrifuged using a Sigma-Aldrich Hettich RotoFix 32 centrifuge (Rotor 1617, Darmstadt, Germany) set at 1000 rpm for 5 minutes. The supernatant was discarded, and the resulting cell pellet was resuspended in fresh culture media using a syringe and a 21G needle. The cell suspension was then counted using an automated cell counter, with 50 µL of the suspension mixed with an equal volume of trypan blue dye. The cell suspension was loaded into a Bio-Rad Cell Counting Slide (Bio-Rad), which was then placed into a Bio-Rad TC20™ Automated Cell Counter (Bio-Rad Laboratories, Hercules, CA, USA) for cell counting. The HEPG2 cells were plated in 24-well plates at a density of 15,000 cells per well, which was calculated based on the cell count results obtained from the cell counter. The plates were then incubated for 24 hours at 37°C in a 5% CO2 atmosphere to allow the cells to adhere to the surface.

- Treatment of cells: On day 2, fresh complete culture media was prepared following the same process as on day 1, described above. The treatment solutions and controls, Dextran and Triton X-100, were also prepared, and they were dissolved/diluted in sterile PBS to achieve the desired final concentrations (Table 3.9).

Table 3.8: Stock solution concentrations

Treatment	Stock Concentration
Dextran	5% w/v
Triton X-100	0.025% v/v
Abacavir/lamivudine	6 mg/ml
Placebo	33 mg/ml
FDC suspension	35 mg/ml

Stock solutions of the treatment group, unformulated abacavir/lamivudine, placebo nanosuspension, and abacavir/lamivudine loaded nanosuspension were prepared using PBS. The suspension formulation contains the same concentration of abacavir and lamivudine as the pure drugs for fair comparison, however, for an accurate representation, the non-drug elements in the formulation are accounted for as well. Each of these stock solutions was then diluted to generate five different concentrations for each treatment. The treatment solutions and control groups were combined with complete media in an 80:20 ratio (media to treatment), ensuring that the final concentrations of dextran and Triton in the media/treatment mixture matched the desired values. These solutions were added to the cells in the 24-well plates as described in section 3.3.1.7. The resulting media/treatment solutions were added to the wells on the plate, with 0.5 mL of solution added to each well. Each treatment concentration was applied to three wells, and the plates were incubated for another 24 hours. Blank control wells, which contained no cells, were included to measure background luminescence from the reagent. Furthermore, wells containing only PBS and media (no treatment) were included as vehicle controls for normalization of the treatments.

Table 3.9: Final concentrations of the treatments (test samples and controls)

	Final Concentration(s) in Media (mg/ml)				
ABC/3TC	0.075	0.15	0.3	0.6	1.2
Placebo	0.4125	0.825	1.65	3.3	6.6
Suspension	0.473	0.875	1.75	3.5	7
Triton X-100	0.005% v/v				
Dextran	1% w/v				

- Cell viability assay: On the third day, the CellTiter-Glo® reagent was diluted with PBS (20:80 ratio). After incubation, the plates were removed from the incubator, and the contents of each well were aspirated. The wells were washed with 0.2 mL of PBS, and the solution was aspirated

again. Subsequently, 0.1 mL of the CellTiter-Glo reagent was added to each well. The plates were mixed on an orbital shaker for 5 minutes at 600 rpm and incubated at room temperature to stabilize the luminescent signal. After stabilization, 80 µL of the solution from each well was transferred into a 96-well white opaque plate, and luminescence was measured using a Synergy™ HT plate reader (Biotek Instrument, CA, USA) with Gen5 (version 2.10.14, Synergy™ software) under luminescence settings. This procedure was repeated in triplicate for each treatment concentration, and the resulting luminescence values were used to assess cell viability. The net values were obtained by subtracting the blank values (no cells) from the total values. The net values were then normalized to the vehicle control groups (PBS/media-only), and statistical analysis was carried out using SigmaPlot (version 12.5 software, Systat Software, Inc., CA, USA).

All statistical analyses were performed using one-way analysis of variance (ANOVA), followed by the Student-Newman-Keuls multiple comparison test where applicable, with a significance level set at $p < 0.05$ (SigmaPlot version 12.5, Systat Software, Inc., CA, USA)

CHAPTER 4: RESULTS AND DISCUSSION

4.0. PRESENTATION AND INTERPRETATION OF RESULTS PHASE 1 — DEVELOPMENT OF THE NANOENCAPSULATED ABACAVIR AND LAMIVUDINE

This section presents the results and discussion involved in the creation and testing of the abacavir and lamivudine nanopowders.

4.0.1. Placebo Formulations

Four distinct drug free polymeric carriers referred to as placebos namely F1, F2, F3, and F4 (Table 3.1) were successfully developed, each exhibiting unique physical characteristics. F1 and F2 produced solid, polymeric films (Figure 4.1 A and B), with F1 being more transparent and F2 more opaque in physical presentation. In contrast, F3 and F4 produced free-flowing powders (Figure 4.1 C and D), which were more practical for the purpose of this study as it allows for easy dispersion within the diluent to produce the nanosuspension. All the placebos were odourless. These powder-like placebos confirmed the effectiveness of the nanoparticle production method (Section 3.1.1.) employed, allowing for further investigation into their compatibility for abacavir and lamivudine encapsulation.

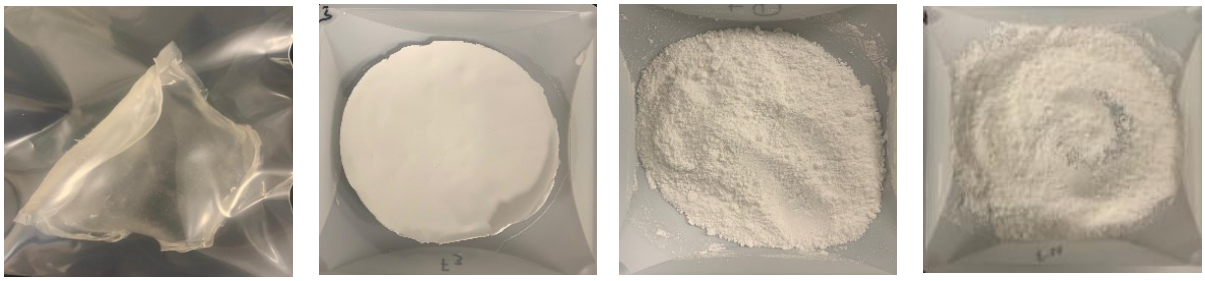

(A) **(B)** **(C)** **(D)**

Figure 4.1. Digital images of placebo formulations.

4.0.2. Nanoencapsulation of Abacavir and Lamivudine

The drug free polymeric carriers (i.e., placebos F3 and F4; Figures 4.1 C and D) that produced free flowing powders were further investigated as encapsulants for the model drugs, abacavir and lamivudine, studied herein. It was found that abacavir was physically compatible with the PVP/PVA system and successfully encapsulated within its matrix (F4), while lamivudine blended well into the PVA carrier and was enclosed within its matrix (F3). The encapsulated abacavir produced a free-flowing powder that exhibited a slight golden color, attributed to the natural hue of the pure drug, and was odorless (Figure 4.2 A). In contrast, the encapsulated lamivudine produced a white, free-flowing powder with a faint characteristic odor like that of the pure drug (Figure 4.2 B).

Furthermore, the co-encapsulation of abacavir and lamivudine within the PVP/PVA matrix (Figure 4.1. D) was also attempted, and this resulted in a free-flowing powder with a deep golden color and a slight characteristic odor, which was noticeably different from the pure, unencapsulated abacavir and lamivudine and their encapsulated forms. Based on these observations, particularly the visible color changes, the decision was made to proceed with the separately encapsulated instead of the co-encapsulated drugs to ensure the stability and compatibility of each drug, as color change could be indicative of drug-excipient incompatibilities (Vranić, 2004).

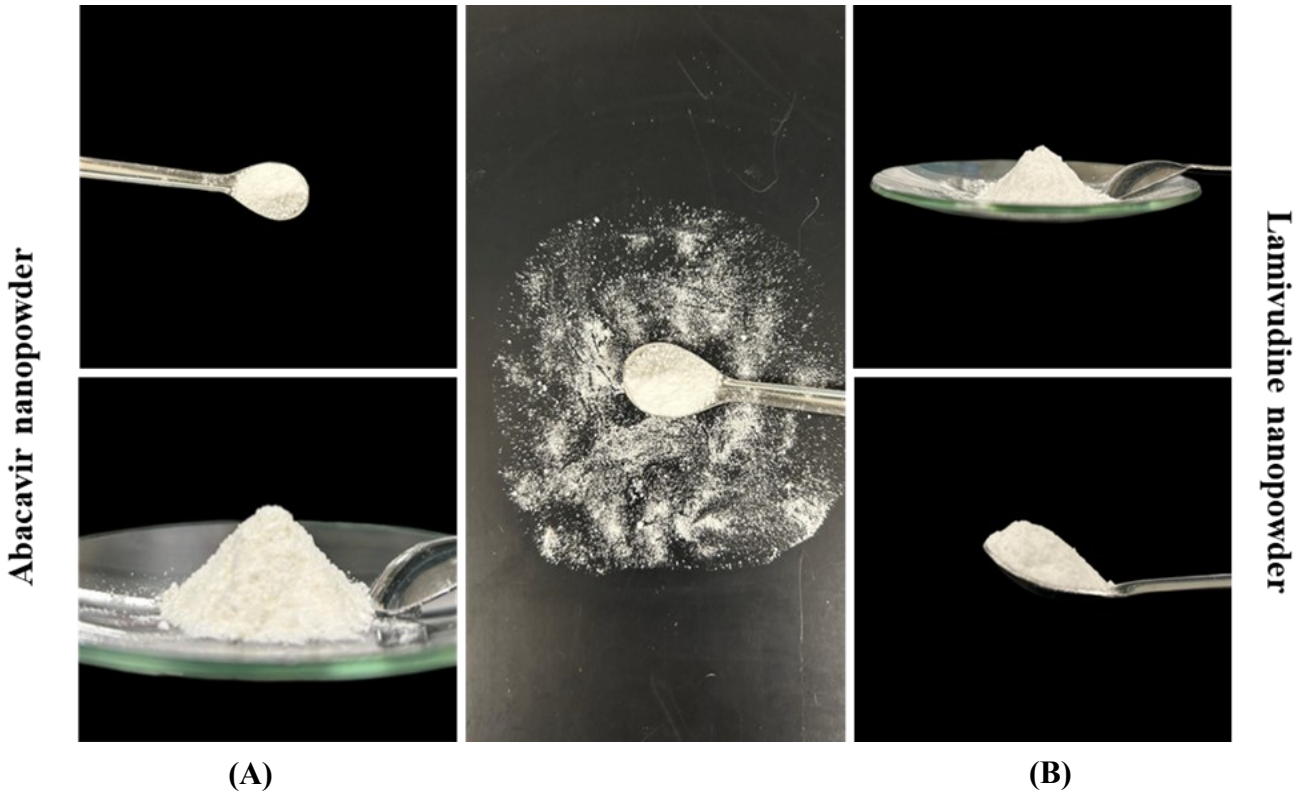

Figure 4.2. Digital photographs of nanoencapsulated abacavir (ABC) and lamivudine (3TC).

4.0.3. Characterization of Abacavir and Lamivudine Nanopowders

4.0.3.1. Transmission Electron Microscopy for Particle Morphology and Size Measurements

4.0.3.1. Transmission Electron Microscopy

Transmission electron microscopy (TEM) analysis revealed that both abacavir (Figure 4.3 A and B) and lamivudine (Figure 4.3 C and D) particles, in their dehydrated states, were spherical in shape and the particle sizes fell within the nano range. Abacavir had a measured average particle size of 64 nm ± 34 nm and lamivudine particles were 77 nm ± 32 nm based on ImageJ analysis. This demonstrated successful nanosizing using the experimental technique utilized in this project.

The TEM images showed that the abacavir particles exhibited slight agglomeration (Figure 4.3 A and B), on the other hand, lamivudine particles had no noticeable agglomeration (Figure 4.3 C and D).

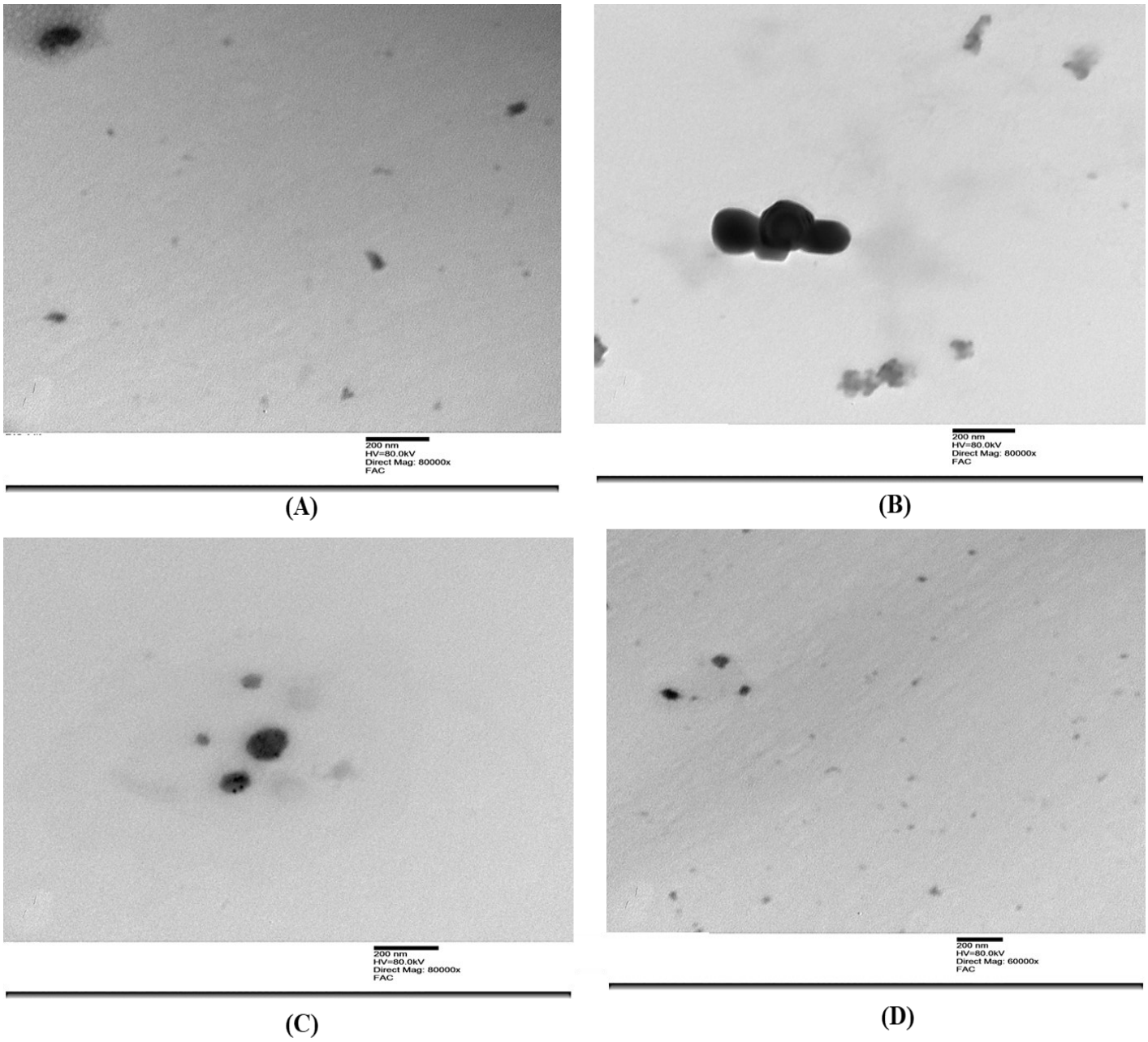

Figure 4.3. TEM images of abacavir (A, B) and lamivudine (C, D).

4.0.3.2. Fourier Transform Infrared Spectroscopy (FTIR)

The FTIR spectra of pure, unformulated abacavir and lamivudine were compared to their respective nanoparticulate formulations. The vibrational frequencies of salient functional groups characteristic for the drugs were generally similar between the pure/unformulated and encapsulated forms. In lamivudine, the C–H stretching band observed at 3204.14 cm^{-1} in the pure lamivudine spectrum was absent in the nanoparticle formulation. The N-H scissoring band, initially observed at 1633.48 cm^{-1}, shifted to 1646.03 cm^{-1} in the nanoparticulate form. A consistent peak at 1607.80 cm^{-1} was observed in both spectra and is attributed to the aromatic C=C stretching of the pyrimidine ring. Its unchanged position suggests that the core structure of lamivudine remained intact post-encapsulation. Minor shifts were also seen in the fingerprint region, specifically the C-N stretching band (from 1057.54 cm^{-1} in the pure drug to 1051.13 cm^{-1} in the nanoparticle), indicating mild interactions with the polymeric matrix. Additionally, a band at 851.03 cm^{-1}, assigned to N-H wagging, was retained in the nanoparticle formulation with reduced intensity (Table 4.1).

Table 4.1: FTIR vibrational frequencies of lamivudine

Functional groups	**Pure lamivudine (cm^{-1})**	**Lamivudine nanoparticles (cm^{-1})**
C-H stretch	3204.14	2024.64
C=C stretch	1607.69	1607.80
C-N stretch	1057.54	1051.13
N-H scissoring	1633.48	1646.03
N-H wagging	851.03	850.84

In the spectrum of pure abacavir, a distinct C-H stretching vibration was observed at 2822.91 cm^{-1}, which was absent in the nanoparticle formulation, similar to the reaction noticed in the lamivudine

nanopowder. The N-H stretching band, initially at 1621.69 cm^{-1}, shifted to 1643.80 cm^{-1} in the nanoparticle formulation. A similar observation was made in the C=O stretching vibration, which shifted from 1660.36 cm^{-1} to 1643.80 cm^{-1}. The C-N stretching band also shifted slightly (from 1290.42 cm^{-1} to 1292.86 cm^{-1}). Key bands such as 621.12 cm^{-1} (N-H wagging) and 1137.50 cm^{-1} (S=O or ring vibration) were retained with minimal shifts in the fingerprint region (Table 4.2).

Table 4.2: FTIR vibrational frequencies of abacavir.

Functional groups	Pure abacavir (cm^{-})	Abacavir nanoparticles (cm^{-})
C-N stretch	1290.42	1292.86
N-H stretch	1621.69	1643.80
N-H wag	621.12	623.22
C-H stretch	2822.91	-
C=O stretch	1660.36	1643.80
S=O stretch	1137.50	1144.80

The FTIR analysis of abacavir and lamivudine, in both their pure/free and encapsulated/nanoparticle forms, revealed notable spectral changes that indicate successful drug encapsulation and possible molecular interactions with formulation excipients. In both cases, the disappearance of the C–H stretching bands in the nanoparticle spectra observed at 2822.91 cm^{-1} for abacavir and 3204.14 cm^{-1} for lamivudine suggests that these groups were likely involved in intermolecular interaction, such as hydrogen bonding or dipole–dipole interactions, with the polymer matrix (Ryu et al., 2011). Additionally, slight shifts in N–H and C=O stretching bands, along with changes in peak intensity, further support the formation of intermolecular interactions, which may have altered the vibration of the functional groups involved. Despite these modifications, the fingerprint region (500 - 1500 cm^{-1}) of both drugs remained largely intact, with minor shifts and preserved characteristic bands, indicating that the core chemical structure of the

drugs was not compromised during nanoparticle formation (Segall, 2019). Overall, the FTIR results confirm the successful nanoencapsulation of both drugs.

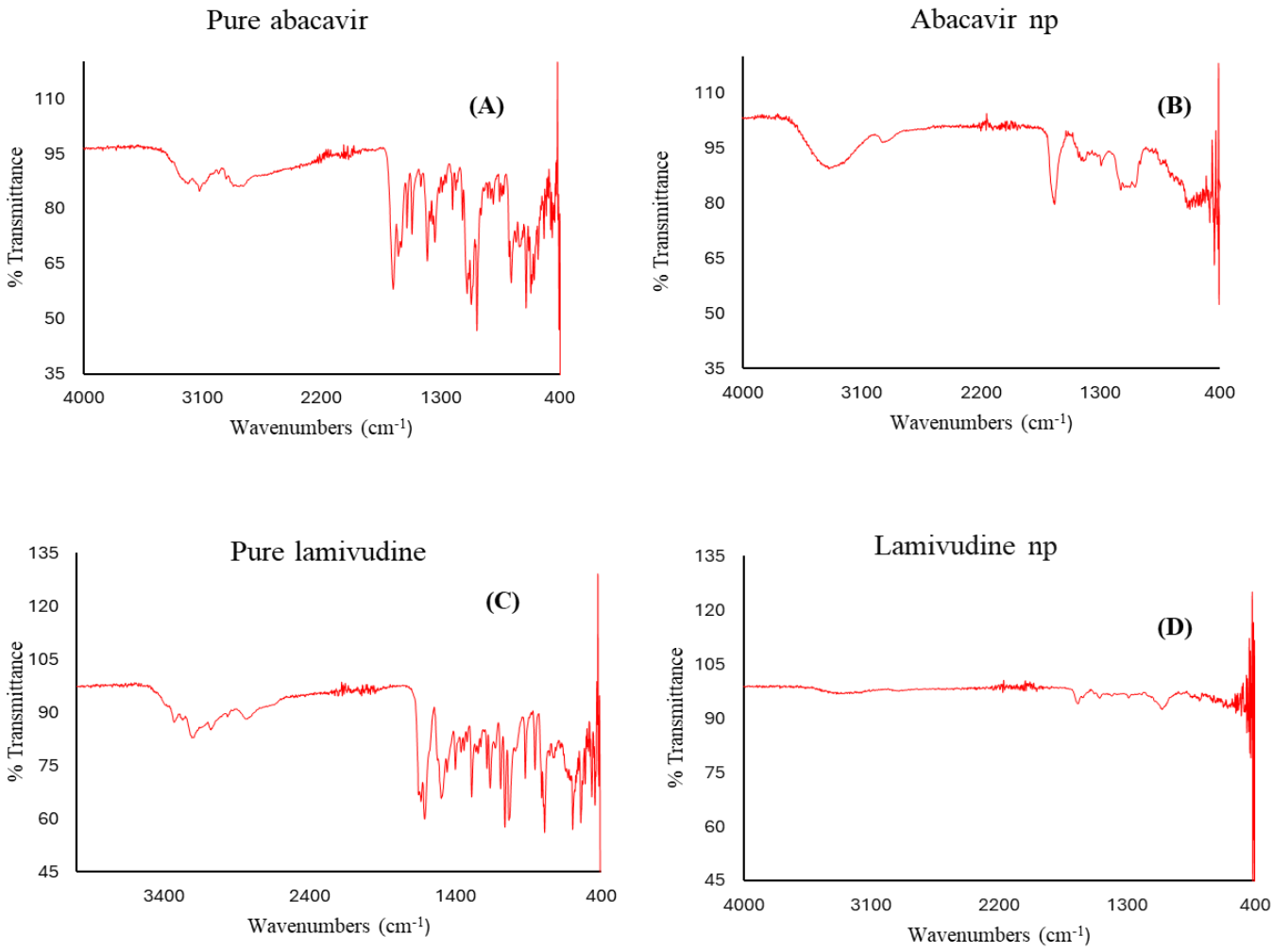

Figure 4.4. FTIR spectra of (A) unformulated abacavir, (B) abacavir nanoparticles, (C) unformulated lamivudine, and (D) lamivudine nanoparticles.

4.0.3.3. Surface morphology of nanoparticles using SEM

Scanning electron microscopy (SEM) images were also used to further analyse the surface morphology of both abacavir and lamivudine nanoparticles, which were also found to be spherical, with some level of agglomeration observed on both free drug particles at higher magnification, as shown in Figure 4.5. (B) and (D). These observations confirmed the findings from the TEM analysis.

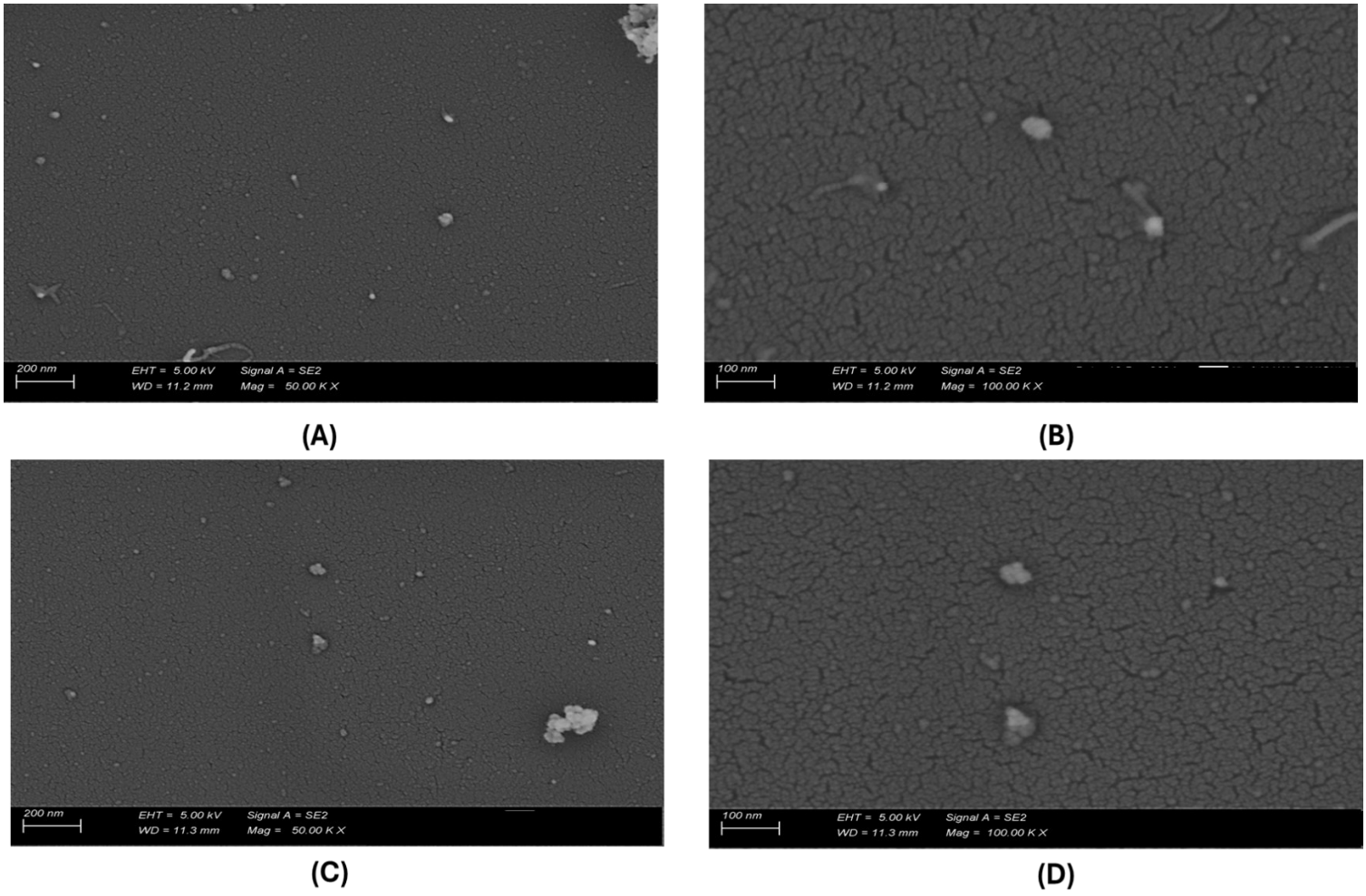

Figure 4.5. SEM images of nanoencapsulated abacavir (A, B) and lamivudine (C, D) (magnification 50,000x and 100,000x).

4.0.3.4. Encapsulation Efficiency

The percentage of drug encapsulated within the nanoparticles was 27% ± 5% for abacavir and 42% ± 5% for lamivudine, indicating the amount of each drug encapsulated within the nanoparticles' core. The noticeably higher encapsulation efficiency of lamivudine compared to abacavir may be attributed to differences in their physicochemical properties, particularly solubility and ionicity. Lamivudine, being more hydrophilic, had favorable interactions with the polymeric matrix, which might have enhanced its entrapment. In contrast, abacavir's comparatively lower solubility and less favorable ionic interactions with the polymers could have limited its incorporation (Cheow & Hadinoto, 2011).

4.0.3.5. Drug Loading Efficiency

The overall drug loading efficiency (which included encapsulated and surface drug) of both Abacavir and Lamivudine was similar, with Abacavir at 84% ± 1% and Lamivudine at 83% ± 2%, confirming the compatibility of both drugs with the excipient and minimal drug loss during the processing method.

4.0.3.6. Hydrodynamic diameter, Polydispersity Index, and Zeta Potential

The hydrodynamic diameter (particle size) confirmed that both abacavir and lamivudine nanoparticulates were within the nano range, with abacavir having an average diameter of 164 nm ± 26 nm and lamivudine at 200 nm ± 26 nm (Figure 4.6). The values obtained are related to those generated from the Image J analysis of the TEM sample images (i.e., abacavir = 64 nm ± 34 nm; lamivudine = 77 nm ± 32 nm). The slightly bigger particle sizes observed with measurements executed with the dynamic light scattering method may be associated with a level of particulate

swelling (peripheral) considering the wet state of the particles tested, while the TEM imaging made use of dehydrated nanoparticulate samples. These further support the earlier findings that the nanoencapsulation of the abacavir and lamivudine within their individual polymeric matrices was achieved.

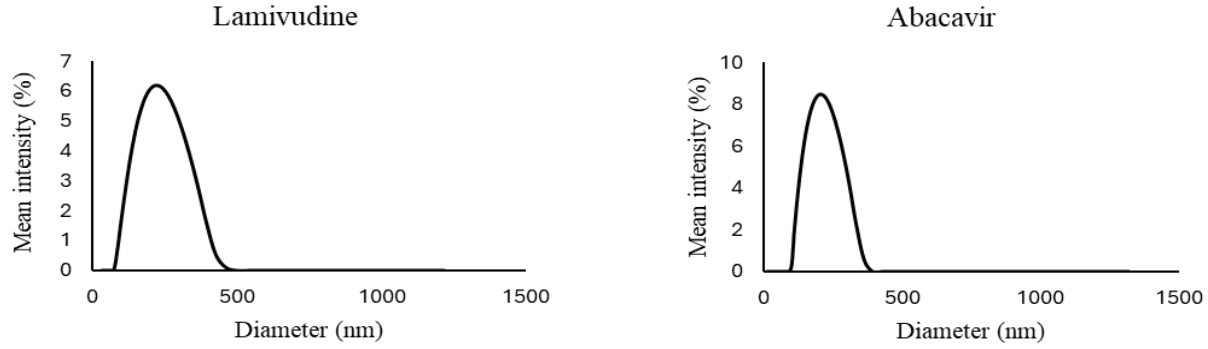

Figure 4.6. Hydrodynamic diameter of lamivudine and abacavir nanoparticles.

The polydispersity index (PDI) of nanoencapsulated abacavir was 0.3000 ± 0.0026, and for lamivudine, it was 0.2800 ± 0.0027. A PDI value of ≤ 0.3 generally indicates a narrow size distribution, which is ideal for ensuring consistent drug release and stability. The zeta potential for abacavir was -31.3 mV ± 1 mV, and for lamivudine, it was -30.7 mV ± 0.8 mV (Figure 4.7). A higher absolute zeta potential (either positive or negative) typically ≥ 30 suggests good colloidal stability and reduces the likelihood of aggregation. Therefore, both values indicate a stable nanodispersion (Németh et al., 2022).

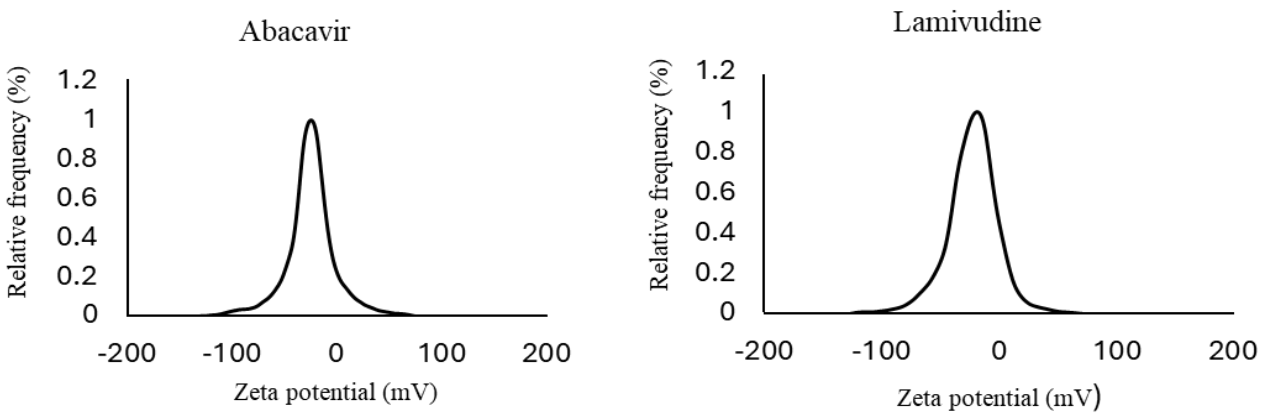

Figure 4.7. Graphical representation of abacavir and lamivudine nanoparticles' zeta potential.

4.0.3.7. Measurement of Powder Flow

With the powder-like physical presentation of the drug-loaded nanoparticulates, powder flow analyses were carried out as one of the quality indicators of the delivery systems fabricated. This was quantified employing the Hausner ratio, which showed that abacavir and lamivudine nanopowders had excellent flow properties following standard scales provided by the United States Pharmacopoeia (Table 3.3; Equation 3.3). The Hausner ratio for abacavir was 1.11 ± 0.04, and that of lamivudine was 1.06 ± 0.02, meaning that both nanopowders have suitable flow properties for further formulation use. Good powder flow is essential for the successful development and manufacturing of solid dosage forms; poor flowability can lead to production inefficiencies, which can affect the dose uniformity, compromise product quality, and increase manufacturing costs. Therefore, ensuring optimal powder flow is essential to achieving formulation homogeneity, process reproducibility, and regulatory compliance in pharmaceutical production (Shah et al., 2023).

4.0.3.8. Pilot Investigation of Environmental Stability of Abacavir and Lamivudine Nanopowders

There was no noticeable change in the physical appearance of the nanopowders over the entire three-month period. Specifically, there were no changes in color or odor. Furthermore, the drug content of both abacavir and lamivudine remained consistent, indicating good stability, with statistical analysis showing no significant differences in drug content over time. For abacavir, the p-value was 0.724, and for lamivudine, it was 0.166, both of which are greater than the significance threshold of 0.05, indicating no statistically significant changes in drug content during the entire study period.

Table 4.3: Drug content of abacavir and lamivudine nanopowders**.**

Time points	**Abacavir (%)**	**Lamivudine (%)**
Day 0	86.5 ± 1.7	84.6 ± 0.5
Week 2	87.3 ± 1.8	83.8 ± 2.8
Week 4	86.6 ± 2.0	81.9 ± 1.7
Week 8	83.5 ± 4.3	87.5 ± 3.3
Week 12	89.7 ± 4.9	83.3 ± 2.2

4.1. PRESENTATION AND INTERPRETATION OF RESULTS PHASE 2 — FABRICATION AND CHARACTERIZATION OF AN OPTIMIZED PHARMACEUTICAL/FLUID GEL

This section reports on the findings associated with the pharmaceutical gel (fluid gel) manufacture, quality assessments and the identification of some typifying characteristics.

4.1.1. Preliminary Screening of the Fluid Gels

The one-variable-at-a-time (OVAT) preliminary, non-systematic screening involved five fluid gels namely HG1, HG2, HG3, HG4, and HG5 (Table 3.4) which were successfully prepared. Upon visual inspection of these drug free entities, HG1 HG2 and HG3 exhibited relatively low viscosity, resulting in gels that were too watery/too thin and lacked the desired consistency to function as diluent for the drug loaded nanopowders. While these all maintained uniform consistencies with no phase separation displayed, their flow properties were not ideal for the intended application. In contrast, HG4 and HG5 produced fluid gels with a more favorable balance between viscosity and flow. The gels were neither too thick nor too thin, demonstrating a preferred consistency and a more appropriate texture compared to HG1, HG2, and HG3. All formulations were not phase separated, transparent, with good clarity, and exhibited no noticeable odor. This suggests that the excipients and method used for producing these fluid gels were well-suited and effective. The results of this experiment were applied as independent variable limits (Table 3.5) for the development of Plackett Burman Experimental Design template utilized for the systematic production and optimization of the fluid gels.

4.1.2. Design of Experiments and Selection of the Final Optimized Fluid Gel Carrier

The 15 pharmaceutical gel formulations were successfully prepared, and the parameters tested (response parameters) namely physical appearance, pH and gel strength (texture) are summarized in Table 4.4. below. On the physical appearance scale used (Section 3.2.2.1.), the gels ranked 1, 3, and 4 were all clear in color and not phase separated, while the gels ranked 2 were cloudy, with noticeable phase separation. Overall, all the fluids gels were odorless. Additionally, all the gels that contained citric acid had low pH ranging between 3 and 4 compared to gels without it which could be because of the acidic nature of citric acid (Lambros et al., 2022).

Table 4.4: Response parameters of each fluid gel.

Fluid Gels	Physical appearance	pH	Gel strength (N)
FG 1	1	5.590 ± 0.310	0.053 ± 0.002
FG 2	2	3.890 ± 0.040	0.056 ± 0.003
FG 3	3	5.710 ± 0.070	0.057 ± 0.003
FG 4	1	3.310 ± 0.010	0.053 ± 0.001
FG 5	3	5.840 ± 0.050	0.056 ± 0.006
FG 6	2	3.480 ± 0.240	0.054 ± 0.006
FG 7	2	3.840 ± 0.050	0.055 ± 0.002
FG 8	1	6.020 ± 0.110	0.053 ± 0.002
FG 9	2	3.310 ± 0.090	0.025 ± 0.002
FG 10	2	3.600 ± 0.100	0.023 ± 0.001
FG 11	1	5.820 ± 0.130	0.053 ± 0.002
FG 12	4	3.370 ± 0.160	0.056 ± 0.001
FG 13	2	3.650 ± 0.150	0.053 ± 0.001
FG 14	2	3.940 ± 0.110	0.055 ± 0.002
FG 15	2	5.760 ± 0.070	0.025 ± 0.000

To select the lead fluid gel that served as an optimal secondary encapsulant for a fixed dose of the abacavir and lamivudine nanopowders, a response surface regression founded on multiple response parameters (i.e., physical appearance, pH and gel strength) generated was applied. This process encompassed constrained simultaneous optimization of the independent variables (Table

3.5) relative to the responses (Table 4.4) using the Minitab® Version 21.1.0 Statistical Software. To accomplish this goal, physical appearance (PA), pH and gel strength (GS) were set at target levels that produced a fluid gel with desirable flow characteristics, closest to neutral pH, non-segregated/homogenous appearance and moderate textural strength. Model fitting generated R^2 values close to 100% and p-values less than 0.05, excluding the physical appearance of the gels, which had an insignificant value of 35.83% and p-value = 0.91. A composite desirability value of 0.97 (with 1 being the best) for the combination of responses optimized was obtained which signifies model reliability and suitability (Rampedi et al., 2023). Although physical appearance displays non-significance, it was still factored into the optimization process because of its relevance to the gels' presentation and applicability as a diluent for the nanopowders to produce the nanosuspension formulation. Following these tasks, an optimized polymeric fluid gel was produced based on predicted responses. The accuracy of the statistical design in predicting the final optimized gel carrier was achieved by preparing the fluid gel based on computed formula and matching the experimentally derived response parameters with the predicted ones. A close relationship between these sets of experimental and predicted readings was found thus corroborating the correctness of the design of experiments strategy utilized. The results are presented in Table 4.5 below.

Table 4.5: Numerical values of the statistical optimization process

Optimized Fluid Gel	**Indicators of Plackett Burman Design Suitability**					
	Responses	**Experimental**	**Predicted**	**R^2 (%)**	**p-value**	**Desirability**
HPMC = 0.100g	PA	1.000 ± 0.001	1.250	35.830	0.936	0.938
HEC = 0.000 g	pH	5.510 ± 0.220	5.783	99.460	0.001	0.993
SSG = 0.100 g	GS (N)	0.054 ± 0.002	0.052	93.280	0.018	0.938
XYL = 2.000 g	**Composite desirability**					**0.969**
PEG/PVA = 0.100 g						
MC = 0.100 g						
GEL = 0.200 g						
CA = 0.000 g						

PA = Physical appearance; HPMC =Hydroxypropyl methylcellulose; HEC = Hydroxy ethyl cellulose; SSG = Sodium starch glycolate; XYL = Xylitol; PEG/PVA = Polyethylene glycol/ Polyvinyl alcohol; MC = Methyl cellulose; GEL = Gelatin; CA = Citric acid

4.1.3. Evaluation and Characterization of Optimized Gel

4.1.3.1. Physicochemical Properties of the Optimized Pharmaceutical Gel

The optimized fluid gel was successfully formulated and its physical appearance as well as its viscosity and gel strength were evaluated. The optimized gel was a clear, homogeneous liquid with a pourable consistency and an odorless nature.

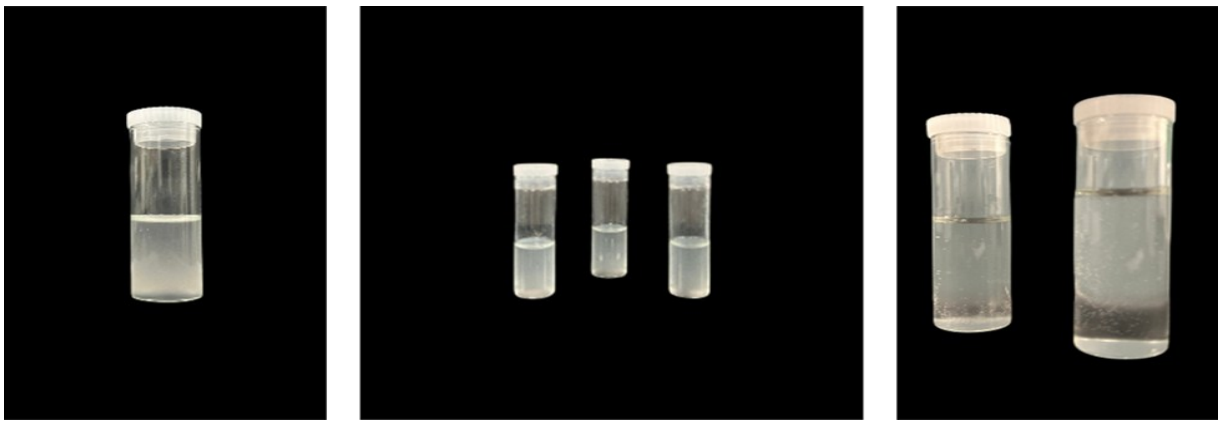

Figure 4.8. Digital images of the optimized pharmaceutical gel.

The experimental values of the physical appearance, pH and gel strength were compared to the predicted values generated by the Minitab software (Table 4.5). Statistical analysis revealed no significant differences between the experimental and predicted values, with p-values for gel strength and pH being 0.281 and 0.199, respectively. The slight differences in values were attributed to random sampling variability.

4.1.3.2. Viscosity of the Optimized gel

The optimized gel's viscosity was measured at 348 mPa.s ± 2.7 mPa.s. The viscosity value is an important parameter as it directly impacts the formulation's gastrointestinal transit time, absorption rates, and drug release profile. (Hassan and Hasari, 2022)

4.1.3.3. Scanning Electron Microscopy Images

The SEM images reveal the gel's sponge-like and porous structure, interconnected by fibrous networks. Additionally, crystal-like formations are observed on the surface. The pores in the gel suggest that it may facilitate the entrapment of the drug molecules to promote controlled release, and the presence of crystalline regions may indicate areas where the crystalline excipients like xylitol are located, which could be relevant for the drug release behavior and the bioavailability of the final drug product.

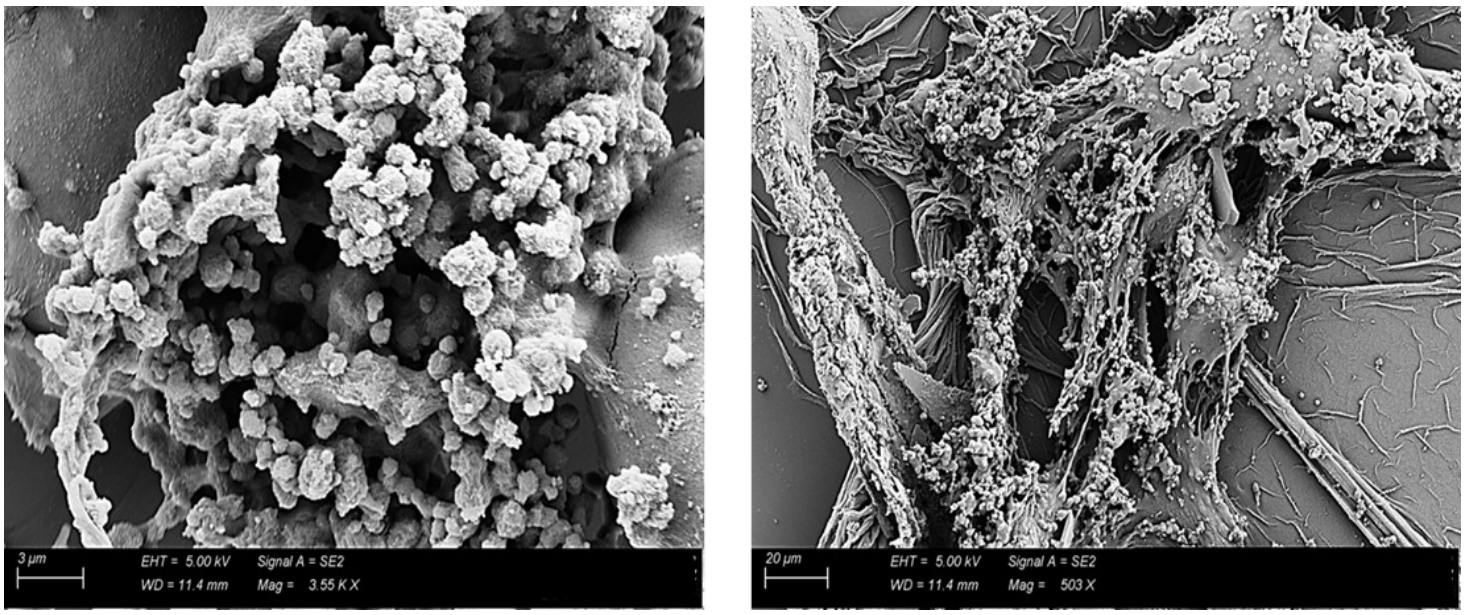

Figure 4.9. SEM images of optimized pharmaceutical gel at different magnifications – 3550x and 503x.

4.1.3.4. Stability Studies of the Optimized Pharmaceutical Gel

The stability of the gels studied over a three-month period demonstrated no changes in overall physical properties such as homogeneity, odor, or color. Additionally, the pH ($p = 0.368$) and gel strength ($p = 0.836$) values showed no statistically significant changes throughout the test period, indicating no degradation over the entire duration.

Table 4.6: Results of stability studies (stability indicators)

Time points	Gel strength (N)	pH
Day 0	0.054 ± 0.002	5.510 ± 0.220
Week 2	0.053 ± 0.001	5.440 ± 0.040
Week 4	0.053 ± 0.001	5.450 ± 0.300
Week 8	0.054 ± 0.001	5.400 ± 0.230
Week 12	0.053 ± 0.001	5.700 ± 0.010

4.2. PRESENTATION AND INTERPRETATION OF RESULTS PHASE 3 — PREPARATION AND EVALUATION OF THE FIXED DOSE ABACAVIR/LAMIVUDINE NANOSUSPENSION FORMULATION

This phase reports the results and evaluation of the nanobased suspension formulation.

4.2.1. Physical Assessment of the Formulated Fixed dose Nanosuspension Formulation

The combination of the abacavir and lamivudine nanopowders and the optimized pharmaceutical gel produced the fixed dose nanosuspension formulation of abacavir and lamivudine (40 mg/20 mg) per 5 mL and formed a stable colloidal suspension that was odorless and exhibited a slight golden color (Figure 4.10). it demonstrated optimal flow characteristics, making it easily dispensable and. The suspension's physical properties were well-suited for its intended purpose, with an aesthetically pleasing subtle golden hue.

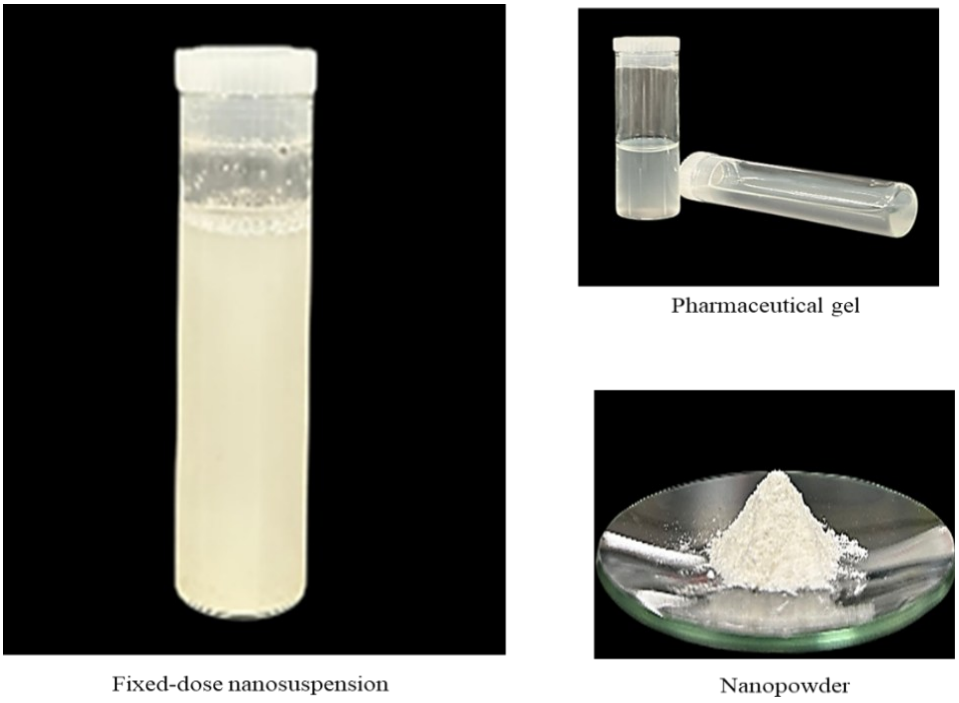

Figure 4.10. Image of the fixed dose nanobased suspension.

4.2.2. Evaluating the Quality of the Nanobased Suspension

4.2.2.1. Studies Comparing Select Physicochemical Properties of the Nanosuspension Formulation with Comparator Products

The physicochemical properties of the suspension such as the strength, pH and viscosity were compared to those of three commercially available gel-like liquid suspension formulations (i.e., Advil®, Motrin® and Tylenol®) as shown in Table 4.7. given below. These were selected as references because to date, no liquid suspension of fixed dose lamivudine/abacavir is available so these prototype paediatric suspension formulations were employed for this comparative analyses (Table 4.7).

Table 4.7: Comparison of the nanosuspension's physicochemical properties with the reference comparator products.

Test parameters	**Abacavir/Lamivudine Nanosuspension**	**Advil®**	**Motrin®**	**Tylenol®**
Gel strength (N)	0.042 ± 0.002	0.052 ± 0.005	0.025 ± 0.002	0.024 ± 0.003
pH	4.100 ± 0.030	4.200 ± 0.130	3.800 ± 0.040	5.400 ± 0.040
Viscosity (mPa.s)	177.3 ± 0.570	303.7 ± 12.40	184.6 ± 0.570	261.0 ± 1.000

The textural strength of the fixed dose nanosuspension developed was significantly different when compared to all three reference formulations ($p < 0.001$). The viscosity of the nanosuspension was significantly lower when compared to both Advil® and Tylenol®, while the comparison with Motrin® was not statistically significant ($p = 0.188$). Similarly, the pH of the suspension was significantly higher than Motrin® and lower than that of Tylenol®, but the difference with Advil® was not statistically significant ($p = 0.789$). This indicates that the nanosuspension possessed similar physical qualities compared with the commercially available paediatric suspension drug products thus demonstrating its practical utilization in these population.

4.2.2.2. Fourier Transform Infrared Spectroscopy on Abacavir/Lamivudine Nanosuspension

The FTIR spectra of abacavir and lamivudine in the nanosuspension formulation were analyzed and compared with those of the nanoencapsulated and free drugs, as shown in Table 4.8. The FTIR spectrum of the fixed dose suspension displayed subtle shifts at similar positions to those observed in the nanoencapsulated formulations of abacavir and lamivudine. Notably, the C-H stretching bands, which were present in the spectra of the pure drugs, were again absent in the suspension spectrum, suggesting a consistent pattern of drug-excipient interactions across both formulation types. These interactions are likely due to hydrogen bonding or dipole-based associations that alter the vibrational environment of the affected functional groups. Despite these changes, the fingerprint region remained largely intact for both drugs, and important peaks, such as the C-N and N-H wagging vibrations, were retained, indicating that the core molecular structures were preserved. These findings suggest that while the suspension matrix interacts with the drugs like the nanoparticle system, it does so without compromising chemical stability, further supporting the suitability of this formulation approach.

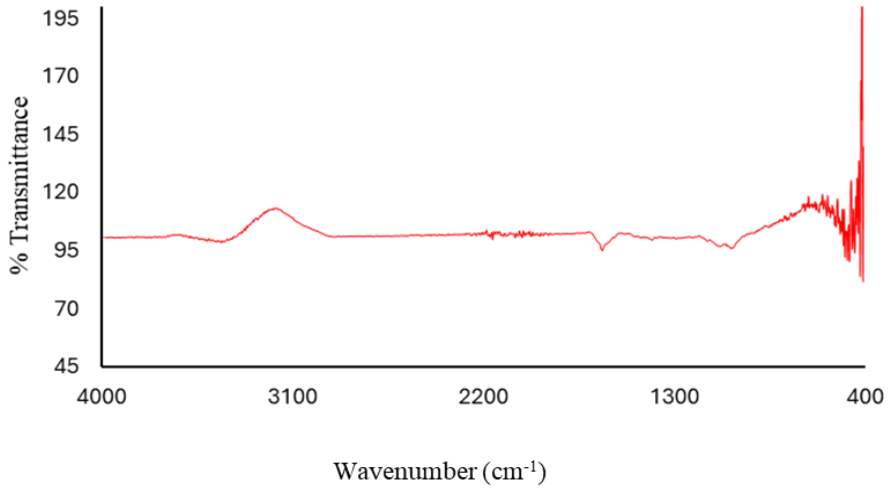

Figure 4.11. FTIR spectra of the suspension

Table 4.8. Vibrational frequencies of abacavir and lamivudine in nanosuspension compared to their respective pure drugs and nanoencapsulated drugs

Drugs	**Functional groups**	**Pure drug (cm^{-1})**	**Nanopowder (cm^{-1})**	**Nanosuspension (cm^{-1})**
Abacavir	C-N stretch	1290.42	1292.86	1119.49
	N-H stretch	1621.69	1643.80	1637.15
	N-H wag	621.12	623.22	625.40
	C-H stretch	2822.91	-	-
	S=O stretch	1137.50	1144.80	1110.49
Lamivudine	C-H stretch	3204.14	-	-
	C=C stretch	1607.69	1607.80	1601.70
	C-N stretch	1057.54	1051.13	1053.17
	N-H scissoring	1633.48	1646.03	1648.56
	N-H wagging	851.03	850.84	854.86

4.2.2.3. Scanning Electron Microscopy

The SEM image of the nanosuspension formulation showed evidence of drug deposition (Figure 4.12 (B)), likely resulting from diffusion or physical entrapment within the gel's pores. The observed aggregation in the image may be attributed to drug crystallization or interactions between the drug and the gel matrix. These structural differences suggest that the formulation successfully encapsulates the drug, supporting the effectiveness of the double encapsulation strategy designed to protect the drug

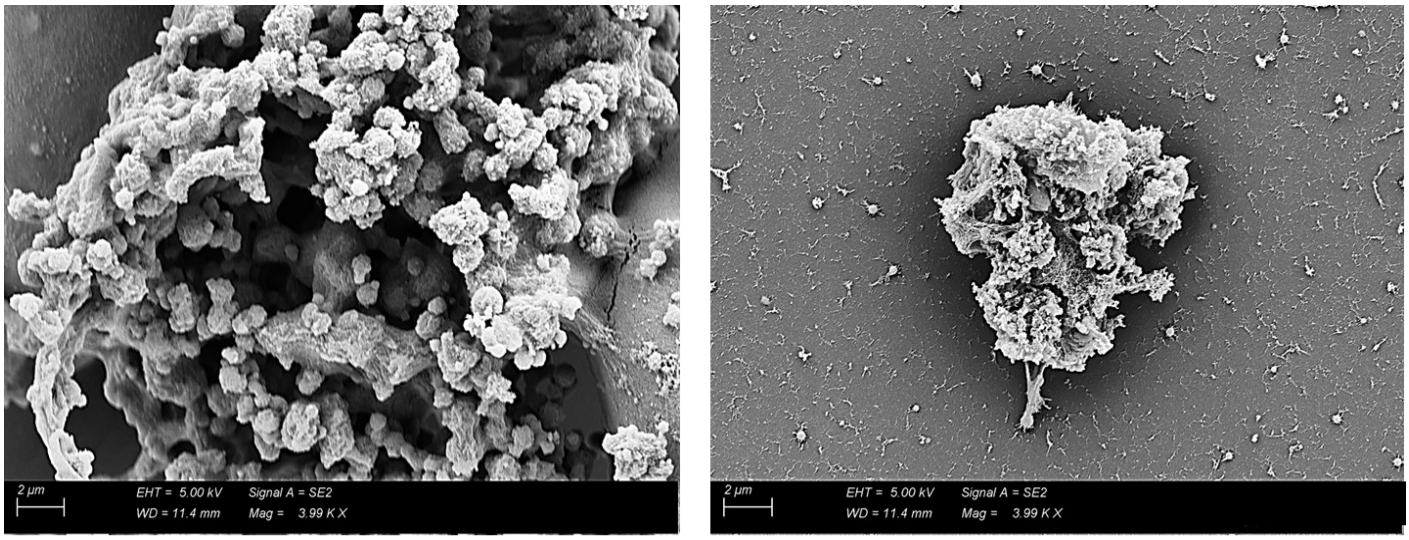

Plain gel **Suspension**

Figure 4.12. SEM images of the pure pharmaceutical/fluid gel and drug loaded nanosuspension formulation

4.2.2.4. Drug Release Kinetics in Simulated Gastric Fluid

The drug release profiles of abacavir and lamivudine from the nanobased suspension formulation exhibited a complete release (≈ 100%) within 15 minutes. Drug release was initiated at 5 minutes for both drugs with 19 % and 25 % attained for abacavir and lamivudine respectively. This immediate release behavior ensures that the active drugs are available for absorption (initiating pharmacotherapy) shortly after administration (Wheless & Phelps, 2018). Interestingly, the concentrations of both drugs were maintained for up to 4 hours, which corresponds to the average gastric emptying time (2-5 hours) (Lee et al., 2014). This suggests that the nanosuspension formulation provides protection from the acidic gastric pH, allowing the drugs to reach the small intestine where absorption occurs (Ensign et al., 2012). The release kinetics of both abacavir and lamivudine from the nanosuspension were best described by the Korsmeyer-Peppas model (with lag phase), as indicated by the highest correlation coefficient (R^2) and the lowest Akaike

Information Criterion (AIC) values. Mathematical analysis performed using the KinetDS software (version 3.0, open-source freeware) revealed an R^2 of 0.692 and an AIC of 97.369 for abacavir, while for lamivudine, the R^2 was 0.701 and the AIC was 71.510, demonstrating a better fit for the Korsmeyer-Peppas model. The lag phase was observed at 5 minutes which was the initial stage of the drug release before the complete release of both drugs. The exponent (n) values of both abacavir and lamivudine were less than 0.5 (0.180 and 0.138) respectively which indicates that drug release is not solely dependent on diffusion (Lisik & Musiał, 2019).

Table 4.9: Drug release models and their fit parameters

Drug release models	**Pure ABC**		**ABC susp**		**Pure 3TC**		**3TC susp**	
	R^2	**AIC**	**R^2**	**AIC**	**R^2**	**AIC**	**R^2**	**AIC**
First order	0.782	56.913	0.140	105.305	0.789	44.604	0.131	79.914
Zero order	0.742	57.407	0.112	102.257	0.737	45.686	0.107	78.069
Korsmeyer Peppas with lag	0.637	65.478	0.692	97.3695	0.673	43.703	0.701	71.510

Note: Pure ABC – unformulated abacavir; ABC susp – Abacavir in Nanosuspension; Pure 3TC =unformulated lamivudine; 3TC susp = Lamivudine in Nanosuspension; AIC = Akaike information criterion

In contrast, the dissolution profiles of the unformulated free drugs showed faster release. Pure lamivudine achieved 100% dissolution within 5 minutes, after which its concentration declined over the subsequent 4 hours, reflecting a rapid release and drug decomposition. Similarly, pure abacavir dissolved rapidly, with over 80% of the drug released within 5 minutes, followed by a decline in concentration over time, which may represent drug degradation. This behavior is explained by the first-order kinetic model, which best fits both drugs with the R2 of abacavir being 0.782 and AIC of 56.913 and that of lamivudine being 0.789 and AIC of 44.604, making it best fitted for the type of drug release observed.

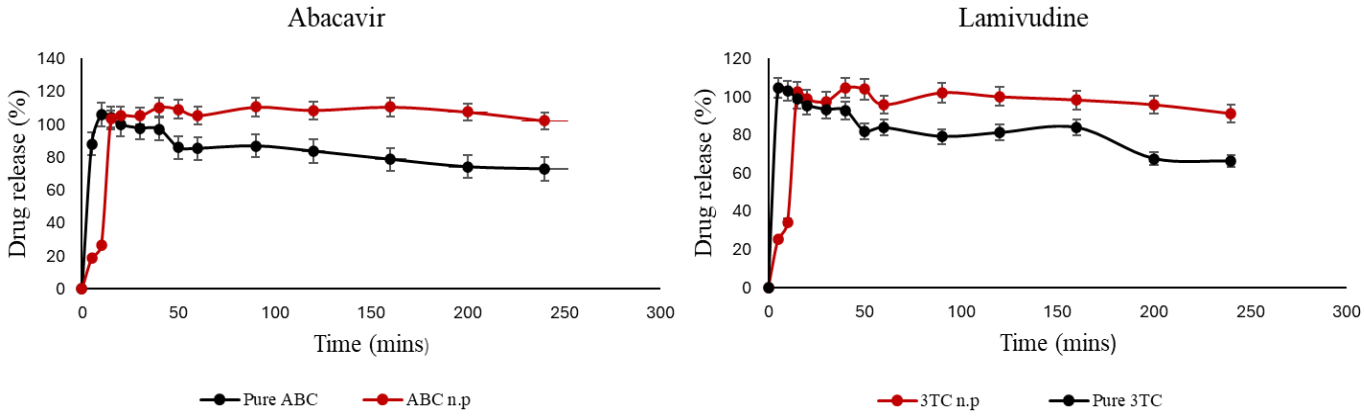

Figure 4.13. Drug release of formulated and unformulated abacavir and lamivudine

4.2.2.5. Stability Studies on the Nanobased Suspension

The abacavir/lamivudine fixed dose nanosuspension formulation demonstrated excellent stability over a 4-week period at 30°C ± 2°C and 65% ± 5% relative humidity, with no statistically significant changes observed across all stability indicators (p values were all above 0.05). The physical appearance of the nanosuspension remained consistent throughout the study, with no noticeable changes in color or smell. Furthermore, the nanosuspension did not exhibit any signs of sedimentation during the entire duration of the study, indicating that it remained stable and homogenous. These results suggest that the formulation is physically stable and that it can maintain its intended characteristics over the 28-day period and possibly more.

Table 4.10: Results of stability indicators

Parameters	Day 0	Week 1	Week 2	Week 3	Week 4
Textural strength (N)	0.043 ± 0.002	0.044 ± 0.001	0.042 ± 0.002	0.044 ± 0.001	0.044 ± 0.001
pH	3.88 ± 0.050	3.75 ± 0.030	3.50 ± 0.050	3.86 ± 0.040	3.83 ± 0.020
Lamivudine drug content (%)	81.6 ± 1.000	80.2% ± 2.400	81.5% ± 2.400	81.9% ± 0.100	87.5% ± 3.300
Abacavir drug content (%)	85.7 ± 2.600	85.5% ± 3.800	88.7% ± 4.600	84.9% ± 4.100	85.1% ± 1.400

Since the nanosuspension was stored under amber conditions, it is reasonable to conclude that optimal storage conditions for this nanosuspension formulation involved protection from light, which may degrade the active ingredients as a lot of drugs are generally sensitive to light which may lead to reduced potency and efficacy of the drugs (Ahmad et al., 2016). The fact that the nanosuspension formulation does not require refrigeration after reconstitution is a significant advantage, especially because HIV is endemic in resource-limited settings where access to electricity and refrigeration may be limited (Hansoti et al., 2017).

4.2.3.6. In-Vitro Cytotoxicity Studies

The cytotoxicity of the nanosuspension formulation was assessed using HepG2 cells (human liver carcinoma cell line), which were chosen because hepatic cells are primarily responsible for most oral drug metabolism; thus, they are commonly used in cytotoxicity testing (Harjumäki et al., 2019). Dextran and Triton X-100 were used as negative and positive controls, respectively. Triton X-100, as a known cytotoxic agent (Choi et al., 2019), demonstrated a significant reduction in cell viability, serving as a positive control, while dextran showed no cytotoxicity.

The cytotoxicity studies revealed that unformulated pure abacavir/lamivudine induced significant toxicity with four out of the five tested concentrations (0.15, 0.3 and 0.6 mg/ml), showing a significant decrease in cell viability ($p < 0.001$) as illustrated in Figure 4.14. The highest

concentration of the unformulated drugs (0.6 mg/ml) was particularly toxic to the cells with only 25.8 % viability, which was lower than Triton-X-100. Whereas the lowest concentration (0.437 mg/ml) did not exhibit any significant cytotoxicity. This finding demonstrates the cytotoxic effect of these drugs when administered in high doses in their pure form.

On the contrary, the drug free nanosuspension suspension showed support for cell growth at the lower concentrations (0.412, 0.825, 1.2 mg/ml). At the highest concentration (6.6 mg/ml), however, significant toxicity with a decrease of up to 42.8% was observed (Figure 4.14) ($p < 0.001$), indicating that while the placebo formulation is generally safe at lower doses, higher concentrations may be detrimental to cell viability.

The abacavir/lamivudine nanosuspension formulation demonstrated improved cytocompatibility compared to the unformulated drugs. At lower concentrations (0.437, 0.875, and 1.75 mg/ml), cell viability was greater than 100%, as seen in Figure 4.14, although they were not statistically significant for the proliferation of HepG2 cells. At these concentrations, the formulated drugs did not exhibit significant toxicity, indicating that the encapsulated or protected formulation of abacavir/lamivudine provided a safer profile compared to the unformulated pure drugs. At higher concentrations, no significant cytotoxicity was observed, demonstrating the potential of the nanosuspension formulation to improve the cytocompatibility of the drugs, likely due to the formulation's protective effect that mitigates the toxic side effects commonly observed with high doses of these therapeutic compounds.

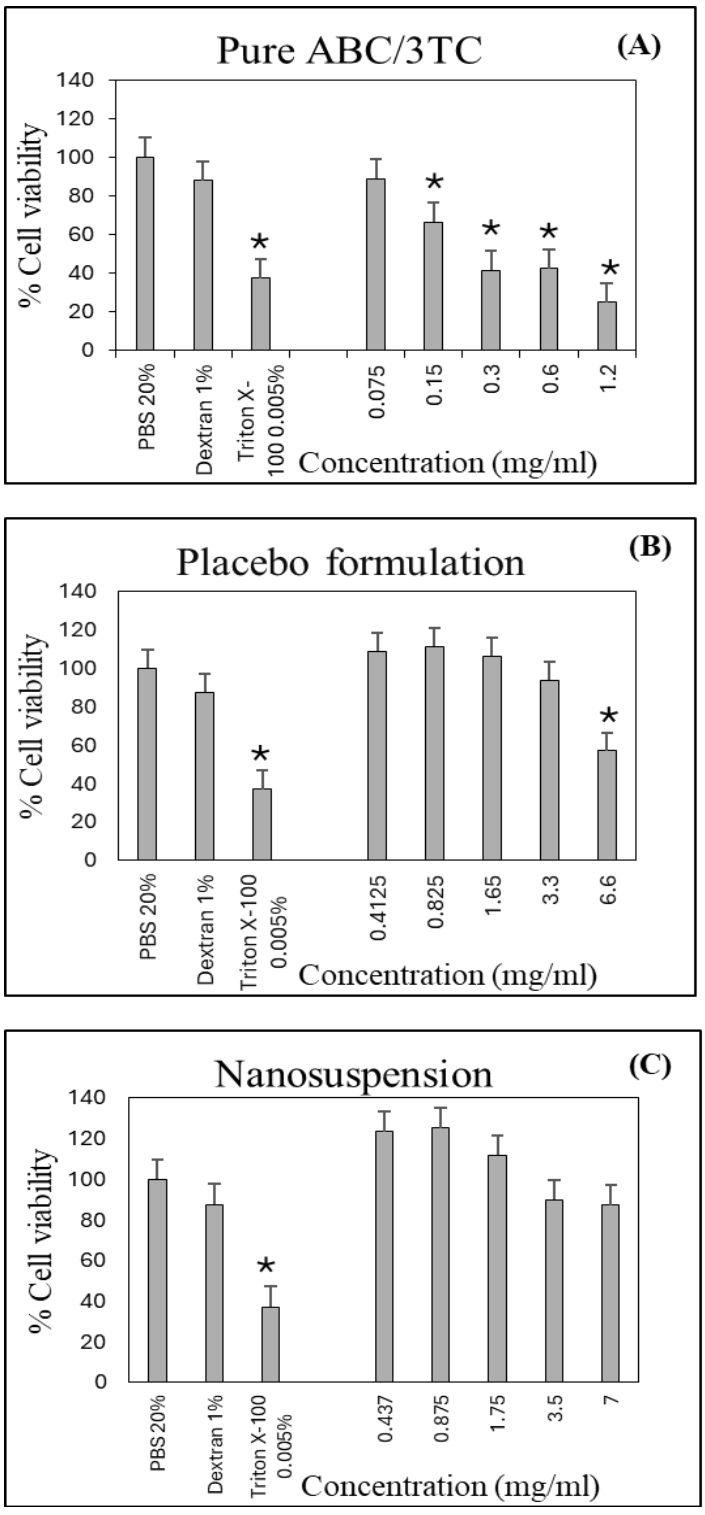

Figure 4.14. Illustration of the cytotoxicity studies of pure abacavir and lamivudine (A), placebo formulation (B), and the nanosuspension (C).

CHAPTER 5: CONCLUSION AND FUTURE PERSPECTIVE

5.0. CONCLUSION

This research successfully developed a fixed dose nanosuspension formulation containing abacavir and lamivudine for the treatment of HIV in children, aiming to provide a more appropriate dosage form for this age group. The nanopowders of abacavir and lamivudine were effectively produced using the salting-out technique, resulting in hydrodynamic diameters of 164 nm ± 26 nm for abacavir and 200 nm ± 26 nm for lamivudine. Transmission and Scanning Electron Microscopy (TEM and SEM) analysis confirmed their spherical morphology. Both nanopowders demonstrated favorable properties, with polydispersity index (PDI) values of 0.3 for abacavir and 0.28 for lamivudine, indicating narrow particle size distributions. The zeta potential values of -31.3 mV ± 1 mV for abacavir and -30.7 mV ± 0.8 for lamivudine suggest a stable system. Furthermore, the nanopowders exhibited stability under room conditions for up to 3 months, with no significant changes in physical appearance or drug content, indicating long-term stability.

The pharmaceutical/fluid gel, which functioned as a dispersion medium (secondary encapsulant), was also optimally fabricated. It exhibited desirable physicochemical properties, including a gel strength of 0.054 N ± 0.002 N and a pH of 5.5 ± 2.02, which is close to the physiological pH of the mouth (6.7–7.3), an important consideration for oral formulations (Baliga et al., 2013). The gel was stable for up to 3 months under ambient conditions

The abacavir and lamivudine nanopowders were incorporated into the optimized fluid gel to produce the fixed dose nanosuspension formulation. The physicochemical properties of the

nanosuspension, including viscosity (177.3 ± 0.6 mPa.s) and pH (4.1 ± 0.030), were comparable to commercially available regular paediatric liquid suspensions such as Motrin® (viscosity: 184.7 ± 0.6) and Advil® (pH: 3.8 ± 0.13), demonstrating its suitability for paediatric use. The drug release profile of the nanosuspension followed zero-order kinetics, indicating the independent release of both drugs in a regulated fashion. Stability studies of the reconstituted suspension stored under ambient conditions (no refrigeration) over one month, showed no drug degradation or changes in the physical appearance of the nanosuspension formulation thus making it an attractive option in resource limited settings where HIV is majorly predominant.

Furthermore, in vitro cytotoxicity studies on HepG2 cells revealed that the formulation exhibited greater cytocompatibility compared to the unformulated drugs or placebo, suggesting that the formulation is safe for further clinical exploration.

Finally, this work contributes to the development of child-friendly fixed dose orally delivered liquid formulations for paediatric HIV treatment and can be used to simplify the treatment of other ailments that require multiple drugs for treatment, providing a viable alternative to current treatment options which often require multiple formulations.it also provides more options to older/adult patients who prefer oral liquid dosage forms or those who are experiencing difficulty swallowing.

5.1. FUTURE RECOMMENDATIONS

Although the proposed drug delivery system successfully encapsulated both abacavir and lamivudine, a complete HIV treatment regimen typically requires the inclusion of three antiretroviral agents. Therefore, incorporating an additional drug (such as Dolutegravir) into the

formulation would be beneficial for providing a comprehensive and effective treatment for paediatric HIV. Additionally, while the drug release profile demonstrated stability in acidic conditions, conducting further drug release studies in simulated intestinal fluid (SIF) is crucial. This will help confirm that the drugs are successfully released in the small intestine, where absorption occurs, ensuring the formulation's effectiveness.

While the pH of the suspension is comparable to Advil®, there was a slight shift in pH when compared to the plain pharmaceutical/fluid gel. To ensure that the formulation remains stable and safe for paediatric use, it may be essential to introduce pH stabilizers to maintain the pH as close to the physiological pH of the mouth (6.7-7.3) as possible.

Since nanoparticles have been shown to enhance drug absorption, potentially reducing the required dosage, pharmacokinetic studies are recommended to assess the absorption, distribution, metabolism, and excretion (ADME) profiles of the formulation in vivo. This would help evaluate the formulation’s performance more comprehensively.

Furthermore, detailed organoleptic studies (e.g., using the electronic tongue, nose) should be conducted to assess and optimize the sensory characteristics (taste, color, and smell) of the formulation, ensuring it is more acceptable and palatable for the paediatric population, which is crucial for adherence to long-term HIV treatment.

Finally, advancing this formulation for commercial use is crucial, but it does not come without challenges, particularly in areas like technology transfer for large-scale manufacturing and meeting

stringent regulatory requirements. To move forward, it will be important to conduct scale-up studies to ensure manufacturing feasibility and begin early engagement with regulatory agencies to navigate paediatric-specific guidelines and ensure compliance.

REFERENCES

1. Abedin, S., & Adeleke, O. A. (2024). State of the art in paediatric nanomedicines. *Drug Delivery and Translational Research*, *14*(9), 2299–2324. https://doi.org/10.1007/s13346-024-01532-x.
2. Achenbach, C. J., Scarsi, K. K., & Murphy, R. L. (2010). Abacavir/Lamivudine Fixed dose Combination Antiretroviral Therapy for the Treatment of HIV. *Advances in Therapy*, *27*(1), 1–16. https://doi.org/10.1007/s12325-010-0006-9.
3. Adeleke, O. A., Hayeshi, R. K., & Davids, H. (2020). Development and Evaluation of a Reconstitutable Dry Suspension Containing Isoniazid for Flexible Paediatric Dosing. *Pharmaceutics*, *12*(3), Article 3. https://doi.org/10.3390/pharmaceutics12030286.
4. Adepu, S., & Ramakrishna, S. (2021). Controlled Drug Delivery Systems: Current Status and Future Directions. *Molecules*, *26*(19), 5905. https://doi.org/10.3390/molecules26195905.
5. Adkison, K., Wolstenholme, A., Lou, Y., Zhang, Z., Eld, A., Perger, T., Vangerow, H., Hayward, K., Shaefer, M., & McCoig, C. (2018). Effect of Sorbitol on the Pharmacokinetic Profile of Lamivudine Oral Solution in Adults: An Open-Label, Randomized Study. *Clinical Pharmacology and Therapeutics*, *103*(3), 402–408. https://doi.org/10.1002/cpt.943.
6. Agathis, N. T. (2023). Mortality Among Children Aged 5 Years Living with HIV Who Are Receiving Antiretroviral Treatment—U.S. President's Emergency Plan for AIDS Relief, 28 Supported Countries and Regions, October 2020–September 2022. *MMWR. Morbidity and Mortality Weekly Report*, *72*. https://doi.org/10.15585/mmwr.mm7248a1.
7. Ahmad, I., Ahmed, S., Anwar, Z., Sheraz, M. A., & Sikorski, M. (2016). Photostability and Photostabilization of Drugs and Drug Products. *International Journal of Photoenergy*, *2016*(1), 8135608. https://doi.org/10.1155/2016/8135608.

8. AIDS and Hepatitis C Professional Group, Society of Infectious Diseases, Chinese Medical Association; Chinese Center for Disease Control and Prevention. (2022). Chinese guidelines for the diagnosis and treatment of HIV/AIDS (2021 edition). *Infectious Diseases & Immunity*, *2*(03), 145-167.
9. Alqahtani, M. S., Kazi, M., Alsenaidy, M. A., & Ahmad, M. Z. (2021). Advances in Oral Drug Delivery. *Frontiers in Pharmacology*, *12*. https://doi.org/10.3389/fphar.2021.618411.
10. Al-Ramahi, R. J., Zaid, A. A. N., & Anabousi, H. (2015). Problems associated with reconstitution, administration, and storage of antibiotic suspensions for paediatrics: A cross-sectional study in Nablus city, Palestine. *BMC Research Notes*, *8*, 760. https://doi.org/10.1186/s13104-015-1746-z.
11. *Antiretroviral Therapy—PAHO/WHO | Pan American Health Organization*. (2020, July 21). https://www.paho.org/en/topics/antiretroviral-therapy.
12. Aziz, Z. H. A., Katas, H., Omar, M. S., Mohamed Shah, N., Mohamad Yusop, S., Shafiee, M. N., & Mohd Tarmizi, S. F. (2022). Preference, Perception, and Acceptability of Fluid Gels as a Potential Age-Appropriate Dosage Form for Elderly Patients with Dysphagia. *Gels*, *8*(4), 218. https://doi.org/10.3390/gels8040218.
13. Begines, B., Ortiz, T., Pérez-Aranda, M., Martínez, G., Merinero, M., Argüelles-Arias, F., & Alcudia, A. (2020). Polymeric Nanoparticles for Drug Delivery: Recent Developments and Future Prospects. *Nanomaterials*, *10*(7), Article 7. https://doi.org/10.3390/nano10071403.
14. Brandt, C., Zvolensky, M. J., Woods, S. P., Gonzalez, A., Safren, S. A., & O'Cleirigh, C. M. (2017). Anxiety symptoms and disorders among adults living with HIV and AIDS: A critical review and integrative synthesis of the empirical literature. *Clinical Psychology Review*, *51*, 164–184. https://doi.org/10.1016/j.cpr.2016.11.005.

15. Berthomieu, C., & Hienerwadel, R. (2009). Fourier transform infrared (FTIR) spectroscopy. *Photosynthesis Research*, *101*(2), 157–170. https://doi.org/10.1007/s11120-009-9439-x

16. Chen, L., Xu, J., & Chen, J. (2015). Applications of scanning electron microscopy in earth sciences. *Science China Earth Sciences*, *58*(10), 1768–1778. https://doi.org/10.1007/s11430-015-5172-9

17. Cheow, W. S., & Hadinoto, K. (2011). Factors affecting drug encapsulation and stability of lipid–polymer hybrid nanoparticles. *Colloids and Surfaces B: Biointerfaces*, *85*(2), 214–220. https://doi.org/10.1016/j.colsurfb.2011.02.033

18. Caplan, M. R., Daar, E. S., & Corado, K. C. (2018). Next generation fixed dose combination pharmacotherapies for treating HIV. *Expert Opinion on Pharmacotherapy*, *19*(6), 589–596. https://doi.org/10.1080/14656566.2018.1450866.

19. Cardenas, M. C., Farnan, S., Hamel, B. L., Mejia Plazas, M. C., Sintim-Aboagye, E., Littlefield, D. R., Behl, S., Punia, S., Enninga, E. A. L., Johnson, E., Temesgen, Z., Theiler, R., Gray, C. M., & Chakraborty, R. (2023). Prevention of the Vertical Transmission of HIV; A Recap of the Journey so Far. *Viruses*, *15*(4), Article 4. https://doi.org/10.3390/v15040849.

20. Choi, H. W., Chan, C., Shterev, I. D., Lynch, H. E., Robinette, T. J., Johnson-Weaver, B. T., Shi, J., Sempowski, G. D., Kim, S. Y., Dickson, J. K., Gooden, D. M., Abraham, S. N., & Staats, H. F. (2019). Identification of Novel Mast Cell Activators Using Cell-Based High-Throughput Screening. *SLAS Discovery: Advancing Life Sciences R & D*, *24*(6), 628–640. https://doi.org/10.1177/2472555219834699.

21. Cihlar, T., & Ray, A. S. (2010). Nucleoside and nucleotide HIV reverse transcriptase inhibitors: 25 years after zidovudine. *Antiviral Research*, *85*(1), 39–58. https://doi.org/10.1016/j.antiviral.2009.09.014.

22. Coelho, J. F., Ferreira, P. C., Alves, P., Cordeiro, R., Fonseca, A. C., Góis, J. R., & Gil, M. H. (2010). Drug delivery systems: Advanced technologies potentially applicable in personalized treatments. *EPMA Journal*, *1*(1), 164–209. https://doi.org/10.1007/s13167-010-0001-x.

23. Contributor, T. W., NT. (2020, June 15). HIV 1: Epidemiology, pathophysiology and transmission. *Nursing Times*. https://www.nursingtimes.net/cancer/hiv-1-epidemiology-pathophysiology-and-transmission-15-06-2020/.

24. Crucho, C. I. C., & Barros, M. T. (2017). Polymeric nanoparticles: A study on the preparation variables and characterization methods. *Materials Science and Engineering: C*, *80*, 771–784. https://doi.org/10.1016/j.msec.2017.06.004.

25. Daanish, A. F., Mushkani, D. E. A., & Atiq, M. A. (2023). *Excessive dilution of oral antibiotic suspensions and oversized bottles: An exploratory survey based on paediatricians' experiences in Kabul*. Research Square. https://doi.org/10.21203/rs.3.rs-3339211/v1.

26. Derman, S. (2015). Caffeic Acid Phenethyl Ester Loaded PLGA Nanoparticles: Effect of Various Process Parameters on Reaction Yield, Encapsulation Efficiency, and Particle Size. *Journal of Nanomaterials*, *2015*(1), 341848. https://doi.org/10.1155/2015/341848.

27. Ekpenyong, M. G., Antai, S. P., Asitok, A. D., & Ekpo, B. O. (2017). Plackett-Burman Design and Response Surface Optimization of Medium Trace Nutrients for Glycolipopeptide Biosurfactant Production. *Iranian Biomedical Journal*, *21*(4), 249–260. https://doi.org/10.18869/acadpub.ibj.21.4.249.

28. Ensign, L. M., Cone, R., & Hanes, J. (2012). Oral Drug Delivery with Polymeric Nanoparticles: The Gastrointestinal Mucus Barriers. *Advanced Drug Delivery Reviews*, *64*(6), 557–570. https://doi.org/10.1016/j.addr.2011.12.009.

29. Ezike, T. C., Okpala, U. S., Onoja, U. L., Nwike, C. P., Ezeako, E. C., Okpara, O. J., Okoroafor, C. C., Eze, S. C., Kalu, O. L., Odoh, E. C., Nwadike, U. G., Ogbodo, J. O., Umeh, B. U., Ossai, E. C., & Nwanguma, B. C. (2023). Advances in drug delivery systems, challenges and future directions. *Heliyon*, *9*(6), e17488. https://doi.org/10.1016/j.heliyon.2023.e17488.

30. Fernandez, J. V. B., & Munir, A. (2025). Abacavir. In *StatPearls*. StatPearls Publishing. http://www.ncbi.nlm.nih.gov/books/NBK537117/.

31. Foka, F. E. T., & Mufhandu, H. T. (2023). Current ARTs, Virologic Failure, and Implications for AIDS Management: A Systematic Review. *Viruses*, *15*(8), Article 8. https://doi.org/10.3390/v15081732.

32. Fadlelmoula, A., Pinho, D., Carvalho, V. H., Catarino, S. O., & Minas, G. (2022). Fourier Transform Infrared (FTIR) Spectroscopy to Analyse Human Blood over the Last 20 Years: A Review towards Lab-on-a-Chip Devices. *Micromachines*, *13*(2), 187. https://doi.org/10.3390/mi13020187

33. Gerets, H. H. J., Tilmant, K., Gerin, B., Chanteux, H., Depelchin, B. O., Dhalluin, S., & Atienzar, F. A. (2012). Characterization of primary human hepatocytes, HepG2 cells, and HepaRG cells at the mRNA level and CYP activity in response to inducers and their predictivity for the detection of human hepatotoxins. *Cell Biology and Toxicology*, *28*(2), 69–87. https://doi.org/10.1007/s10565-011-9208-4

34. Gaikwad, S. S., Morales, J. O., Lande, N. B., Catalán-Figueroa, J., Laddha, U. D., & Kshirsagar, S. J. (2024). Exploring paediatric oral suspension development: Challenges, requirements, and formulation advancements. *International Journal of Pharmaceutics*, *657*, 124169. https://doi.org/10.1016/j.ijpharm.2024.124169.

35. Gandhi, R. T., Landovitz, R. J., Sax, P. E., Smith, D. M., Springer, S. A., Günthard, H. F., Thompson, M. A., Bedimo, R. J., Benson, C. A., Buchbinder, S. P., Crabtree-Ramirez, B. E., del Rio, C., Eaton, E. F., Eron, J. J., Jr, Hoy, J. F., Lehmann, C., Molina, J.-M., Jacobsen, D. M., & Saag, M. S. (2024). Antiretroviral Drugs for Treatment and Prevention of HIV in Adults: 2024 Recommendations of the International Antiviral Society–USA Panel. *JAMA*. https://doi.org/10.1001/jama.2024.24543.

36. Gibas, K. M., Kelly, S. G., Arribas, J. R., Cahn, P., Orkin, C., Daar, E. S., Sax, P. E., & Taiwo, B. O. (2022). Two-drug regimens for HIV treatment. *The Lancet. HIV*, *9*(12), e868–e883. https://doi.org/10.1016/S2352-3018(22)00249-1.

37. González-González, O., Ramirez, I. O., Ramirez, B. I., O'Connell, P., Ballesteros, M. P., Torrado, J. J., & Serrano, D. R. (2022). Drug Stability: ICH versus Accelerated Predictive Stability Studies. *Pharmaceutics*, *14*(11), Article 11. https://doi.org/10.3390/pharmaceutics14112324.

38. Govender, R. D., Hashim, M. J., Khan, M. A., Mustafa, H., & Khan, G. (2021). Global epidemiology of HIV/AIDS: a resurgence in North America and Europe. *Journal of epidemiology and global health*, *11*(3), 296-301.

39. Guo, H., Li, F., Qiu, H., Liu, J., Qin, S., Hou, Y., & Wang, C. (2020). Preparation and Characterization of Chitosan Nanoparticles for Chemotherapy of Melanoma Through Enhancing Tumor Penetration. *Frontiers in Pharmacology*, *11*. https://doi.org/10.3389/fphar.2020.00317.

40. Hassan, D. S., & Hasary, H. J. (2022). The impact of viscosity on the dissolution of naproxen immediate-release tablets. *Journal of Taibah University Medical Sciences*, *18*(4), 687–695. https://doi.org/10.1016/j.jtumed.2022.12.009.

41. Haleem, A., Javaid, M., Singh, R. P., Rab, S., & Suman, R. (2023). Applications of nanotechnology in medical field: A brief review. *Global Health Journal*, *7*(2), 70–77. https://doi.org/10.1016/j.glohj.2023.02.008.

42. Hansoti, B., Kelen, G. D., Quinn, T. C., Whalen, M. M., DesRosiers, T. T., Reynolds, S. J., Redd, A., & Rothman, R. E. (2017). A systematic review of emergency department-based HIV testing and linkage to care initiatives in low resource settings. *PLOS ONE*, *12*(11), e0187443. https://doi.org/10.1371/journal.pone.0187443.

43. Harjumäki, R., Nugroho, R. W. N., Zhang, X., Lou, Y.-R., Yliperttula, M., Valle-Delgado, J. J., & Österberg, M. (2019). Quantified forces between HepG2 hepatocarcinoma and WA07 pluripotent stem cells with natural biomaterials correlate with in vitro cell behavior. *Scientific Reports*, *9*(1), 7354. https://doi.org/10.1038/s41598-019-43669-7.

44. Heu, R., Shahbazmohamadi, S., Yorston, J., & Capeder, P. (2019). Target material selection for sputter coating of SEM samples. *Microscopy Today*, *27*(4), 32-36.

45. *HIV statistics - global and regional trends* (2023) *UNICEF DATA*. Available at: https://data.unicef.org/topic/hivaids/global-regional-trends/ (Accessed: 23 December 2024)

46. *How is HIV transmitted? | NICHD - Eunice Kennedy Shriver National Institute of Child Health and Human Development*. (2021, August 10). https://www.nichd.nih.gov/health/topics/hiv/conditioninfo/transmission.

47. Huston, M., DeBella, M., DiBella, M., & Gupta, A. (2021). Green synthesis of nanomaterials. *Nanomaterials*, *11*(8), 2130.

48. Huynh, K., Vaqar, S., & Gulick, P. G. (2024). HIV Prevention. In *StatPearls*. StatPearls Publishing. http://www.ncbi.nlm.nih.gov/books/NBK470281/.

49. Jesson, J., Saint-Lary, L., Revegue, M. H. D. T., O'Rourke, J., Townsend, C. L., Renaud, F., Penazzato, M., & Leroy, V. (2022). Safety and efficacy of abacavir for treating infants, children, and adolescents living with HIV: A systematic review and meta-analysis. *The Lancet Child & Adolescent Health*, *6*(10), 692–704. https://doi.org/10.1016/S2352-4642(22)00213-9

50. Kannan, M., 2018. Transmission electron microscope—Principle, components and applications. *A textbook on fundamentals and applications of nanotechnology*, pp.93-102.

51. Khan, D., Kirby, D., Bryson, S., Shah, M., & Rahman Mohammed, A. (2022). Paediatric specific dosage forms: Patient and formulation considerations. *International Journal of Pharmaceutics*, *616*, 121501. https://doi.org/10.1016/j.ijpharm.2022.121501.

52. Kim, D.-W., & Weon, K. Y. (2021). Pharmaceutical application and development of fixed dose combination: Dosage form review. *Journal of Pharmaceutical Investigation*, *51*(5), 555–570. https://doi.org/10.1007/s40005-021-00543-x.

53. Konan, Y. N., Gurny, R., & Allémann, E. (2002). Preparation and characterization of sterile and freeze-dried sub-200 nm nanoparticles. *International Journal of Pharmaceutics*, *233*(1), 239–252. https://doi.org/10.1016/S0378-5173(01)00944-9.

54. Kumari, A., Singla, R., Guliani, A., & Yadav, S. K. (2014). Nanoencapsulation for drug delivery. *EXCLI Journal*, *13*, 265–286.

55. Kumari, S., Goyal, A., Sönmez Gürer, E., Algın Yapar, E., Garg, M., Sood, M., & Sindhu, R. K. (2022). Bioactive Loaded Novel Nano-Formulations for Targeted Drug Delivery and Their Therapeutic Potential. *Pharmaceutics*, *14*(5), Article 5. https://doi.org/10.3390/pharmaceutics14051091.

56. Kaszuba, M., Corbett, J., Watson, F. M., & Jones, A. (2010). High-concentration zeta potential measurements using light-scattering techniques. *Philosophical Transactions. Series A,*

Mathematical, Physical, and Engineering Sciences, *368*(1927), 4439–4451. https://doi.org/10.1098/rsta.2010.0175

57. Lau, A. J., Yang, G., Rajaraman, G., Baucom, C. C., & Chang, T. K. H. (2010). Human Pregnane X Receptor Agonism by *Ginkgo biloba* Extract: Assessment of the Role of Individual Ginkgolides. *The Journal of Pharmacology and Experimental Therapeutics*, *335*(3), 771–780. https://doi.org/10.1124/jpet.110.172338
58. Margolis, A. M., Heverling, H., Pham, P. A., & Stolbach, A. (2014). A Review of the Toxicity of HIV Medications. *Journal of Medical Toxicology*, *10*(1), 26–39. https://doi.org/10.1007/s13181-013-0325-8
59. Lambros, M., Tran, T. (Henry), Fei, Q., & Nicolaou, M. (2022). Citric Acid: A Multifunctional Pharmaceutical Excipient. *Pharmaceutics*, *14*(5), 972. https://doi.org/10.3390/pharmaceutics14050972.
60. Lee, C., Sapasap, J., LaRochelle, J., Smith, R. O., & Badowski, M. E. (2021). Antiretroviral Therapy in Children and Adolescents: A Look Into Modern Single Tablet Regimens. *The Journal of Paediatric Pharmacology and Therapeutics: JPPT*, *26*(8), 783–794. https://doi.org/10.5863/1551-6776-26.8.783.
61. Lee, Y. Y., Erdogan, A., & Rao, S. S. C. (2014). How to Assess Regional and Whole Gut Transit Time with Wireless Motility Capsule. *Journal of Neurogastroenterology and Motility*, *20*(2), 265–270. https://doi.org/10.5056/jnm.2014.20.2.265.
62. Lim, Z. C., Hoo, G. S., Ang, J. H., Teng, C. B., Ang, L. W., Lee, C. C., Leo, Y. S., Law, H. L., Ng, O. T., & Wong, C. S. (2021). Safety and effectiveness of switching to Abacavir/Lamivudine plus rilpivirine for maintenance therapy in virologically suppressed

HIV-1 individuals in Singapore (SEALS). *AIDS Research and Therapy*, *18*(1), Article 1. https://doi.org/10.1186/s12981-021-00402-7.

63. Lisik, A., & Musiał, W. (2019). Conductomeric Evaluation of the Release Kinetics of Active Substances from Pharmaceutical Preparations Containing Iron Ions. *Materials*, *12*(5), 730. https://doi.org/10.3390/ma12050730.
64. López-Cabeza, R., Kah, M., Grillo, R., Bílková, Z., & Hofman, J. (2021). Is centrifugal ultrafiltration a robust method for determining encapsulation efficiency of pesticide nanoformulations? *Nanoscale*, *13*(10), 5410–5418. https://doi.org/10.1039/D0NR08693B.
65. Lv, Z., Chu, Y., & Wang, Y. (2015). HIV protease inhibitors: A review of molecular selectivity and toxicity. *HIV/AIDS (Auckland, N.Z.)*, *7*, 95–104. https://doi.org/10.2147/HIV.S79956.
66. Mack, I., Sharland, M., Brussee, J. M., Rehm, S., Rentsch, K., & Bielicki, J. (2021). Insufficient stability of clavulanic acid in widely used child-appropriate formulations. *Antibiotics*, *10*(2), 225.
67. Mahdi, M. H., Conway, B. R., & Smith, A. M. (2014). Evaluation of gellan gum fluid gels as modified release oral liquids. *International Journal of Pharmaceutics*, *475*(1), 335–343. https://doi.org/10.1016/j.ijpharm.2014.08.044.
68. Malamatari, M., Somavarapu, S., Taylor, K. M. G., & Buckton, G. (2016). Solidification of nanosuspensions for the production of solid oral dosage forms and inhalable dry powders. *Expert Opinion on Drug Delivery*, *13*(3), 435–450. https://doi.org/10.1517/17425247.2016.1142524.
69. Manoharan, C., Basarkar, A., & Singh, J. (2010). Various Pharmaceutical Disperse Systems. In A. K. Kulshreshtha, O. N. Singh, & G. M. Wall (Eds.), *Pharmaceutical Suspensions: From*

Formulation Development to Manufacturing (pp. 1–37). Springer. https://doi.org/10.1007/978-1-4419-1087-5_1.

70. Mega, T. A., Usamo, F. B., & Negera, G. Z. (2020). Abacavir versus Zidovudine-based regimens for treatment of HIV-infected children in resource limited settings: A retrospective cohort study. *BMC Paediatrics*, *20*(1), 99. https://doi.org/10.1186/s12887-020-1995-4.
71. Mengesha, M. M., Embibel, M., Gobena, T., Tunje, A., Jerene, D., & Hallström, I. K. (2022). Antiretroviral therapy non-adherence among children living with HIV in Dire Dawa, Eastern Ethiopia: A case-control study. *BMC Paediatrics*, *22*(1), 653. https://doi.org/10.1186/s12887-022-03697-1.
72. Mohammadzadeh, R., & Javadzadeh, Y. (2018). An overview on oral drug delivery via nano-based formulations. *Pharmaceutical and Biomedical Research*. https://doi.org/10.18502/pbr.v4i1.139.
73. Mohd Shahrizan, M. S., Abd Aziz, Z. H., & Katas, H. (2022). Fluid gels: A systematic review towards their application in pharmaceutical dosage forms and drug delivery systems. *Journal of Drug Delivery Science and Technology*, *67*, 102947. https://doi.org/10.1016/j.jddst.2021.102947.
74. M.Sc, M. G. (2023, July 17). *Polymeric Nanoparticles: Properties and Applications*. AZoNano. https://www.azonano.com/article.aspx?ArticleID=6504.
75. NCBI (National Center for Biotechnology Information), 2025. *PubChem Compound Summary for CID 441300, Abacavir*. [online] Available at: https://pubchem.ncbi.nlm.nih.gov/compound/Abacavir [Accessed 7 Apr. 2025].

76. NCBI (National Center for Biotechnology Information), 2025. *PubChem Compound Summary for CID 60825, Lamivudine*. [online] Available at: https://pubchem.ncbi.nlm.nih.gov/compound/Lamivudine [Accessed 7 Apr. 2025].

77. Nagata, J. M., Miller, J. D., Cohen, C. R., Frongillo, E. A., Weke, E., Burger, R., Wekesa, P., Sheira, L. A., Mocello, A. R., Otieno, P., Butler, L. M., Bukusi, E. A., Weiser, S. D., & Young, S. L. (2022). Water Insecurity is Associated with Lack of Viral Suppression and Greater Odds of AIDS-Defining Illnesses Among Adults with HIV in Western Kenya. *AIDS and Behavior*, *26*(2), 549–555. https://doi.org/10.1007/s10461-021-03410-w.

78. Németh, Z., Csóka, I., Semnani Jazani, R., Sipos, B., Haspel, H., Kozma, G., Kónya, Z., & Dobó, D. G. (2022). Quality by Design-Driven Zeta Potential Optimisation Study of Liposomes with Charge Imparting Membrane Additives. *Pharmaceutics*, *14*(9), 1798. https://doi.org/10.3390/pharmaceutics14091798.

79. Pereira, M.D.C., Nunes, D., Andrade, S., Ramalho, M.J., & Loureiro, J. (2022, April 06). Nanoparticles-Loaded Hydrogel System. *In Encyclopedia*. https://encyclopedia.pub/entry/21398.

80. Penazzato, M., Townsend, C. L., Sam-Agudu, N. A., Ruel, T. D., Archary, M., Bekker, A., Cressey, T. R., Colbers, A., Sugandhi, N., Rojo, P., Rakhmanina, N., Watkins, M., Frigati, L., Mukui, I., Hafiz, A., Vicari, M., Capparelli, E. V., Abrams, E. J., Abrams, E., … Watkins, M. (2022). Advancing the prevention and treatment of HIV in children: Priorities for research and development. *The Lancet HIV*, *9*(9), e658–e666. https://doi.org/10.1016/S2352-3018(22)00101-1.

81. Phanuphak, N., & Gulick, R. M. (2020). HIV treatment and prevention 2019: Current standards of care. *Current Opinion in HIV and AIDS*, *15*(1), 4. https://doi.org/10.1097/COH.0000000000000588.

82. Pooranagangadevi, N., & Padmapriyadarsini, C. (2022). Treatment of Tuberculosis and the Drug Interactions Associated With HIV-TB Co-Infection Treatment. *Frontiers in Tropical Diseases*, *3*. https://doi.org/10.3389/fitd.2022.834013.

83. Quercia, R., Perno, C.-F., Koteff, J., Moore, K., McCoig, C., St. Clair, M., & Kuritzkes, D. (2018). Twenty-Five Years of Lamivudine: Current and Future Use for the Treatment of HIV-1 Infection. *JAIDS Journal of Acquired Immune Deficiency Syndromes*, *78*(2), 125. https://doi.org/10.1097/QAI.0000000000001660.

84. Rampedi, P. N., Ogunrombi, M. O., Wesley-Smith, J., & Adeleke, O. A. (2023). A Micro-Configured Multiparticulate Reconstitutable Suspension Powder of Fixed Dose Rifampicin and Pyrazinamide: Optimal Fabrication and In Vitro Quality Evaluation. *Pharmaceutics*, *15*(1), Article 1. https://doi.org/10.3390/pharmaceutics15010064.

85. Riss, T., Niles, A., Moravec, R., Karassina, N., & Vidugiriene, J. (2004). Cytotoxicity Assays: In Vitro Methods to Measure Dead Cells. In S. Markossian, A. Grossman, M. Arkin, D. Auld, C. Austin, J. Baell, K. Brimacombe, T. D. Y. Chung, N. P. Coussens, J. L. Dahlin, V. Devanarayan, T. L. Foley, M. Glicksman, K. Gorshkov, J. V. Haas, M. D. Hall, S. Hoare, J. Inglese, P. W. Iversen, … X. Xu (Eds.), *Assay Guidance Manual*. Eli Lilly & Company and the National Center for Advancing Translational Sciences. http://www.ncbi.nlm.nih.gov/books/NBK540958/

86. Segall, A. I. (2019). Preformulation: The use of FTIR in compatibility studies. *Journal of Innovations in Applied Pharmaceutical Science*, *4*(3), 1–6. https://www.jiapsonline.com/admin/php/uploads/291_pdf.

87. Shah, D. S., Moravkar, K. K., Jha, D. K., Lonkar, V., Amin, P. D., & Chalikwar, S. S. (2023). A concise summary of powder processing methodologies for flow enhancement. *Heliyon*, *9*(6), e16498. https://doi.org/10.1016/j.heliyon.2023.e16498

88. Sivasubramanian, G., Frempong-Manso, E., & MacArthur, R. D. (2010). Abacavir/lamivudine combination in the treatment of HIV: A review. *Therapeutics and Clinical Risk Management*, *6*, 83–94.

89. Stetefeld, J., McKenna, S. A., & Patel, T. R. (2016). Dynamic light scattering: A practical guide and applications in biomedical sciences. *Biophysical Reviews*, *8*(4), 409–427. https://doi.org/10.1007/s12551-016-0218-6

90. Tkachenko, Y., & Niedzielski, P. (2022). FTIR as a Method for Qualitative Assessment of Solid Samples in Geochemical Research: A Review. *Molecules*, *27*(24), Article 24. https://doi.org/10.3390/molecules27248846

91. Saag, M. S., Gandhi, R. T., Hoy, J. F., Landovitz, R. J., Thompson, M. A., Sax, P. E., Smith, D. M., Benson, C. A., Buchbinder, S. P., del Rio, C., Eron, J. J., Jr, Fätkenheuer, G., Günthard, H. F., Molina, J.-M., Jacobsen, D. M., & Volberding, P. A. (2020). Antiretroviral Drugs for Treatment and Prevention of HIV Infection in Adults: 2020 Recommendations of the International Antiviral Society–USA Panel. *JAMA*, *324*(16), 1651–1669. https://doi.org/10.1001/jama.2020.17025.

92. Saran, A. K., Holden, N. A., & Garrison, S. R. (2022). Concerns regarding tablet splitting: A systematic review. *BJGP Open*, *6*(3), BJGPO.2022.0001. https://doi.org/10.3399/BJGPO.2022.0001.

93. Schlatter, A. F., Deathe, A. R., & Vreeman, R. C. (2016). The Need for Paediatric Formulations to Treat Children with HIV. *AIDS Research and Treatment*, *2016*(1), 1654938. https://doi.org/10.1155/2016/1654938.

94. Shah, D. S., Moravkar, K. K., Jha, D. K., Lonkar, V., Amin, P. D., & Chalikwar, S. S. (2023). A concise summary of powder processing methodologies for flow enhancement. *Heliyon*, *9*(6), e16498. https://doi.org/10.1016/j.heliyon.2023.e16498.

95. Sherman, E. M., Agwu, A. L., Ambrosioni, J., Behrens, G. M. N., Chu, C., Collins, L. F., Jimenez, H. R., Koren, D. E., McGorman, L., Nguyen, N. N., Nicol, M. R., Pandit, N. S., Pierre, N., Scarsi, K. K., Spinner, G. F., Tseng, A., Young, J. D., & Badowski, M. E. (2024). Consensus recommendations for use of long-acting antiretroviral medications in the treatment and prevention of HIV-1: Endorsed by the American Academy of HIV Medicine, American College of Clinical Pharmacy, Canadian HIV and Viral Hepatitis Pharmacists Network, European AIDS Clinical Society, and Society of Infectious Diseases Pharmacists. *Pharmacotherapy: The Journal of Human Pharmacology and Drug Therapy*, *44*(7), 494–538. https://doi.org/10.1002/phar.2922**.**

96. Pinto, R. M., Hall, E., & Tomlin, R. (2023). Injectable Long-Acting Cabotegravir-Rilpivirine Therapy for People Living With HIV/AIDS: Addressing Implementation Barriers from the Start. *The Journal of the Association of Nurses in AIDS Care: JANAC*, *34*(2), 216–220. https://doi.org/10.1097/JNC.0000000000000386.

97. Sharma, M. U., Arjariya, S., Chouksey, R., & Sharma, N. (2022). A review: formulation and evaluation of pharmaceutical gel. *Journal of Pharmaceutical Negative Results*, 1344-1362.

98. Shiau, S., Arpadi, S. M., & Yin, M. T. (2020). Bone Update: Is It Still an Issue Without Tenofovir Disoproxil Fumarate? *Current HIV/AIDS Reports*, *17*(1), 1–5. https://doi.org/10.1007/s11904-019-00474-1.

99. Singh, J., Dutta, T., Kim, K. H., Rawat, M., Samddar, P., & Kumar, P. (2018). 'Green'synthesis of metals and their oxide nanoparticles: applications for environmental remediation. *Journal of nanobiotechnology*, *16*, 1-24.

100. Sorour, G., Sipambo, N., & Archary, M. (2023). Paediatric antiretroviral update. *Southern African Journal of HIV Medicine*, *24*(1), 1506. https://doi.org/10.4102/sajhivmed.v24i1.1506

101. Srisuwan, Y., & Baimark, Y. (2014). Biodegradable Poly(D, L-Lactide)/Lipid Blend Microparticles Prepared by Oil-in-Water Emulsion Method for Controlled Release Drug Delivery. *Oriental Journal of Chemistry*, *30*(1), 63–69.

102. Swinkels, H. M., Justiz Vaillant, A. A., Nguyen, A. D., & Gulick, P. G. (2024). HIV and AIDS. In *StatPearls*. StatPearls Publishing. http://www.ncbi.nlm.nih.gov/books/NBK534860/.

103. Taylor, K., Fritz, K., Pellegrini, M. V., & Parmar, M. (2025). Lamivudine. In *StatPearls*. StatPearls Publishing. http://www.ncbi.nlm.nih.gov/books/NBK559252/.

104. Thang, N. H., Chien, T. B., & Cuong, D. X. (2023). Polymer-Based Hydrogels Applied in Drug Delivery: An Overview. *Gels*, *9*(7), Article 7. https://doi.org/10.3390/gels9070523.

105. Tressler, R., & Godfrey, C. (2012). NRTI Backbone in HIV Treatment. *Drugs*, *72*(16), 2051–2062. https://doi.org/10.2165/11640830-000000000-00000.

106. Tu, Y., Zheng, R., Yu, F., Xiao, X., Jiang, M., & Yuan, Y. (2021). Dual drug delivery system with flexible and controllable drug ratios for synergistic chemotherapy. *Science China Chemistry*, *64*(6), 1020–1030. https://doi.org/10.1007/s11426-020-9964-x.

107. Vanangamudi, M., Kurup, S., & Namasivayam, V. (2020). Non-nucleoside reverse transcriptase inhibitors (NNRTIs): A brief overview of clinically approved drugs and combination regimens. *Current Opinion in Pharmacology*, *54*, 179–187. https://doi.org/10.1016/j.coph.2020.10.009.

108. Vijayan, V., Naeem, F., & Veesenmeyer, A. F. (2021). Management of Infants Born to Mothers with HIV Infection. *American Family Physician*, *104*(1), 58–62.

109. Vranić, E. (2004). Basic Principles of Drug- Excipients Interactions. *Bosnian Journal of Basic Medical Sciences*, *4*(2), 56–58.

110. Wang, C., Cheng, S., Zhang, Y., Ding, Y., Chong, H., Xing, H., Jiang, S., Li, X., & Ma, L. (2019). Long-Acting HIV-1 Fusion Inhibitory Peptides and their Mechanisms of Action. *Viruses*, *11*(9), Article 9. https://doi.org/10.3390/v11090811.

111. Wang, Y., De Clercq, E., & Li, G. (2019). Current and emerging non-nucleoside reverse transcriptase inhibitors (NNRTIs) for HIV-1 treatment. *Expert Opinion on Drug Metabolism & Toxicology*, *15*(10), 813–829. https://doi.org/10.1080/17425255.2019.1673367.

112. Wheless, J. W., & Phelps, S. J. (2018). A Clinician's Guide to Oral Extended-Release Drug Delivery Systems in Epilepsy. *The Journal of Paediatric Pharmacology and Therapeutics: JPPT*, *23*(4), 277–292. https://doi.org/10.5863/1551-6776-23.4.277.

113. Wilkins, C. A., Hamman, H., Hamman, J. H., & Steenekamp, J. H. (2024). Fixed dose Combination Formulations in Solid Oral Drug Therapy: Advantages, Limitations, and Design Features. *Pharmaceutics*, *16*(2), 178. https://doi.org/10.3390/pharmaceutics16020178.

114. WHO. (2023, July 13). *HIV and AIDS*. World Health Organization. https://www.who.int/news-room/fact-sheets/detail/hiv-aids.

115. Yusuf Aliyu, A., & Adeleke, O. A. (2024). Latest Progress on Tuberculosis and HIV Co-Infection: A Closer Look at People of Different Ages. *Advanced Therapeutics*, 2400033. https://doi.org/10.1002/adtp.202400033.

116. Zhao, A. V., Crutchley, R. D., Guduru, R. C., Ton, K., Lam, T., & Min, A. C. (2022). A clinical review of HIV integrase strand transfer inhibitors (INSTIs) for the prevention and treatment of HIV-1 infection. *Retrovirology*, *19*(1), 22. https://doi.org/10.1186/s12977-022-00608-.